ISSN 0736-5306

SCIENCE OF TSUNAMI HAZARDS

The International Journal of The Tsunami Society

Volume 4 Number 2 1986

OBJECTIVE: The Tsunami Society publishes this journal to increase and disseminate knowledge about tsunamis and their hazards.

DISCLAIMER: The Tsunami Society publishes this journal to disseminate information relating to tsunamis. Although these articles have been technically reviewed by peers, The Tsunami Society is not responsible for the variety of any statement, opinion, or consequences.

EDITOR'S NOTE

The Tsunami Society is now four years old. The society wishes to introduce new items in addition to those in the Tsunami Dialogue, of which the first issue has already been published. This journal will now include a new section entitled "Forum" which will involve brief discussions on technical matters related to tsunamis and comments on articles that appeared in any issue, up to one year ago. Please note that papers submitted to the Forum must be limited to four typed pages, double-spaced. If your discussion must be longer in length it should be submitted as a paper on its own merit. Non-technical items may be published in Dialog.

Submit manuscripts of articles, notes, or letters to:
T. S. Murty Technical Editor
Institute of Ocean Sciences
Department of Fisheries and Oceans
Sidney, B.C., Canada V8L 4B2

If article is accepted for publication the author(s) must submit a camera ready manuscript. A voluntary $50.00 page charge will include 50 reprints.

SUBSCRIPTION INFORMATION: Price per copy $20.00 USA Hardcopy

EDITOR'S NOTE

The timely publication of the information in these articles was judged to be more important than the need to improve the grammar.

ISSN 0736-5306

Published by **The Tsunami Society** in Honolulu, Hawaii, U.S.A.

HYDRODYNAMIC NATURE OF DISASTERS BY THE TSUNAMIS OF THE JAPAN SEA EARTHQUAKE OF MAY 1984

TOSHIO IWASAKI
Dr. Professor Emeritus of Tohoku University
Professor of Ashikaga Institute of Technology
268 OMAE,ASHIKAGA 326,JAPAN

ABSTRACT

Catastrophic accidents caused by the tsunamis of the Japan Sea Earthquake of May 1983 are described in detail especially accounting on their hydrodynamic nature. Instructions to diminish disasters by large tsunami are suggested. Several problems which should be investigated in the future are also pointed out.

1. INTRODUCTION

On May 26,1983 an earthquake occurred on the northeastern part of the Japan main island in the Japan Sea. This was called the Japan Sea Earthquake. Since people had believed that large tsunamis would not occur in the Japan Sea, it was big surprise when such large Tsunami attacked. There was a loss of 103 lives which were mostly tourists or people hobby fishing who were not knowledgeable about tsunamis. This is different from recognition by people living in the Sanriku coast facing the Pacific coast.

The major object of investigation of tsunami is to defend it or to minimize its effects. One wishes to forecast the magnitude and the time of attack so as to give people enough time to evacuate,or to construct counter measures to stop or to compromise tsunami energy. This paper describes major catastrophic cases and the hydrodynamic investigation on the cause. It is hoped on this point that such investigation might be useful for the establishment of counter tsunami measures in the future.

2. DATA OF THE EARTHQUAKE AND THE WAVE SOURCE

Table-1 shows the general data of the Japan Sea Earthquake.

Table-1

Epicenter disclosed firstly by JMA was
40° 21'N 139° 05'E with the focal depth of 14km
and that corrected in the evening of May 26 by JMA was
40° 24'N 138° 54'E with the focal depth of 5km.
Epicenter reported by Faculty of Science,Tohoku University was
40° 41'N 139° 08'E with the focal depth of 15 km
Arrival time of seismic wave recorded at Akita Met. Observatory was
for P-wave at 12h 00m 17.8s and for S-wave at 12h 00m 36.5s.
Magnitude of the earthquake was 7.7.
Mechanism of the seismic motion was estimated such that
direction of the fault plane was N110° -120°E,
sloping angle was 20° - 30°,
faulting was adverse dip slip with low angle,
the length of the plane was 120-130 km running from N to S and the breadth of the focal zone was about 40km from E to W.

Fig. 1(a) shows the distribution of the epicenters of the aftershock observed during May 26 and 31 by the Observation Center for Earthquake Prediction,Faculty of Science,Tohoku University and Hirosaki University. Fig. 1(b) shows the corresponding distribution during May 26 and July 31. Bathymetrical lines are also shown and the aftershock area is shown as a horse shoe shape in the zone of 2000-3000 meters deep.

The fault line was estimated to run along the 3000 meters bathymetrical line and the upheaval movement occurred on the west side of this line. The tsunami generation zone was investigated by the method of adverse propagation wave rays using the arrival time of many tidal stations by which it was concluded that, in the above aftershock area,the sea bottom was raised and subsidence occurred between the aftershock area and the edge of the shelf where there was a steep slope from 200 meters to 3000 meters in a narrow distance as shown in the figure.

A tsunami was evoked by such movement of the sea bed. It was very important to the history of tsunami research that many video records and snapshots were taken by citizens. Thus a clear image of the tsunami could be constructed.

Generally speaking,from the Oga Peninsula to the coast including Noshiro,Minehama and Yatsumori the first wave group was led by solitons and outside of this region,that was Funakawa, Akita in the south and Tsugaru Peninsula,and Oshima Peninsula in the north such dispersive waves were not observed.

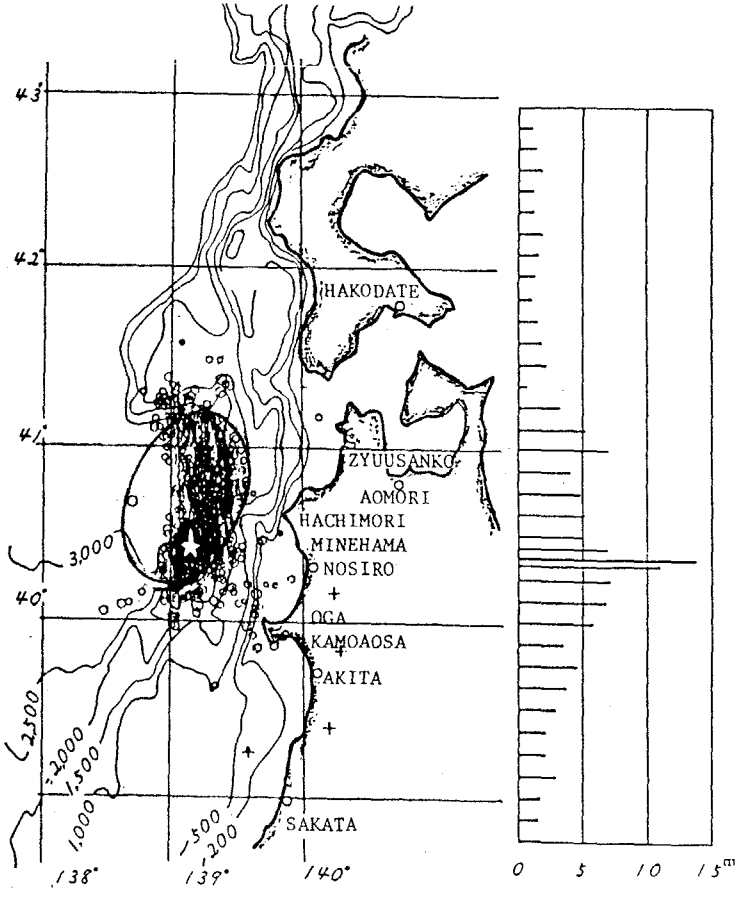

Fig. 1(a) Epicenters of Main Shock and Aftershock during May 26 and 31 1983 with the estimated Source Ellipse and Distribution of Tsunami Traces.

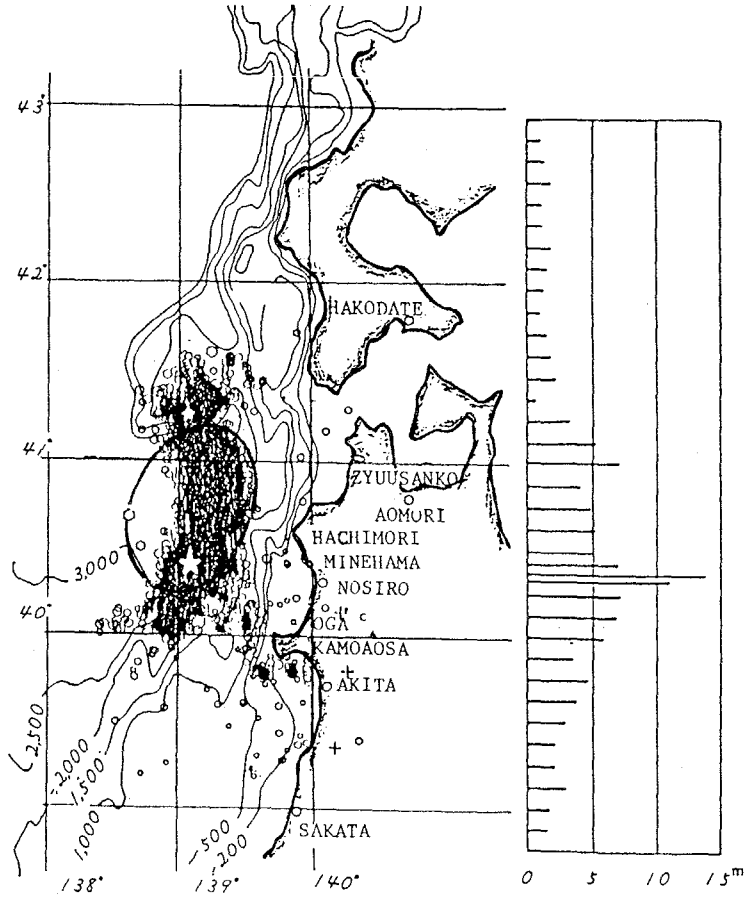

Fig. 1(b) Epicenters of Main Shock and Aftershock during May 26 and July 31, 1983 with the estimated Source Ellipse and Distribution of Tsunami Traces.

3. SCALE OF THE WAVE SOURCE AND THE DEFORMATION OF THE SEA BOTTOM

Equations to estimate the wave source area have been given by B.Wilson, K.Iida and T.Iwasaki (Iwasaki,1973). They are as follows.

$$m=2.61M-18.44 \quad (1)$$

$$M=6.27 + 0.76 \log_{10} L \quad (2)$$

$$ips = \tanh [1.5 \tanh \{(PAI/2021)^{1/2} * L^{2/3}\}] \quad (3)$$

$$2a = L/ips, \quad 2b = L*(1-ips^2)^{1/2}/ips \quad (4)$$

$$S = PAI*a*b \quad (5)$$

$$\log E_t = 0.6*m + 11.4 - \log_{10} 9.8 \quad (6)$$

where m and M are magnitudes of tsunami and the earthquake respectively. ips,L,a,b and S are the eccentricity,the distance between foci,the half length of the major and the minor axes and the source area of the assumed ellipse,respectively. E_t is the tsunami energy in ton-meter units,and M=7.7. Then the above equations give m=1.657, L =76113 km, ips =0.7243, a=52.55 km, b=36.24 km, S=5983 sq.km and $E_t=2.529*10^{11}$ ton-m.

The mean upheaval of the sea bed is

$$teta = (2E_t/(wS))^{1/2}$$

$$= (2*2.529*10^{11}/1.02*5.983*10^{9})^{1/2} = 9.104 \quad (7)$$

In fig. 1 the source ellipse is shown. The aftershock area has a longer dimension in the S-N direction than the assumed ellipse which is quite different from those in the Sanriku District.

4. SOLITONS ON THE NOSHIRO COAST

Many records by videos and photographs of the tsunami front show that soliton dispersion occurred on the Noshiro Coast (Shuto 1983,Li-San Hwang and Hammack 1984). Street, Chan and Fromm show results of numerical,finite-difference models for long waves on the continental slope such that "solitary waves break down into undular bores when the waves propagate onto a stepped slope"(Street,Chan and Fromm 1970). Camfield summerized solitons and soliton-induced dispersion (Camfield 1980). Then the condition for instability was obtained by Mason and Keulegan(1944) as

$$(a_1*L_1)^{1/2} > 2*d_2 \quad (8)$$

where a_1 and L_1 are the amplitude and the length in deep water and d_2 is the depth in shallow water. If we assume L_1 and d_2 as 76130 m (the length of the minor axis) and 200 m (the depth of the Noshiro shelf),the above equation gives for the unstable condition as,

$$a_1 > 2.1 \text{ m}$$

Eq.(7) gives much higher amplitude than this criterion which illustrates generation of solitons.

5. HYDRODYNAMIC NATURE OF DISASTERS

Among many cases,five examples are shown which are important for references to the planning of counter measures in the future. They are 1)the case of school children at Kamoaosa, 2)the case of fishermen at Zyuusanko, 3)the case at the Oga Aquarium, 4) scattering of 4-ton hexapods at the Minehama beach and 5) disaster at the construction site and translation and dislocation of caissons,weighing about 4000 tons, in the Noshiro Harbor.

1) The case of school children at Kamoaosa

The Kamoaosa coast is located on the south side of the Oga Peninsula. Fig. 2 shows its sketch. A highway runs about 10 meters higher than the coast. When the earthquake was generated,a micro-bus was going down on the sloping lane from this highway to the coast in which 45 children of the Aikawa Grammar School were with their two teachers and two fathers. Since shock was not so strong in the bus and the school was in the inland area,they had never suspected the generation and attack of the tsunami. So they proceeded onto the beach and sat on seaside rocks opening their lunch-boxes when the tsunami came in the terror. Mr.M.Ootomo,a fisherman of 47 years old,told that the sea withdrew 30 cms at 15 minutes after the earthquake, followed by return swelling up from the foot which caught the children and floated altogether at once,then washed offshore very rapidly. Another fisherman, Mr.K.Sasaki, 65 years old, said "the highest wave level was estimated about T.P.7 m by the overflow depth on the top level of the breakwater T.P. 4 m. In the fish port, a big swirl appeared with a roaring noise." And almost all of the people floated around a small island about 300 meters off the coast where all adults and 32 children were rescued by fishermen since there currents were not so strong and people could be floated and be rescued.

Thus the following facts are pointed out.

a. Tsunamis at the Kamoaosa coast were not solitons nor breaking waves, but the upsurge which followed the small downsurge.

b. People were taken off seaward as soon as they were floated.

c. There occurred a swirl in the fish port.

d. There was a rather calm area 300 meters off the shore where three fourths of the children were rescued,which suggests all members might have been rescued if they were wearing life jackets.

It had been generally considered that there was no way to be rescued when they were caught by tsunami. However the experience at Kamoaosa taught that there were still high possibility to be safe in the offshore region where current velocity becomes weak. Such possibility becomes higher when people could float on sea surface by wearing life jackets.

2) The case of fishermen at Zyuusanko

Photo-1 and 2 show six fishermen before and just at the instant of being caught by the tsunami front,which were taken by Mr.N.Nara,an officer of Ichiura Village of Aomori Prefecture who was patrolling since the tsunami warning was announced to the village and found the accident about 0:45 pm from a bridge "Zyuusankyo". One who is just being caught in the photo-2 is the fourth from the left in the photo-1. His two locations was measured as 88 meters by our field survey. Also the distance of the tsunami front in two pictures was measured as 99 meters. Our laboratory member made a simulation run carrying such cooler and wearing boots.It took 37 seconds between two locations. So his running speed was 2.38 m/sec and the front velocity of the tsunami was 2.67 m/sec. Since the Froude number of the front is usually assumed as 2, the depth at the front is calculated as 18 cms. Photos show clearly the shallowness at the front. However when people were caught by the tsunami, the depth increases so rapidly that the fishermen were quickly caught and were drowned as shown in photo. 2. It is said when the depth is 50 cms, they cannot run. Then the following instructions are deduced.

a. It should be noticed that there was a small building behind them. We knew that a ladder was installed to the roof. If they might evacuate to there, all of them could be safe. This showsthe importance of evacuation to a higher place. We were told on the survey tour that several fishermen were rescued from top of rocks in the sea.

b. It was very curious that the man who was just being caught by the tsunami did not thrown off his cooler which contained his gains in that morning. There is a person still pushing his motor bike in photo-1. What we must consider as an important problem is how to find out the critical moment. It is not ridiculous but related with the way of existence.

c. It should be noted that the tsunami front overtook them from the right side where there was a defense dike with the height of T.P. 5 meters and not from the river mouth. Thus the tsunami waves were not solitons but surges like those at Kamoaosa.

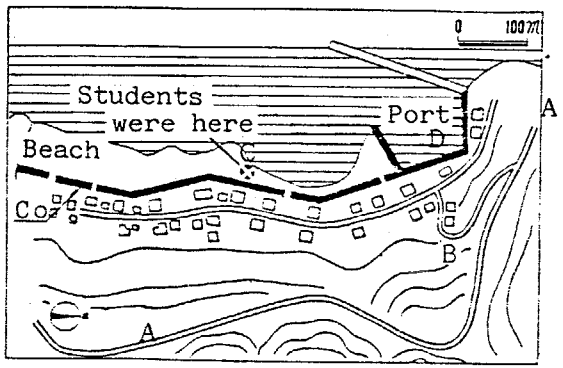

Fig. 2 A Sketch of the Kamo-aosa Coast south side in the Oga Peninsula where 13 School Children lost their Lives.

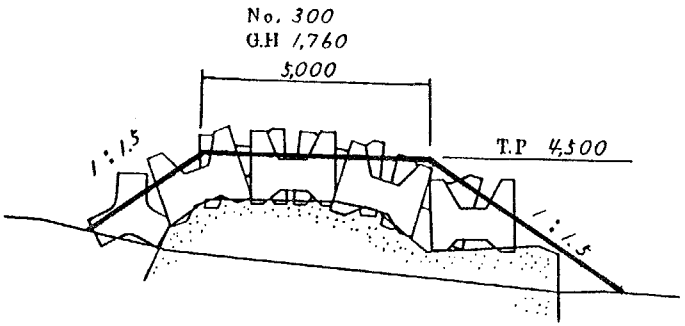

Fig. 3 The Cross Section of Sand Dike Protection of 4-ton Hexapods at Minehama.

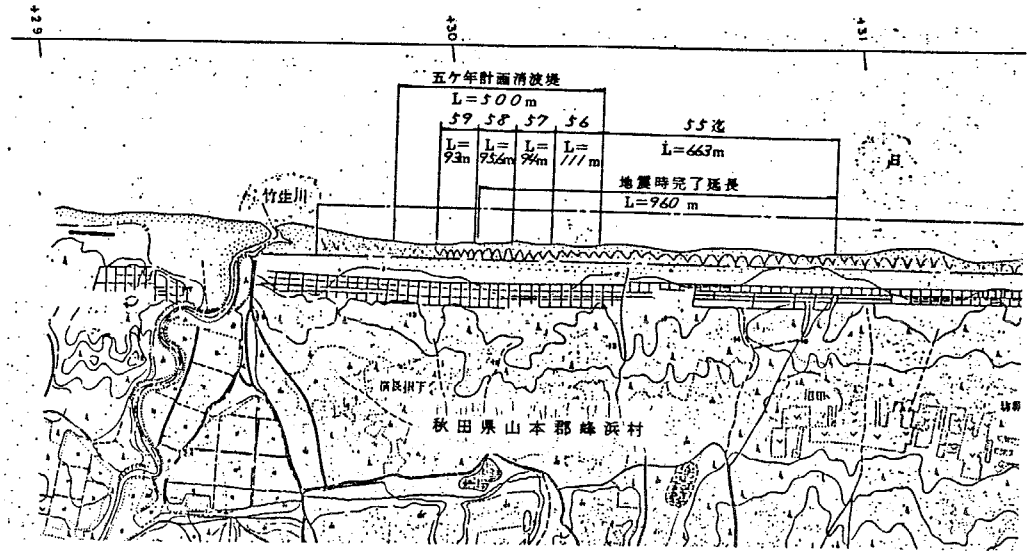

Fig. 4 Plan of the Construction Site of the Sand Dike Protection Work of 4-tons Hexapods at Minehama.

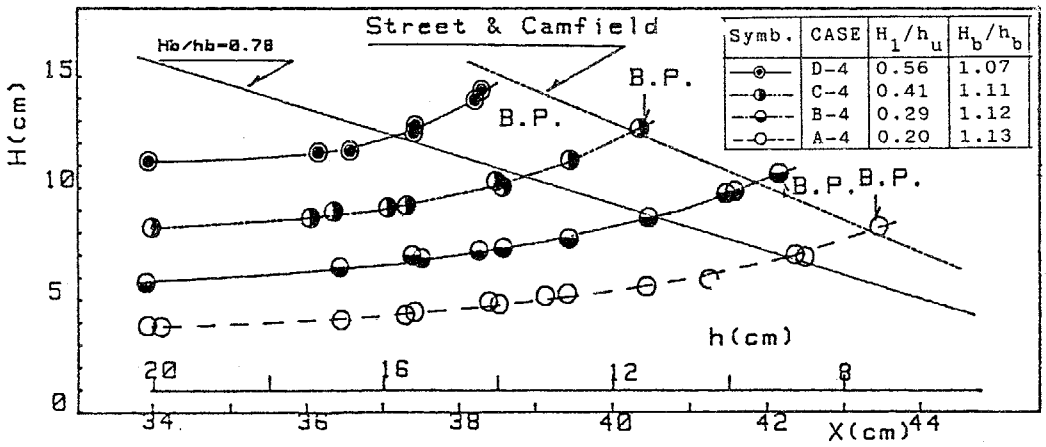

Fig. 5 Change of the Wave Height of the First Solitons with the distant from the Generation Section where the depths are 70 cm from x=0 m to 22.5 m, 20 cm from x=23 m to 34 m respectively and then the Bed Bed Slope is 1/75. Depth at each points is shown on the Ordinate.

Photo-1. At 0:45 pm the Second Tsunami attacked the River Mouth of Iwaki. The front three could evacuate. But others were caught.

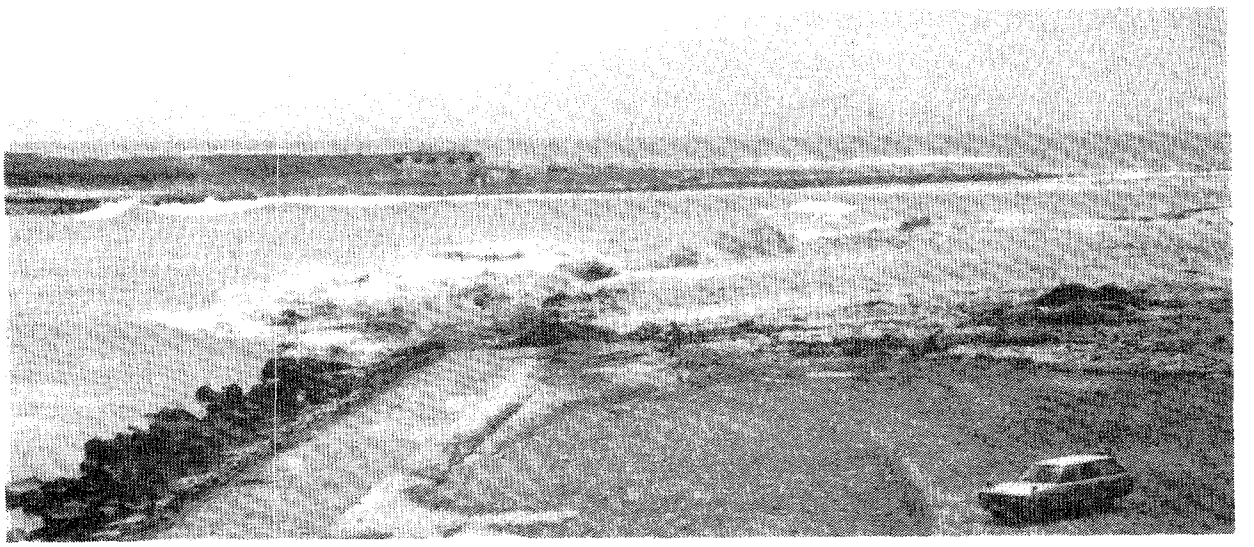

Photo-2. A Fisherman is now being caught by the Tsunami Front which came from the Right Side. He may be the fourth from the left in Photo-1.

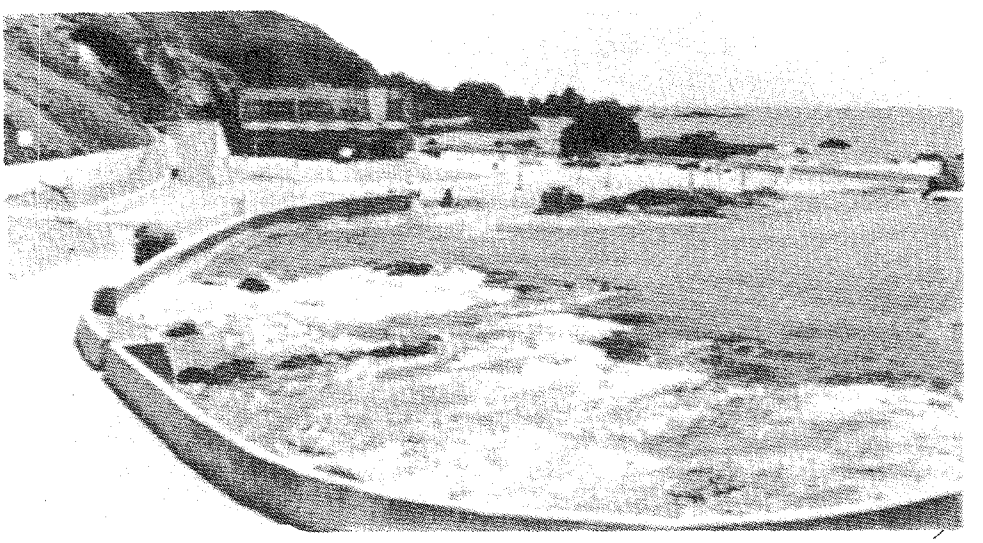

Photo-3. First Swell at the Oga Aquarium at 12:15 pm. Mr.Hosoi gave warning by a Walkie-talkie.

3)The case at the Oga Aquarium

Photo 3-8 were taken by Mr. S.Sato of the Suzuki Construction Co.Ltd. and were presented to us by Mr. T.Hosoi , a member of the Oga Aquarium. Since he had experienced the Niigata Earthquake Tsunami in 1964, he had paid attention to the offshore before the tsunami front came. Although Oga situated nearest to the wave source and the tsunami came only 7 minutes after the earthquake,he could notice the tsunami front in the offshore and made announcement by the loud-speaker of the aquarium and let about 100 visitors in the aquarium evacuate to the higher place. Then he went outside and made caution by a handy microphone, charged fortunately few days before,to the tourists. Photo-3 shows the sight of the lower ground from the Aquarium at about 13 minutes after the earthquake. Rapid rise of the water level is shown in these successive pictures. Also solitons cannot be recognized. One of our survey team made here also simulation running on the slope in photo-4 and it took 30 secs. Thus the time difference might be 15-20 sec between each pictures. It is surprising that how rapid water surface rose. Especially by photo-6 and 7, at the instant the level in front of the wall got maximum, water in the sea begun to withdraw forming a steep fall at the shoreline. Thus in this case any materials might be drawn into the sea as soon as they were floated by the incoming wave. However there was very effective guidance for people to evacuate and only one tragedy among two hundred tourists was occurred on a lady who came from Switzerland,the country in Alps and might be unfamiliar to such disaster. More attention should be paid to the way of precaution to such strange visitors.

Then the followings are summarized.

a. It is very much effective to have trained people in charge of watching on the sea and make caution when tsunami comes with powerful handy microphones. The minimum time for the tsunami warning is legally decided as 20 minutes in Japan. However our coasts are very near to the seismic sources and usually it is too late for people along the sea to evacuate if they move after the issue of warning. Now it is impossible to shorten the warning time of JMA less than 20 min. Numerical technique have developed in recent years and computer speeds increased very much. However how people can decide the location and six components of the fault plane before the tsunami comes. Also I-O technique is still time consuming comparedto computer run itself. Authorities tend to consume budgets for installing large scale caution towers equipped with modern facilities. However broad and dense network of caution system may be built up by such trained men of caution with very cheap expense.

b. The case of Oga Aquarium is to be compared with the case at Kamoaosa. There was remarkable discrepancy on the consideration on visitors. In this tsunami, most of the suffered people were unfamiliar with the phenomena on coasts or guests of hobby fishing who were isolated from the warning or announcements sitting all day long along shore. Also how to protect unfamiliar foreigners from the tsunami disaster is a big problem.

4) Scattering of 4-tons hexapods at the Minehama beach

Fig. 3 shows the cross section of a structure made of 4-tons hexapods which were designed for sand dikes against erosion by winter storm waves. The latter protect the Noshiro Plane from the wind-blown sand. Fig. 4 is the plan which shows the structure has been constructed already with the length of 960 meters. Among 1000 blocks,233 were scattered over 27,900 square meters of which 36 were broken. Maximum wave trace was 13 m above MSL and the dislocation distances were between 70 to 135 m.

In Tohoku University,a channel of 100 meters long was installed where a number of tests on the effects of solitons were conducted (Iwasaki et al 1984). In this test a single hump was formed in the deep portion of depth of 70 cms by pushing a vertical plate shoreward and was dispersed into three solitons on the flat of 20 cms deep after running up the slope of 45 degree. Fig. 5 shows the change of the wave height of the first solitons on the flat which shows the height is increased to the shore and finally breaks where the ratio of the wave height to the depth coincides with the results by Street and Camfield for the bed slope of 1/75 (Street and Camfield 1966). After breaking, the first soliton decreases its height very rapidly. However since the soliton is similar to a solitary wave, there is no phase of seaward motion and the whole mass of the first

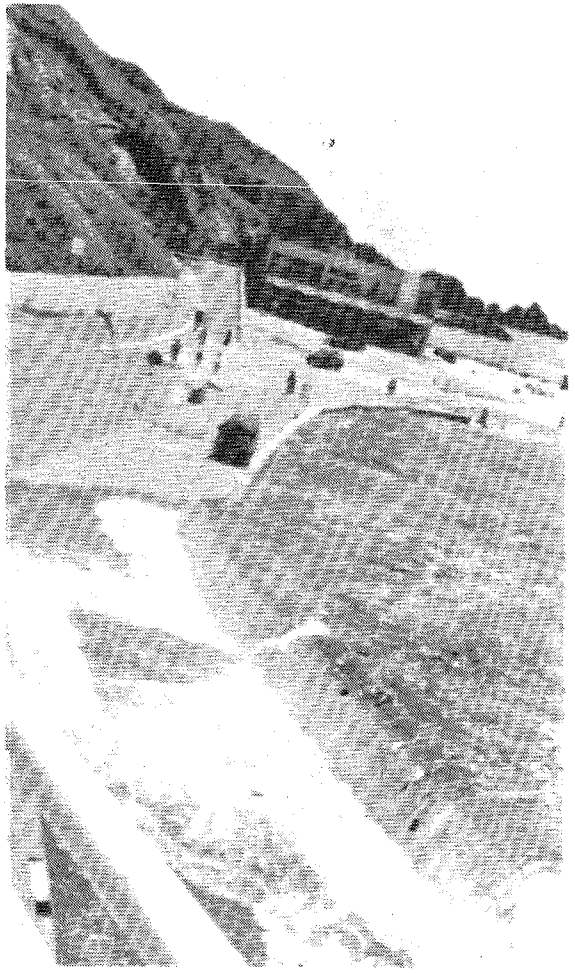

Photo-4. After 15-20 sec of Photo-3, tsunami swells up. Tourists are running on the Slope.

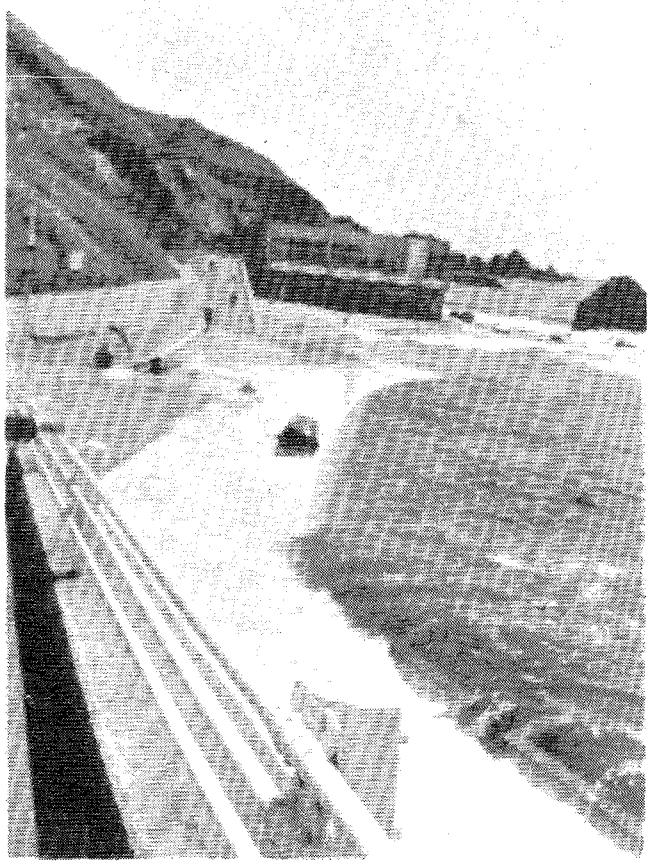

Photo-5. Most Tourists could evacuate except a lady who had came from Switzerland.

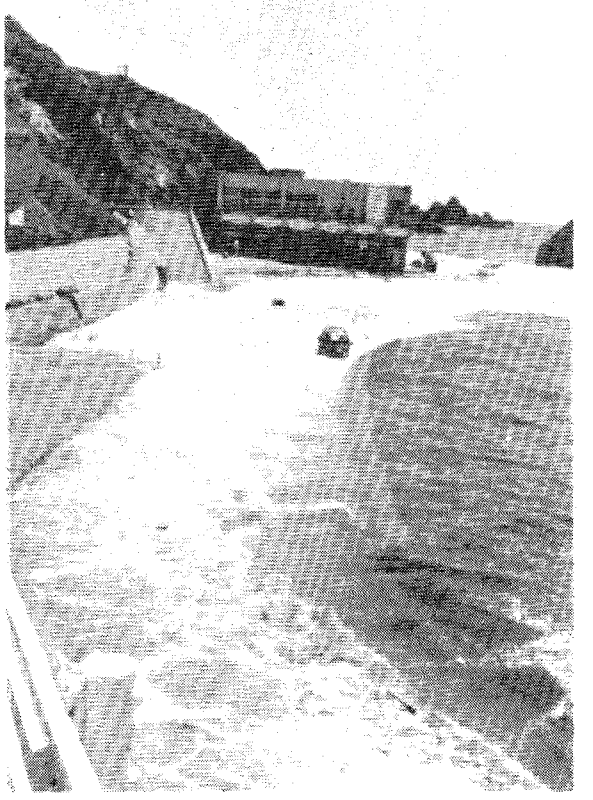

Photo-6. The Height of the Tsunami is now nearly equal to the Maximum. Marked Trace is T.P. 3.33 m.

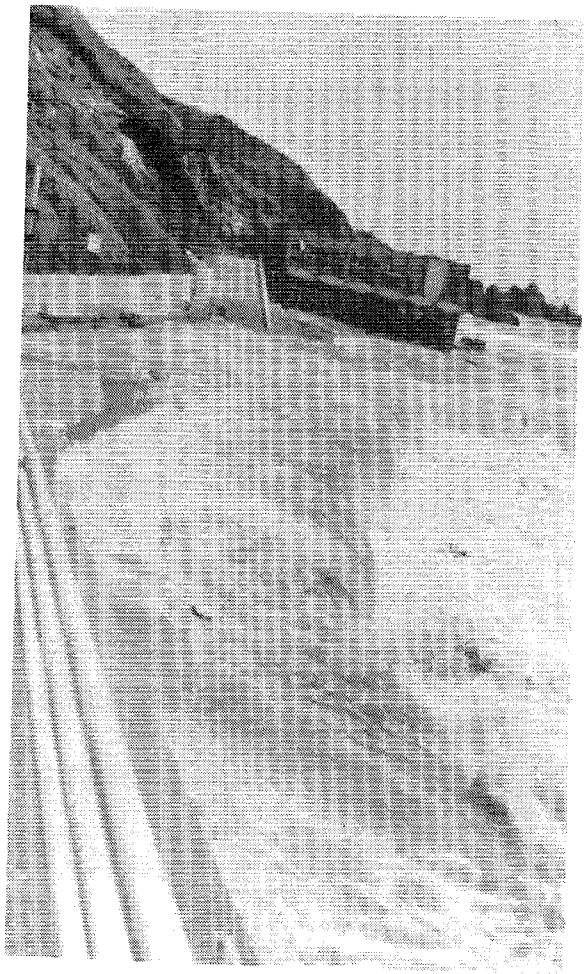

Photo-7. As soon as the water level get maximum, the sea begins to withdraw. A waterfall is created.

Photo-8. Here there are rocks roaring by the receding tsunamis. However a number of fishermen could survive by climbing up to the top of rocks.

soliton is distributed in the surf zone resulting the increase of the depth. We call this increase the soliton setup which should be discriminated from the wave setup. Thus the second soliton proceeds shoreward on the increased depth. This setup makes the breaking point of the second soliton nearer to the shore as the bottom slope compensates the setup by the difference of bed level. This is again repeated by the second soliton to the third. Fig. 6 shows this result clearly by the time-distance trajectories of solitons and the third soliton breaks just near the shoreline. Fig. 7 shows the velocity distributions under the crest of the third soliton as it proceeds to the shore which indicates the increase of the velocity before breaking.

Usually solitons lose their energy after breaking and any serious damages are not caused which was the situation at Hachimori shown in fig. 9B of the paper by Li-San Hwang and Hammack. However the reason why the hexapods were scattered by solitons in Minehama is illustrated by the above discussion that in Minehama the breaking of the third soliton occurred just on the shoreline due to the soliton setup. Also due to our tests it is proved that the maximum runup height is twice the wave height on the shoreline. It was reported at Minehama where there was no such blocks that the maximum height of the tsunami runup was 15 meters. Then the maximum height on the shoreline was estimated as 7.5 meters.

5) Disaster at the construction site and translation and dislocation of caissons of about 4000 tons in the Noshiro Harbor

In the Noshiro Harbor,revetments for the new Noshiro Thermal Power Plant were under construction. Fig. 8 shows the plan of the site. Dimension of the ground is 870 m * 1900 m ,rectangular shaped and the cross section of the revetments is designed as shown in fig. 9. The main structure is a concrete caisson which section is 11.0 m wide, 8.5 m high with the length of 20 m. This caisson is supported by backfill heap of rubbles of 5 to 15 cm diameter for the winter wave pressure and also in the offshore side tetrapod, hexapod or tribar mounds of 30 tons are designed to heap in order to dissipate the winter wave energy. Concrete layer of 2 m depth covers the caisson. The caisson is built on the broad foundation of rubble stones of 200-500 kg and the wave dissipater is on rubbles of 1 tons. As for the foundation protection, 6-tons concrete blocks are used.

When the tsunami attacked, 306 people were working there. Loss of lives amounted to 34, in which 9 were in ships and 25 were on caissons. Among 67 ships in charge for construction, 40 were destroyed. All six cranes and trucks on caissons were washed away.

It was remarkable that the ratio of the lost lives to the total was 4% (9 per 226) on ships to be compared 66.7% ,the ratio of the damaged ships to the total(40 per 60). Captains said ships could sail against the tsunami by directing ship nose to the coming wave if the wave height is less than the half of ship length. They said however a ship shorter than above was overturned in pitching plane by the wave steepness. It should be investigated also in the future that how to make divers evacuate from the underwater since 9 lost were mostly them.

On the caisson,80 people were working. Among them,25 were lost. Messrs. Ito,Morita and Inaba of the Daito Kougyo Co.Ltd. who were on a pontoon saw the first wave overflowed the caisson with the depth of 0.7 meters above the crest level of T.P.4 m, when people could withstand the flow. However they saw the second wave washed all people on caissons away into the sea,when the overflow depth was estimated as 4 m. There were proof that in this harbor the tsunami height was over 10 meters. Among the lost some people were found under the concrete blocks and others got damage by being collided by rubble stones in the water.

The problem of warning was most serious here. Mr.K.Yaguchi,an engineer of the Noshiro Harbor of the Akita Prefecture,told us that as soon as he listened the tsunami warning by the radio,he went up to the roof and found the wave coming already. Situation was almost the same at the offices of the construction companies that they promptly transmitted the warning to workers on caissons by walkie talkies. However it was too late since tsunami was attacking the site at that moment.

Very much surprising facts were translation or dislocation of the caissons of about 4000 tons! There were three zones contracted by different companies. In the zone presided by Goyou Co.Ltd.,six caissons were totally dislocated,one was tilted and one was translated among 22

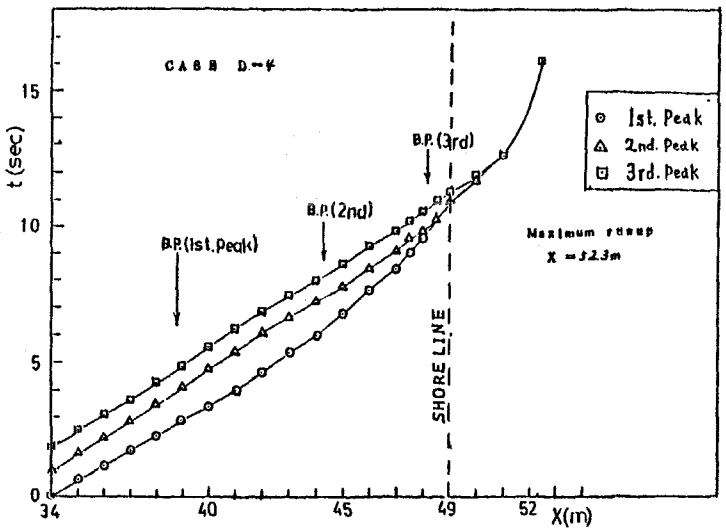

Fig. 6 Time-distance Trajectories of Successive Solitons.

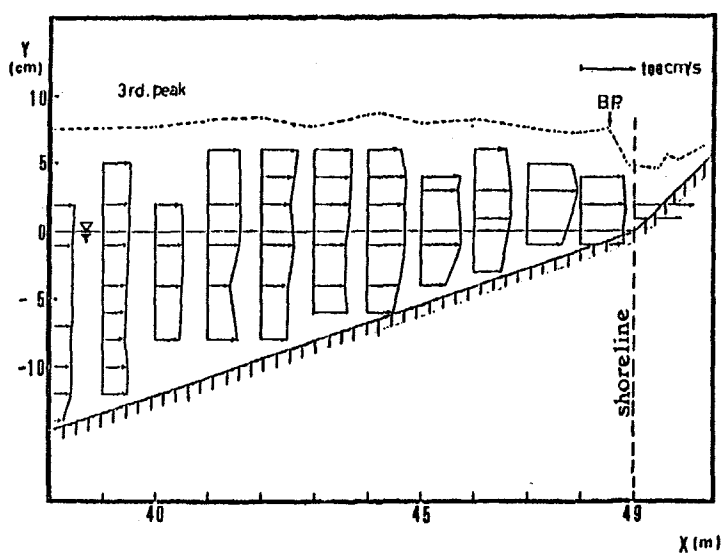

Fig. 7 Change of Velocity Distribution under the Crest of the Third Soliton.

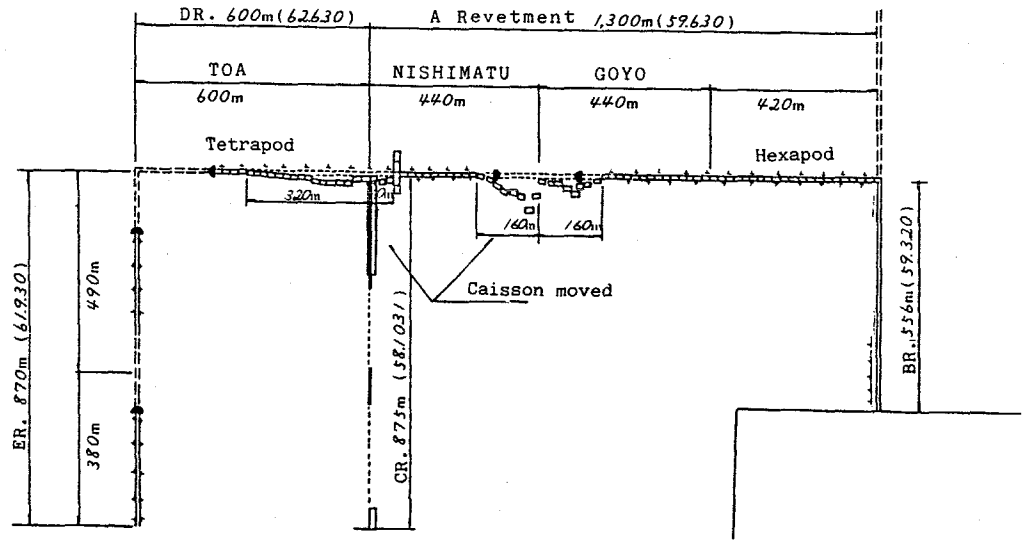

Fig. 8 Plan of the Construction Site of Revetments in which Location of Destructed Caissons is shown.

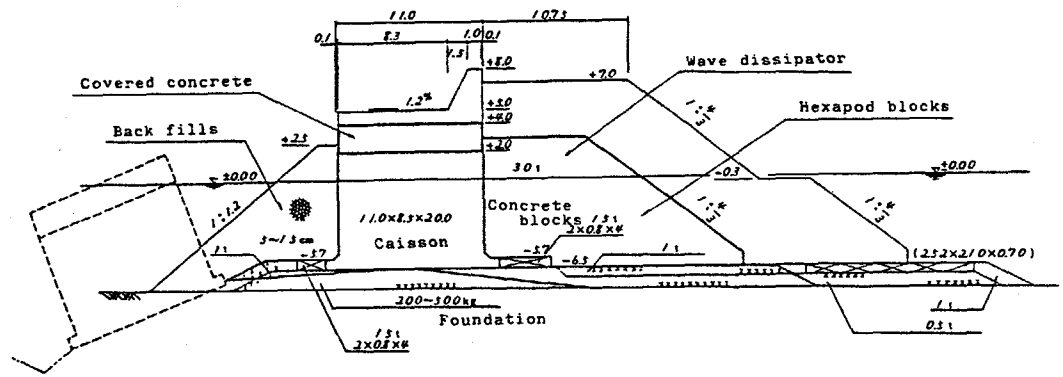

Fig. 9 Cross Section of the Revetment with an Example of Dislocated Caissons.

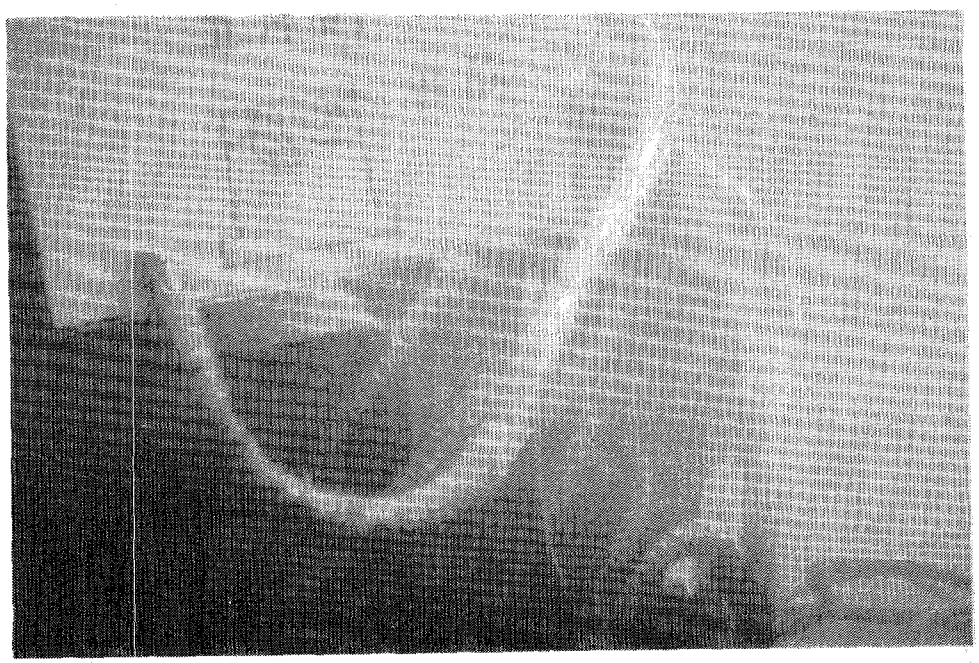

Photo-9 Underwater View of Exposed Ferro-concrete Bars of Reinforcement of a Broken Caisson No. 20. (Courtesy to Nishimatsu Construction Co. Ltd.).

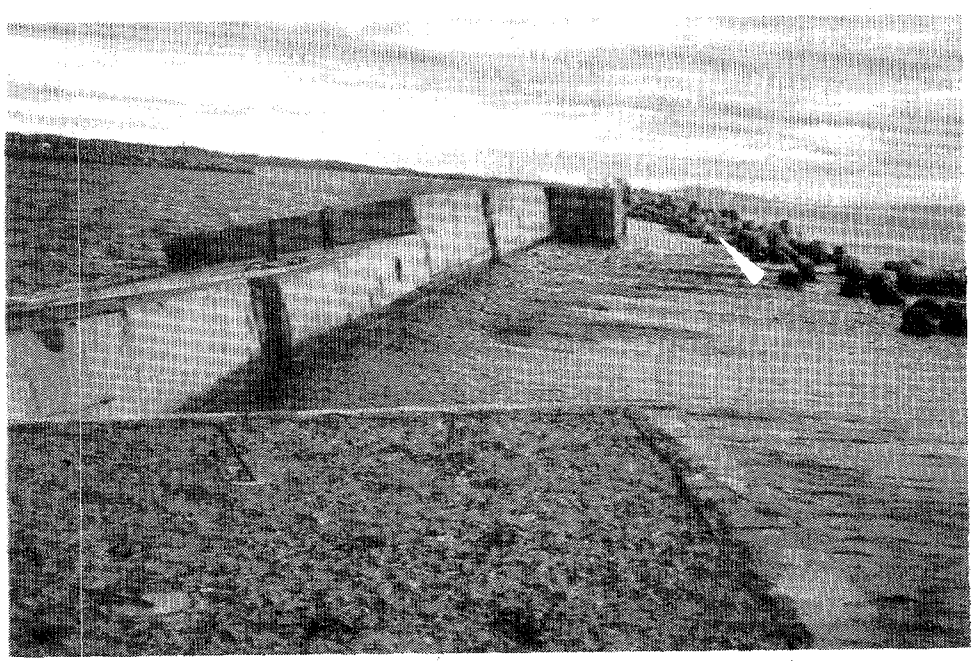

Photo-10 View of a Row of Translated Caissons of the Zone presided by the Toa Construction Co. Ltd. at the Noshiro Harbor.

caissons. In the Nishimatsu Co.Ltd. zone, six were dislocated, one was tilted and four were translated among 26 caissons. In the Toa Co.Ltd. zone,five caissons were tilted, 14 were translated among 20 caissons. It was found that the damage of caissons depended on stages of completion. Suffering was classified as follows.

1. There was no damage on caissons which construction was completed.
2. Tilting, that is minor dislocation within 50 cms and remain still on the foundation, occurred on caissons which had concrete block dissipators on the offshore side, but were not supported by backfill heap on the shoreward side.
3. Dislocation, that is totally dislocated from the base, occurred on caissons which had neither wave dissipater on the offshore side nor backfill support on the shoreward side. The distance of the dislocation was from 10 m to 66 m at the maximum. Divers made pictures of drowned caisson in which bars of reinforcement were exposed and turned as wheat gluten as shown in photo-9. Photo-10 shows the translated caissons.

Messrs. S.Shimada and H.Tanaka,engineers of the Central Research Inst. of the Electric Power Co.Ltd. investigated the safety of the structures. They assumed the tsunami height was 11 m and checked also for the designed wind wave of the height of 5.8 m and the period of 14 sec. Results are abbreviated as follows.

1. Dead weight of the caisson with concrete overlayer to T.P. 5m is 5632 tons and buoyancy force is 2606 tons.
2. Friction resistance is (5632-2606)*0.6=1816 tons.
3. Passive earth pressure with the coefficient of 0.671 is 598 tons.

Then the tsunami force is larger than 1816 tons but smaller than the sum of 2 and 3,that is 2414 tons. The pressure of the wind wave is 2316 tons which is between above two values.

If the tsunami pressure P is assumed by

$$P=CwH \qquad (9)$$

where w is the unit weight of water, H is the wave height and C is the coefficient,above two values give the range of C between 0.77 and 1.03. They also pointed out that the effect of the wave dissipater were very small for the tsunami since these were not dislocated when the caissons were translated remarkably as shown in photo-10.

6. CONCLUSION

Following is the conclusion of this investigation.

a. The tsunami after the Japan sea earthquake was generated by the sea bed deformation due to the low angle adverse dip slip, upheaval in the deep zone and subsidence in the slope of the island.

b. On the Noshiro shelf where the depth are 200-100 meters and there is relatively flat zone of 30 km wide,soliton dispersion was observed. North to and south to the shelf rapid swelling followed to slight depression.

c. Where soliton dispersive waves approached, the wave height increased and broke where the ratio H_b/h_b became the value predicted by Street and Camfield,which was 1.08 for the bed slope of 1/75. Setup by the breaking made the following solitons break nearer to the shore. The dynamic effect is most predominant just before breaking. At Minehama third soliton broke on the shoreline but in Noshiro Harbor second soliton was almost breaking at the construction site. Scattering of hexapods at Minehama and translation and dislocation of caissons in Noshiro Harbor were the results of breaking at each cites.

d. Tsunami warning was effective at Oga Aquarium and lack of warning caused serious disaster on visitors at other places.

e. Life jackets might save people even if they were washed out in the offshore region where the tsunami velocity decreased remarkably. However submarine divers or laborers on offshore structures were in serious situations for evacuation.

f. On the shore,speed of the tsunami front was not so high such that people could evacuate if they run at their most. However since the depth increased very rapidly,they could not withstand and were washed away once they were caught by the front. As soon as the depth got maximum,very

rapid drawdown followed which resulted people were taken away into the sea. Evacuation to the higher place was essential.
g. Design method for the soliton pressure was proposed such that the method for the wind wave could also be applied by taking the pressure coefficient as 1.03.
h. There remained the problem on warning system. Wide and dense distribution of warning teams composed by trained inspectors with handy microphones and walkie talkies who are watching the movement of the sea surface are recommended. Special consideration should be paid for tourists, especially for strangers from countries unfamiliar with tsunamis.

REFERENCE

1) Camfield,F.E., "Tsunami Engineering", Special Rep. no.6, C.E.R.C.,SR-6,1980,pp.80-87.
2) Iwasaki,T.,"The Wave Source of the Designed Tsunami." Proc. of 20th Symposium on Coastal Engineering in Japan., 1973, pp.163-166.(in Japanese)
3) Iwasaki,T.,A.Mano,M.Nagatomi,E.Tomabechi, "On the Hydrodynamic Force of Tsunamis of The Japan Sea Earthquake." Rep. of the Experimental Station for Prevention of Tsunami Disasters,Fac.Engg.Tohoku Univ.1984,pp.27-40 (in Japanese)
4) Iwasaki,T.,"Records on the disaster in the Noshiro Harbor caused by The Tsunami of the Japan Sea Earthquake." Special Issue of the Experimental Station for Prevention of Tsunami Disasters,Fac.Engg.Tohoku Univ. and Goyou Construction Co.Ltd. 1984,pp.1-134 (in Japanese)
5) Li-San Hwang and J.Hammack,"The Japan Sea Central Region Tsunami of May 26,1983,A Reconnaissance Report." Committee on Natural Disasters, Commission on Engineering and Technical Systems, National Research Council,1984,pp.1-29
6) Shimada,S and H.Tanaka,"Report on the Scale of Tsunami and Disasters due to the Japan Sea Earthquake." (draft printing in Japanese)
7)Shuto,N.,"The Nihonkai Chubu Earthquake Tsunami." Special Report, Tsunami Newsletter Dec. 1983,vol XVI,No.2 pp31-40
8)Street,R.L. and F.E.Camfield,"Observations and Experiments on Solitary Wave Deformation." Proc. of Tenth Conf. on Coastal Engineering 1966,pp.284-301.
9)Street,R.L., Chan, R.K.C. and Fromm,J.E., " The Numerical Simulation of Long Water Waves:Progress on Two Fronts." Tsunamis in the Pacific Ocean. ed. by W.M.Adams. Hawaii, 1970, pp.453-473.

THE GREAT WAVES, by Douglas Myles, with foreword by George Pararas-Carayannis. Published by McGraw Hill Book Company, 1221 Avenue of the Americas, New York, NY 10020. $16.96.

The author has documented in very explicit narrative form, the important destructive historic tsunamis throught the world from the beginning of recorded history to the present. He presents the complete recorded accounts of eyewitnesses and inside glimpses of the history of each particular era. Some of the tsunami events described include the Krakatoa tsunami, the Unimak Island and Scotch Cap Lighthouse disaster, as well as the effects of the April 1, 1946, tsunami on Hilo and other parts of Hawaii. The Chile, May 21, 1960, Alaska, March 27, 1964, and various tsunamis in Japan are described. Graphic descriptions of the tsunamis of the seventeenth and eighteenth centuries include the destruction of Port Royal, Jamaica and Lisbon, Portugal. The "ultimate wave" that occurred at Lituya Bay on July 9, 1958, is well documented in this book.

When the author discusses ancient disasters, he becomes more of a journalist and speculates with a very vivid imagination. His attempts to explain the Biblical flood or parting of the Red Sea as tsunami related are interesting reading, but this reviewer is more comfortable with even the divine intervention theory. The author concludes the book with an excellent description of the tsunami warning centers in Hawaii and Alaska. He has high praise for the Palmer observatory computerized data-gathering and analysis systems. The book issues a tsunami warning of its own. The warning is that tsunamis are very likely in the Atlantic and Indian Oceans and that warning systems should be organized for those areas of the world. The author states that worldwide ignorance of tsunamis and their effects is a significant cause of the majority of deaths. We join with the author in hoping that this book may be instrumental in reducing the number of deaths caused by tsunami waves.

Reviewed by Charles L. Mader

TSUNAMIGENIC EARTHQUAKES IN THE PACIFIC AND THE JAPAN SEA

Junji Koyama
Geophysical Institute, Faculty of Science
Tohoku University, Sendai 980 Japan
and
Masahiro Kosuga
Department of Earth Sciences, Faculty of Science
Hirosaki University, Hirosaki 036 Japan

ABSTRACT

A study is made to compare the seismic excitations and tsunami excitations due to submarine earthquakes in the Pacific and the Japan sea. It has been believed that Japan sea earthquakes with high angle of faultings effectively generate tsunamis. Ocean bottom vertical deformation V_s has been calculated from fault parameters of sixteen tsunamigenic earthquakes near Japan. Although tsunami source volume V_t is closely related to V_s, V_t is systematically large for the Japan sea events compared to the Pacific events. This indicates that the effective excitation of tsunamis in the Japan sea side is not completely attributed to the dip angle of faultings. The relatively larger dislocation on the shallow part of faults than that in the Pacific may be a cause of the effective tsunami excitations in the Japan sea. The regional difference in tsunami excitations should be taken into account for the tsunami hazard reduction program, which is shown in this study as large as 1.0 in the tsunami magnitude scale.

INTRODUCTION

In this century there were more than fifty earthquakes in and near Japan that generated tsunamis. Some of the tsunamis were so large that they caused disasters to the coasts of Japan. Although most of these tsunamigenic earthquakes occurred along the deep-sea trenches in the western Pacific, some in the Japan sea also generated large tsunamis (Fig. 1). The latest one was the 1983 Japan sea earthquake of May 26.

Tsunami source volume V_t has been evaluated for Japanese earthquakes from tsunami source area S_t by inverse refraction diagrams and from inundation and/or tide-gauge wave heights by Green's law (Abe, 1973: Hatori, 1984). Considering the seismic moment of the earthquakes, it has been shown that the tsunamis in the Japan sea side are much larger than those in the Pacific for the same size of earthquakes (Abe, 1985: Hatori, 1984: Takemura and Koyama, 1983).

In order to study the physical basis underlying tsunami excitations due to earthquake faultings, we investigate the ocean bottom deformation of each earthquake taking account of fault length and width, average dislocation, dip and slip angles of faulting.

ANALYSIS METHOD

An approximate expression for the volume V_t of displaced water at the tsunami source in terms of earthquake source parameters is

$$V_t = (M_o / \mu) \sin \delta \sin \lambda \qquad (1)$$

where M_o is seismic moment, μ is rigidity at the source, δ and λ are dip and slip angles of the submarine fault plane (Kanamori, 1972a: Kajiura, 1981). Fig. 2 reproduces the results by Hatori (1984) showing the validity of eq. (1). Tsunamigenic earthquakes in the Japan sea also satisfy the relation (1) but their tsunami excitations are by far larger than those in the Pacific. The dip angles δ are large (about 45 to 60 degrees) for the Japan sea events and small (about 15 to 20 degrees) for the Pacific events, thus the different relations in Fig. 2 may be understood from eq. (1) (Fukao and Furumoto, 1975: Takemura and Koyama, 1983).

Sato et al. (1984) showed that the dip angle of faultings by the 1983 Japan sea earthquake, which is the largest event ever recorded in the Japan sea, to be about 20 degrees from the precise hypocenter determination of aftershocks. Therefore, the above understanding is not true for the case of the 1983 Japan sea event. Satake and Abe (1983) re-examined the fault model of the 1964 Niigata earthquake on the basis of crustal deformations by the geodetic survey and ocean bottom deformations

by echo sounding. They are in favor of the low-angle thrust faulting not the high angle reverse faulting for the mechanism of the 1964 Niigata earthquake.

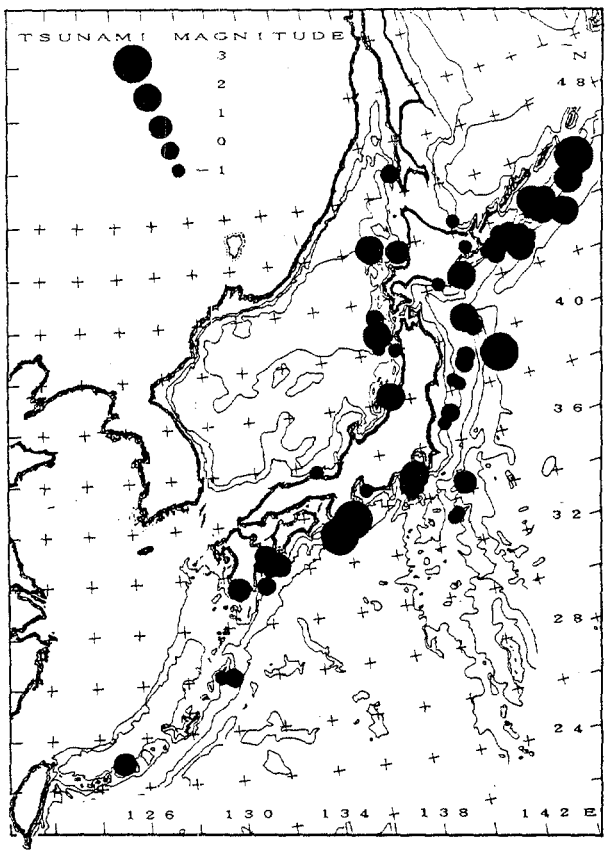

Figure 1 : Tsunamigenic earthquakes near Japan in this century. Tsunami magnitude of each earthquake is illustrated on its epicenter.

The total tsunami energy will be roughly estimated from the potential energy of the water surface disturbance. The latter energy can be computed from the instantaneous ocean-bottom deformation due to earthquake faultings, if the water depth is not so large compared with the size of submarine faults (Takahashi, 1942: Yamashita and Sato, 1974). The ocean bottom vertical deformation due to a dipping finite fault will be given as

$$U_z = \int u_k \, w^z_{kj} \, n_j \, ds \qquad (2)$$

where u_k is the dislocation components on the fault, n_j is the direction cosines of the fault normal, ds is the surface element, and w^z_{kj} is the displacement tensor given in Maruyama (1964). This is used to evaluate the vertical deformation of a surface due to a fault with finite length and width, giving dip and slip angles of the faulting. The above integration is evaluated numerically by dividing the fault plane into 2.0x2.0 km or 5.0x5.0 km elements. For the purpose of comparison with V_t, we calculate the net ocean bottom vertical deformation V_s as

$$V_s = \int |U_z| \, da \qquad (3)$$

where the integration is extended over all the deformed area surrounding the fault. We find that V_s is nearly equal to the square root of $S_t \times \int U_z^2 \, da$, which is a direct measure of potential energy of the tsunami, where S_t is the tsunami source area.

DATA OF EARTHQUAKE PARAMETERS

Table 1 lists the earthquakes whose faulting parameters are estimated from the seismological observations and tsunami source volumes that were obtained by Hatori (1984). Although there are some more earthquakes for which we know the fault parameters from geodetic and/or tsunami observations, we do not include them in the analysis. Five out of sixteen earthquakes occurred in the back-arc Japan sea, which are marked by asterisks in the table. The largest event in the Japan sea is the 1983 Japan sea earthquake of May 26 with M_s of 7.8.

Table 1: List of earthquakes analyzed.

	Year	Place	Length	Width	Dip	Slip	Dislocation
(1)	1933	Off-Sanriku	185km	100km	45	90	5.1m
(2)	1938	Off-Fukushima	75	40	10	80	3.0
(3)	1938	Off-Fukushima	100	60	10	85	2.6
(4)	1938	Off-Fukushima	100	60	10	72	1.8
(5)	1940	Kamui Penin.*	170	50	45	90	0.8
(6)	1944	Tonankai	120	80	10	90	3.5
(7)	1946	Nankaido	120	80	10	90	3.5
(8)	1964	Off-Oga*	50	20	45	90	0.9
(9)	1964	Niigata*	80	30	31	90	3.0
(10)	1968	Off-Tokachi	150	100	20	142	4.1
(11)	1969	E. Hokkaido	180	85	16	90	3.2
(12)	1971	Sakhalin*	70	25	38	90	1.2
(13)	1973	Off-Nemuro	100	60	27	70	2.5
(14)	1978	Off-Miyagi	30	80	20	104	2.9
(15)	1982	Urakawa	30	20	50	70	1.0
(16)	1983	Japan Sea*	30	35	20	60	6.0
			60	40	20	90	4.0

(1): Kanamori(1971a); (2), (3), (4): Abe(1977); (5), (8), (12): Fukao & Furumoto(1975); (6), (7): Kanamori(1972b); (9): Satake & Abe(1983); (10): Kanamori(1971b); (11): Abe(1973); (13): Shimazaki(1974); (14): Seno et al.(1980); (15) Takeo et al.(1982); (16): Kosuga et al.(1984).

Also summarized in Table 1 are faulting parameters used to calculate the ocean bottom vertical deformation from eq. (2). Most of them are estimated from the focal mechanism solutions by P- and S-wave initial motions and/or radiation patterns of mantle surface-waves. The last column indicates the average dislocation on the fault evaluated from seismic moment divided by fault area. In the above calculation the rigidity μ is assumed to be 4.5×10^{11} dyne/cm^2 irrespective to the seismic source regions except for the 1933 Sanriku earthquake, which is believed to have occurred within the Pacific plate (Kanamori, 1971a). This assumption is very important as seen in eq. (1) to evaluate the tsunami excitation from faulting parameters and will be discussed later.

RESULT AND DISCUSSION

The ocean bottom vertical deformation for each earthquake is calculated under the seismological constraints and is illustrated in Fig. 3. We find a close correlation between V_t and V_s for the Pacific earthquakes in a wide dynamic range. However, we also see that the tsunami excitation due to earthquakes in the Japan sea is much larger than that in the Pacific. Since we have considered the dip angle of faults and slip angle of dislocations, the larger excitation of tsunamis can not be completely attributed to the high angle of faultings with small strike-slip component.

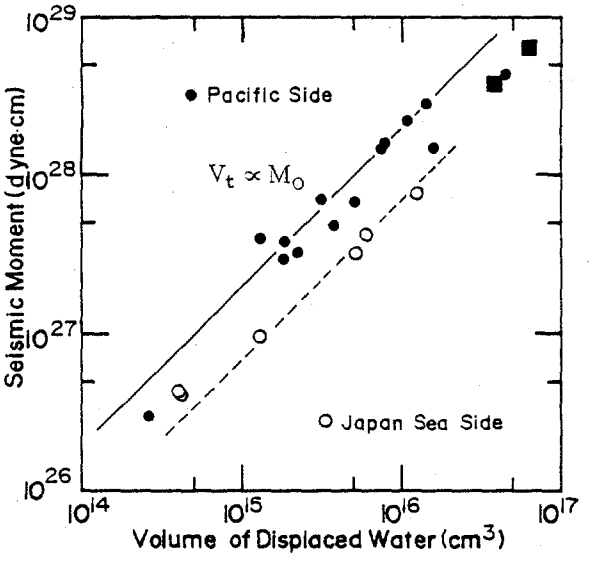

Figure 2: Seismic moment and volume of displaced water at the tsunami source area. Data are quoted mainly from Hatori(1984). Solid and open circles indicate tsunamigenic earthquakes in the Pacific and the Japan sea. Solid squares show tsunami earthquakes of the 1896 Sanriku and 1946 Aleutian earthquakes by Kanamori(1972a).

A mean value of the rigidity in the sources is used to calculate the average dislocation on the faults. Although 5.0 to 7.0 x 10^{11} dyne/cm^2 is usually assumed for the interplate earthquakes in the Pacific and 4.0 to 5.0 x 10^{11} dyne/cm^2 is adopted for the Japan sea events, it is apparent that the difference between the rigidity values does not compensate for the difference in Fig. 3. Therefore, the effective excitation of tsunamis in the Japan sea compared to that of the same seismic-moment earthquakes in the Pacific is not due merely to the large potency by Ben-Menahem and Rosenman (1972) (seismic moment divided by the source rigidity).

The basic assumption to evaluate tsunami excitations is the long-wave approximation. The maximum tsunami height or the inundation level would be in proportion to the largest value of ocean bottom vertical deformations (Ben-Menahem & Rosenman, 1972; Kajiura, 1981; Takahasi, 1942). When the potency of the earthquake and the depth of the fault are unchanged, we observe almost identical V_s values even though the dislocation is not uniformly distributed on the fault but changes as a function of depth. The largest value of the ocean-bottom deformations increases when the dislocation is piled up at the shallow part of the faults. Thus, a large value of water surface disturbances is expected for the pile-up dislocation at the shallow part of the fault.

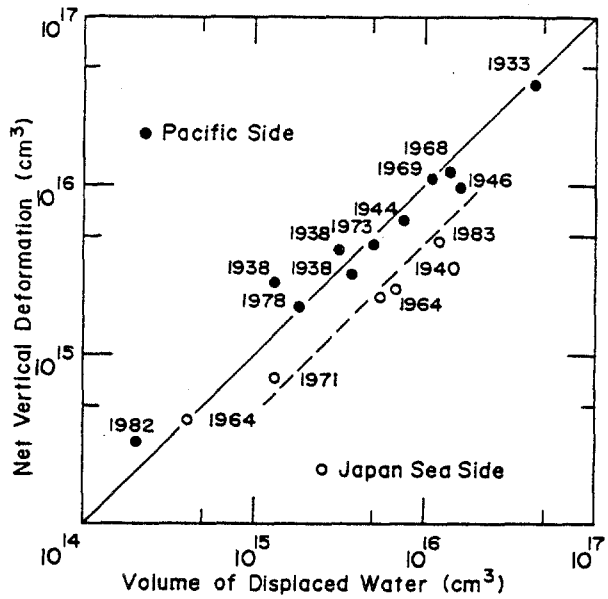

Figure 3 : Total volume of ocean bottom deformation and volume of displaced water at the tsunami source area. Solid and open circles indicate tsunamigenic earthquakes in the Pacific and the Japan sea. Numerals attached to the circles show the year of the events in Table 1.

The above result compromises the fact that the average vertical deformation in the source area is approximately equal to the average wave

height (Abe, 1973; Fukao & Furumoto, 1975) with that the effective tsunami excitation in the Japan sea for the same size of earthquakes. Of course, other models such as a slow slippage on the fault and/or a propagation effect may be considered to explain the effective tsunami excitation. The former would be sensitive to the continuous geodetic measurements, which is sometimes found accompanied by the subduction-zone earthquakes in the Pacific (Kanamori, 1972a; Kasahara & Kato, 1981; Thatcher, 1984). However, the dense and precise geodetic observations on the crustal deformation would not reveal any peculiar characteristics of slow-slippages on the faults in the Japan sea (Fujii, 1976; Noritomi, 1984).

Synthetic mareograms have been made numerically taking into account the complex structures along the coast lines for the 1964 Niigata and 1983 Japan sea earthquakes (Kuniaki Abe, 1978; Satake, 1984). The fault models needed to explain the observations are fairly consistent with the seismological models. This would indicate there is no unusual propagation effect on tsunamis in the Japan sea.

Of course, it would be more realistic to consider that some combinations of the effects mentioned above in addition to the pile-up dislocations on the shallow part of faults are responsible for the effective excitation of tsunamis in the Japan sea.

It is expected that the young subduction-zone and intraplate earthquakes would be under the strong-coupling of slipping planes. Strain energy release in such case would be much easier on the shallower part of the fault rather than extending faults deep into the crust and the mantle. Earthquakes along the deep-sea trenches in the subduction-zones would be a stick-slip faulting on a pre-existing fault plane. The latter would extend the faulting deep into the mantle. Precise hypocenter-determination of aftershocks of large earthquakes supports the above suggestion (Sato et al., 1985).

There is a large regionality in the tsunami excitation which is as much as 1.0 in tsunami magnitude scale even for the same size of earthquakes. This should be involved in the tsunami hazard reduction program for the precise prediction of tsunamis from the seismological data.

Acknowledgement

We would like to thank Dr. Y. Izutani of Shinshu University for his stimulative discussions.

References

Abe, Katsuyuki (1973). Tsunami and mechanism of great earthquakes, Phys. Earth Planet. Inter., 7, 143-153.

Abe, Katsuyuki (1977). Tectonic implications of the large Shioya-oki earthquakes of 1938, Tectonophysics, 41, 269-289.

Abe, Katsuyuki (1985). Quantification of major earthquake tsunami of the Japan sea, Phys. Earth Planet. Inter., 38, 214-223.

Abe, Kuniaki (1978). Determination of the fault model consistent with the tsunami generation of the 1964 Niigata earthquakes, Marine Geology, 1, 313-330.

Ben-Menahem, A. and M. Rosenman (1972). Amplitude patterns of tsunami waves from submarine earthquakes, J. Geophys. Res., 77, 3097-3128.

Fujii, Y. (1976). Pre-slip as forerunner of earthquake occurrence, Symp. Earthq. Predct. Res., 127-137.

Fukao, Y. and M. Furumoto (1975). Mechanism of large earthquakes along the eastern margin of the Japan sea, Tectonophysics, 26, 247-266.

Hatori, T. (1984). Sea-level disturbance at the source area of the 1983 Nihonkai-Chubu tsunami- Relation between volume of the displaced water and seismic moment, Zisin II, 37, 23-29.

Kajiura, K. (1981). Tsunami energy in relation to parameters of the earthquake fault model, Bull. Earthq. Res. Inst., 56, 415-440.

Kanamori, H. (1971a). Seismological evidence for a lithospheric normal faulting - The Sanriku earthquake of 1933, Phys. Earth Planet. Inter., 4, 289-300.

Kanamori, H. (1971b). Focal mechanisms of the Tokachi-oki earthquake of May 16, 1968: Contortion of the lithosphere at a junction of two trenches, Tectonophysics, 12, 1-13.

Kanamori, H. (1972a). Mechanism of tsunami earthquakes, Phys. Earth Planet. Inter., 6, 346-359.

Kanamori, H. (1972b). Tectonic implications of the 1944 Tonankai and the 1946 Nankaido earthquakes, Phys. Earth Planet. Inter., 5, 129-139.

Kasahara, K. and T. Kato (1981). Aseismic faulting following the 1973 Nemuro-oki earthquake, Hokkaido, Japan (a retrospective study), PAGEOPH, 11, 392-403.

Kosuga, M., T. Sato, K. Tanaka and H. Sato (1984). Aftershock activities and fault model of the Japan sea earthquake of 1983, Sci. Rep. Hirosaki Univ., 31, 55-69.

Maruyama, T. (1964). Statical elastic dislocations in an infinite and semi-infinite medium, Bull. Earthq. Res. Inst., 42, 289-368.

Noritomi, K. (1984). Strain and tilt observations, General Rep. 1983 Japan Sea Earthq., 31-35.

Satake, K. (1984). The mechanism of the 1983 Japan sea earthquake as inferred from long-period surface waves and tsunamis, Phys. Earth Planet. Inter., 37, 249-260.

Satake, K. & K. Abe (1983). A fault model for the Niigata, Japan, earthquake of June 16, 1964, J. Phys. Earth, 31, 217-223.

Sato, T., M. Kosuga, K. Tanaka and H. Sato (1984). Aftershock distribution of the Japan sea earthquake, 1983: Redetermination of hypocenters by an inclined structure model, Tohoku Disas. Sci., 20, 1-6.

Seno, T., K. Shimazaki, P. Sommervill, T. Eguchi, and K. Sudo (1980). Rupture process of the Miyagi-oki, Japan, earthquake of June 12, 1978, Phys. Earth Planet. Inter., 23, 39-61.

Shimazaki, K. (1974). Nemuro-oki earthquake of June 17, 1973: A lithospheric rebound at the upper half of the interface, Phys. Earth Planet. Inter., 9, 314-327.

Takahasi, R. (1942). On the seismic sea waves caused by deformation of the sea bottom, Bull. Earthq. Res. Inst., 20, 357-400.

Takemura, M. and J. Koyama (1983). Seismic source spectrum of tsunami and ordinary earthquake: A quatitative estimation of tsunami from forecoming seismic waves, Tohoku Geophys. J., 29, 115-128.

Takeo, M., M. Kasahara and K. Abe (1982). Focal process of the Urakawa-oki earthquake of March 21, 1982, General Rep. Urakawa-Oki, Japan, Earthq. March 21, 1982, 1, 1-12.

Thatcher, W. (1984). The earthquake deformation cycle at the Nankai trough, southwest Japan, J. Geophys. Res., 89, 3087-3101.

Yamashita, T. and R. Sato (1974). Generation of tsunami by a fault model, J. Phys. Earth, 22, 415-440.

COMPARISON OF OBSERVED AND NUMERICALLY CALCULATED HEIGHTS OF THE 1983 JAPAN SEA TSUNAMI

Yoshinobu TSUJI
Earthquake Research Institute,
the University of Tokyo
1-1-1, Yayoi, Bunkyou-ku, Tokyo, 113 Japan

ABSTRACT

Earthquake-Tsunamis frequently outbreak in the north east part of the Japan Sea. Among these tsunamis, the Japan Sea Earthquake-Tsunami of 1983 (M = 7.7, tsunami magnitude m = 2.5, after Hatori,1983), the Kamuimisaki-Oki Earthquake Tsunami of 1940 (M = 7.5, m = 3), and the Kampo Earthquake-Tsunami of 1741 (M = 7.5, m = 3) are discussed. Damages of these big tsunamis have been recorded not only on the coast close to their epicenters, but also on the far coasts, for example , on the coasts of Noto Peninsula, Oki Islands and on the east coasts of the Korean Peninsula. Minute survey of inundation height of the 1983 Japan Sea tsunami was made along the coast of the Japanese Islands and of the southern part of the Korean Peninsula.

On the other hand, sea bottom deformation due to the earthquake was estimated on the basis of the data of distributions of aftershocks, stress drops, initial movement of tsunami records, and land surveying along the coasts. And moreover, the magnetic tape of sea bottom topography of the Japan Sea with grid intervals of 3 minutes was compiled by the Hydrographic Department of the Maritime Safety Agency of Japan, and so the numerical calculation of the propagation of the tsunamis for the Japan Sea area have become possible.

In the present study, we discuss the distribution of height of these tsunamis and the results of the numerical calculations for them.

1. Introduction

In the area off the west coasts of the northern part of the Honshu and Hokkaido Islands, 21 tsunamis were recorded (Table. 1). Earthquake-Tsunamis outbroke only in a narrow strip of sea area which runs along the the north part of the Japanese Islands. They frequently outbroke within the periods of 1741 through 1834, and after 1939, and no tsunami occurred during 1614 to 1740, and 1834 to 1938. The reason on such a deviation of frequency is not clear.

In the present study, we discuss on the distribution of tsunami inundation height of the 1983 Japan Sea Tsunami with the numerical calculation. We also discuss on the 1940 Kamuimisaki-Oki and the 1741 Kampo Tsunamis.

2. The 1983 Japan Sea Earthquake-Tsunami (1983 V 26, M = 7.7, m = 2.5)

2.1 Inundation height and damages

Damages of human beings and properties caused by the 1983 Japan Sea Earthquake-Tsunami in Japan and South Korea are listed in Table 2. Just 100 persons were killed by the tsunami and 4 persons were killed due to the earthquake in Japan. Prominent damages were done on the west coasts of Hokkaido Island, Aomori and Akita Prefectures. The coasts of Shimane Prefecture, and of the Korean Peninsula, which are 700km to 1,000 km apart from the origin, are also badly damaged. One person was killed at Donghae City and two persons were lost at Imweon Port in Samcheok Town in Gangweon-Do Province in South Korea due to the tsunami.

Just after the occurrence of the earthquake-tsunami, survey researches of traces and witnesses were made by scientists and engineers of universities and institutes, and several kinds of reports were published. Inundation height of the tsunami was measured at more than 600 points on the Japanese coast in total, and surveyed area covers almost all the coasts facing to the Japan Sea in Japanese side.

Fig. 2 shows the general map of the distribution of tsunami height. Tsunami height of 14.93m above the level of Tokyo Pale (T.P., the standard level of land maps in Japan), at Minehama Village in the northern part of Akita Prefecture was mentioned in the report of the Public Work Research Institute(1985), and it is the maximum record of the present tsunami. We should notice that, except the coast close to the origin, eminent peaks also exist at several places; the tip of Shakotan Peninsula on Hokkaido, the northern point of Sado Island, the outside coasts of Noto Peninsula, Oki Islands in Shimane Prefecture, and Imweon Port and its vicinity on the east of the Korean Peninsula. Oki Islands and the east coast of Korea are located about 700km and 1,000km far from the tsunami origin, respectively.

Figs. 3, 4, and 5 show the detailed distribution of tsunami height for coasts of Hokkaido Island, northern part of Honshu Island, and western part of the Japanese Islands, respectively.

Baek(1983), the chief of the statistical section of the Central Meteorological Observatory of Korea, reported the distribution of tsunami height and the statistics of the damages in South Korea (Table 2 and Fig. 6). A prominent peak appears at

Imweon Port, Samcheok Eup(Town) of Gangweon-Do, where tsunami height of 3.6-4.0 meters was measured by the trace of sea water on the outside wall of buildings.

No information has come from the northern part of the Korean Peninsula and few articles of information have been obtained for the coast of USSR till end of October of 1985.

2.2 Numerical calculation

Tsunami source area was estimated by Hatori(1983), and it has the size of 90km in WE and 140km in NS directions (Fig.7). Initial sea bed deformation was suggested by Aida(1983) as Fig. 8. He regarded the movement as dislocations of two faults, and decided the parameters of them so as to the observed data of the distributions of aftershocks, stress drop, results of upheaval/subsidence of land, initial motion of the tsunami agree well to the idealized faults that he suggested. Fig. 8 shows the sea bottom deformation calculated for the model faults.

Magnetic tape with sea bottom topography of the Japan Sea with grid intervals of 3 minutes in both WE and NS directions had been compiled by Hydrographic Department, Maritime Safety Agency of Japan. We regarded the point (39°N, 139°E) as the center of the Japan Sea, and assumed the tangential plane of the Earth at the point. Each grid point was projected on the plane and a grid mesh with size of 252x311 in intervals of 5x5km was newly set on the plane, and numerical calculation was made.

Influences of the rotation of the Earth, surface curvature of the Earth, viscosity of sea water, friction at sea bottom, non-linear terms of the equation of motion, and dispersion of wave were neglected.

As we can not well simulate the behavior of wave in shallower sea region by using such a single mesh, and so sea area with depth of less than 200 meters was replaced with sea of 200 depth (Fig. 9). We also assumed that wave is perfectly reflected at the coastline. Calculation was made in finite difference method with time step of 12 second for 2hours 40 minutes of actual situation. In order to check whether the calculation was reasonably proceeded or not, we made calculation of the total mass, kinematic and dynamic energies every 50 steps and confirmed that the value was holding steady.

Fig.10 shows the result of the calculation. Bars in graphs show the maximum height of tsunami, which is experienced at each coastal grid till the end of the calculation. One mesh interval of each graph is 50cm. Tsunami height for smaller islands is shown with bars on the middle column.

We can recognize that the distribution pattern of tsunami height is generally well simulated in the following points.

i. The Maximum peak exists at the north part of Akita Prefecture.
ii. A peak exists at the southern tip of Hokkaido Island.
iii. Higher tsunami was calculated on Okushiri Island than on the mainland of Hokkaido.
iv. A sharp peak appears at the north tip of Sado Island.
v. Tsunami was low around the coast of Toyama Bay.
vi. Eminent peak appears outside coast of Noto Peninsula.

vii. Gently-sloping peak exists at Oku-Tango Peninsula.
viii. High tsunami was simulated at Oki Islands, in spite of long distance (about 700km) from the origin.
ix. Eminent peak appears at Imweon Port on the Korean Coast.
x. Tsunami height around the port of Pusan, the south-east corner of the Korean Peninsula, was very small.

As the influence of amplification of tsunami in shallower sea region is not taken into account, the absolute value of tsunami height is not agree with the observed one. The latter is about 3 to 6 times of the former. We make consideration on the influence of amplification in the shallower sea region on the next section.

2.3 Amplification of tsunami height on continental shelf region

As we used the calculation mesh without shallower slope of continental shelf region, the effect of amplification of tsunami wave was not taken into account in the simulation, and absolute value of tsunami height of calculated result is so small as one third to one sixth of the observed height (Fig. 2 and Fig. 10). Shuto(1972) gave the amplification formula under the condition that the depth changes linearly on the slope, deeper sea is flat and have a uniform depth, and the incident wave is stationary and sinusoidal. We assume that tsunami height at the outside boundary of the shelf is a, and run-up height at the coast is R, then the formula is as follows,

$$R/a=2\left\{J_0^2\left(\frac{4\pi L}{\sqrt{gD}\,T}\right)+J_1^2\left(\frac{4\pi L}{\sqrt{gD}\,T}\right)\right\}^{\frac{1}{2}} \qquad (1)$$

where, L, T, and D are length of slope, period of wave, and depth at outside boundary of slope, respectively. The condition which Shuto assumed, and that of approaching of tsunami wave to the coast is different each other, and therefore, strictly speaking, we can not always justify in applying the formula to the amplification of tsunami. But Kinoshita et al.(1984) showed that the formula also gives good agreement in estimation of amplification of tsunami in the shallower sea region.

If we put L = 0 in formula (1), then a/R converges to 2, which means that in the case that the length of slope is zero, the incident wave would be reflected perfectly, and sea water would climb up to the height of twice of the amplitude of the incident wave, which is just of the condition of our simulation. We write the ratio of net amplification R/2a as r. Relationship between slope length L and r for wave period T = 5, 7, 10, 15, and 20 minutes is shown as Fig.11.

In actual topography of the coasts facing to the Japan Sea, the length of shelf L is about 10 to 30km in general. We can recognize that the superior period of the tsunami is 7 to 10 minutes and therefore, it is reasonable that actually observed tsunami height is three to sixth times of the calculated height of our simulation(Fig. 12).

2.4 Effect of Yamato Rise

In the center of the Japan Sea, there is an eminent table shaped sea region called "Yamato Rise", the top of which is about

300 meters and depth of the surrounding sea is about 3,000 meters. It has the size of 300km and 150km in WE and NS directions, respectively. Prominent peaks at Oki Island, Shimane Peninsula in Japan, and at Imweon Port on Korean coast in the distribution of observed tsunami height (Figs. 2 and 6) and calculated one (Fig.10) appear just near at the counter point of the tsunami source as the rise to be the center. Giving a glance at these figures, we are apt to jump to the conclusion that the rise took a role of a lens on the propagation of the tsunami (Miyoshi, 1984, Tsuji et al., 1984). Kang et al.(1985) made calculation of the refraction diagram by using Ippen(1966)'s method(Fig. 13), and pointed out that rays would be converged at Oki Island, Shimane Peninsula, and the coast of Gangweon-Do, in the Korean Peninsula due to the existence of the Yamato Rise.

In order to verify whether the idea hold good or not, we made numerical calculation once more with removing the rise and replaced by the sea region with 3,000 meters depth. Then, we obtained the result as Fig. 14. Tsunami height on the east coast of the Korea became higher than in the case of the rise present. As for the lens effect of the rise, we can not make a quantitative verification, and there is much left to discuss.

2.5 Calculation with simplified initial sea bed deformation

As the distribution of the initial sea bed deformation suggested by Aida(1984, Fig. 8) was decided on the basis of many kind of seismological and hydrographical data, any of which were obtained as a result of much of efforts offered by many seismologist and oceanologist who had made fine networks of observation stations of various kind. We can not always hope to get such a blessed condition to decide parameters of fault accurately as the present case. If we had no information of the distribution of the initial sea bed deformation except the location and general outline of the source, can we not make numerical calculation of tsunami propagation any more? Is it impossible to make reasonable numerical calculations for any historical tsunamis?

In order to make clear the validity of numerical calculation of this kind for such case that the information on the initial sea bed deformation is not blessed, we made another numerical calculation under the condition that the initial deformation is simplified as Fig.15 with maximum deformation = 2m.

The result is shown as Fig. 16. Comparing it with Fig. 10 we can recognize that the pattern of the distributions of the calculated results very much resembles each other except on the coast close to the tsunami source region. We can simulate the general pattern of the tsunami distribution for almost all parts of coasts around the Japan Sea even if we assume the initial sea bed deformation to be simplified as Fig. 15.

3. Kamuimisaki-Oki Earthquake-Tsunami (1940 VIII 2, M = 7.5, m = 2)

Kamuimisaki-Oki Earthquake outbroke at 0h08m (JST) of 2nd August, 1940 (15h08m of 1st in GMT) in west off sea region of Hokkaido Island, and tsunami with height of 2-3m hit the west

coast of it. Ten persons were killed at the river mouth of the Teshio River. Tsunami with 1-2m was also recorded on Sakhalin Island, and at several points on Honshu Island. Recently, descriptions of this tsunami of Korean side coast was found out (Baek, 1983, Tsuji et al.,1984), and we can make the map of the distribution of tsunami height around the Japan Sea as Fig. 17. It should be noticed that rather high tsunami with 1.5-2m observed at Oki Islands, Uljin and Samcheok Ports on the east coast of Korea. Imweon Port, where the maximum height was recorded on the Korean Peninsula for the 1983 Japan Sea Tsunami, is situated between Uljin and Samcheok Ports.

We assumed the initial sea bed deformation simplified as Fig. 15, and made numerical calculation. The result is shown as Fig. 18. Peaks of the distribution of height of the tsunami at several far points, for examples, Oki Islands, Uljin Port on the Korea are well simulated.

4. Kampo Earthquake-Tsunami (1741 VIII 29, M = 7.5, m = 3)

On the south-west tip of Hokkaido, 1,467 persons were killed due to the 1741 Kampo Tsunami, and Hatori et al.(1977) estimated the height at the coast about 9-15 meters. Several persons were also killed in Aomori Prefecture, the northern most district of Honshu Island. Tsunami was also recorded at Sado Island, outside coast of Noto Peninsula, and at Obama City, about 50km north of Kyoto. Recently, a Korean side record of this tsunami was found out in the diary of the Choseon Dynasty (Tsuji et al., 1984).

The old document mentioned that houses were swept and vessels were destroyed on the coasts of Gangweon-Do Province. The source area and distribution of tsunami height is shown as Fig. 19.

The result of numerical calculation of this tsunami with assuming the maximum sea bed deformation as 2m was shown as Fig. 20. Higher peaks at Sado Island, Noto Peninsula on Honshu Island, and Gangweon-Do Province on Korean Peninsula are well corresponded with the recorded ones.

5. Discussion and conclusion

Comparing the distribution patterns of the height of the observed or recorded three tsunamis with the result of the numerical calculations, we might conclude as follows;

i) There are several specific coasts where tsunami height becomes higher than the neighbouring coasts whenever the tsunami source might be located at any sea area in the north-east part of the Japan Sea. Sado Island, outside coast of Noto Peninsula, Oki Islands, Shimane Peninsula in Japan, and some area of the coast of Gangweon-Do Province in Korea are the examples of such specific coasts.

ii) Several ten percent of those "specific coasts" are the coasts having the shape of top of peninsula with protruding in the direction to the tsunami source region.

iii) Pattern of the distribution of tsunami height can be simulated with calculation using the 5x5km grid mesh in which the shelf slope region was replaced into sea of 200 m depth. If we consider the effect of amplification on the shelf region, we

might give rather good estimation by using Shuto's formula.

iv) Except the coast close to the source, the pattern of distribution of tsunami height can be also well simulated by the simplified sea bed deformation model shown as Fig. 15.

v) We should be prudent to give explanation on the of tsunami energy with so called "lens effect".

vi) If we wish to make explanation more local pattern of distribution of tsunami height, it is necessary to use finer mesh for shallower sea region. Then, we could discuss sharp concentration of tsunami energy.

6. Acknowledgment

The present study was begun as a part of the comprehensive research on the 1983 Japan Sea Earthquake-Tsunami, which was sponsored by the Science and Technology Agency of Japan. The present author wishes to express his thanks to Mr. T. Konishi, the officer of the Oceanographical Division of Marine Department, Japan Meteorological Agency, who gave me many helpful suggestions, and also to Dr. T. Kinoshita, the chief of the first research division of the National Research Center for Disaster Prevention for his active support.

REFERENCES

Aida, I., 1984, A source Model of the tsunami accompanying the 1983 Nihonkai-Chubu Earthquake, Bull. Earthq. Res. Inst. 59, 93-104 (in Japanese).

Baek, W. S., 1983, Report of the 1983 Tonghae (Japan Sea) Earthquake-Tsunami, Central Meteorological Agency, Republic of Korea, pp69 (in Korean).

Hatori, T. and M. Katayama, 1977, Tsunami behavior and source areas of historical tsunamis in the Japan Sea, Bull. Earthq. Res. Inst., 52, 49-70 (in Japanese).

Hatori, T., 1979, Religious Monuments of the Oshima Tsunami in 1741, west Hokkaido, Bull. Earthq. Res. Inst., 54, 343-350 (in Japanese).

Hatori, T., 1983, Tsunami magnitude and source area of the Nihonkai-Chubu (the Japan Sea) Earthquake in 1983, Bull. Earthq. Res. Inst. 58, 723-734 (in Japanese).

Hatori, T., 1984, Reexamination of wave behavior of the Hokkaido-Oshima (the Japan Sea) Tsunami in 1741, -Their comparison with the 1983 Nihonkai-Chubu Tsunami-, Bull. Earthq. Res. Inst., 58, 723-734 (in Japanese).

Ippen, A. T., 1966, Estuary and coastline hydrodynamics, McGraw-Hill, New York.

Japan Meteorological Agency 1984, Report on the Nihonkai-chubu Earthquake, 1983 (The Mid-Japan Sea Earthquake,1983), Report of JMA, 106, pp252.

Kang, S. W. et al., 1985, A study on marine forecasting system for disaster prevention in Korea(I), Korean Ocean Res. and Development Inst., pp317 (in Korean).

Kinoshita, T., T. Konishi, Y. Tsuji, 1984, Magnification factor for tsunami risk evaluation, Report of National Res.

Center for Disaster Prevention, 33,15-22 (in Japanese).
Kinoshita, T., S. Kumagai, Y. Tsuji, N. Ogawa, N. Numano, O. Abe, and T. Konishi, 1984, Survey research report of the disaster of the Nihonkai-Chubu Earthquake, Principal Disaster Report 23, NRCDP, pp164 (in Japanese).
Miyoshi, H., 1984, General discussion: The Nihonkai-Chubu Earthquake-Tsunami, Kaiyoukagaku, 16, 9, 490-495.
Public Work Research Institute, 1985, Report on the disaster caused by the Nihon-kai-chubu Earthquake of 1983, Report of PWRI, 165, pp346 (in Japanese).
Shuto, N., 1972, Standing waves in front of a sloping dike, Coastal Engineering in Japan, 15, 13-23.
Tanimoto, K., T. Takayama, K. Murakami, S. Murata, K. Tsuruya, S. Takahashi, M. Morikawa, Y. Yoshimoto, S. Nakano, and T. Hiraishi, 1983, Field and laboratory investigations of the Tsunami caused by 1983 Nihonkai Chubu Earthquake, Tech. Note of the Port and Harbor Res. Inst., 470, pp299.
Tsuji, Y., T. Konishi, K. Kinoshita, N.Numano, and O. Abe, 1984, Survey sheets of the heights of the tsunami caused by Nihonkai-Chubu Earthquake, 1983, Review of Res. for Disaster Prevention, 87, NRCDP, pp306 (in Japanese).
Tsuji, Y., W. S. Baek, K. S. Chu, H. S. An, 1985, Report of the Nihonkai Chubu Earthquake Tsunami along the East Coast of the Republic of Korea, Review of Res. for Disaster Prevention, 90, NRCDP, pp96.

Table 1. List of earthquake-tsunamis in Japan Sea.

No	Date	Earthquake Magnitude	Epicentre lati. N	Epicentre long. E	Tsunami Magnitude	Remarks
1	850 ? ?	7.0	39.1°	140.0°	2	Yamagata Prefecture
2	887-VIII-2	6.5	37.5.	138.1	2	several thousands killed
3	1092-IX-13	-	"	"	"	uncertain
4	1341-X-31	"	"	"	"	Tsugaru Pen.. Aomori Pref
5	1614-XI-26	7.7	37.5.	138.0	2	uncertain
6	1741-VIII-29	7.5	41.5.	139.4	3	about 1,500 killed. see text
7	1762-X-31	6.6	38.1.	138.7	1	26 houses washed
8	1766-III-8	6.9	40.8.	140.6	-	in Mutsu Bay. Aomori Pref.
9	1792-VI-13	6.9	43.6.	140.3	2	near Shakotan Pen. Hokkaido
10	1793-II-8	6.9	40.7.	140.0	1	Tsugaru Pen.. Aomori Pref.
11	1804-VII-10	7.1	39.0.	140.0	1	Kisakata. Yamagata Pref.
12	1810-IX-25	6.6	39.9	139.9	1?	Oga Pen.. Akita Pref.
13	1833-XII-27	7.4	38.7.	139.2	2	off Yamagata Pref.
14	1834-II-9	6.4	43.3.	141.4	-	Isikari. Hokkaido
15	1939-V-1	7.0	40.0.	139.8	-1	Oga Pen.. Akita Pref.
16	1940-VIII-2	7.5	44.1.	139.5	2	10 killed. see text
17	1947-XI-4	7.0	43.8.	141.0	1	off Rumoi. Hokkaido
18	1964-V-7	6.9	40.3.	139.0	1	off Aomori Pref.
19	1964-VI-16	7.5	38.4.	139.2	2	"Niigata Earthquake"
20	1983-V-26	7.7	40.4.	139.1	2.5	"Nihonkai Chubu Earthquake"
21	1983-VI-21	7.0	41.3.	139.2	0	largest aftershock of No 20

Fig. 1 Locations of the Earthquake-Tsunamis listed in Table 1.
○...M ≥ 7.0. ○...M ≤ 6.9.

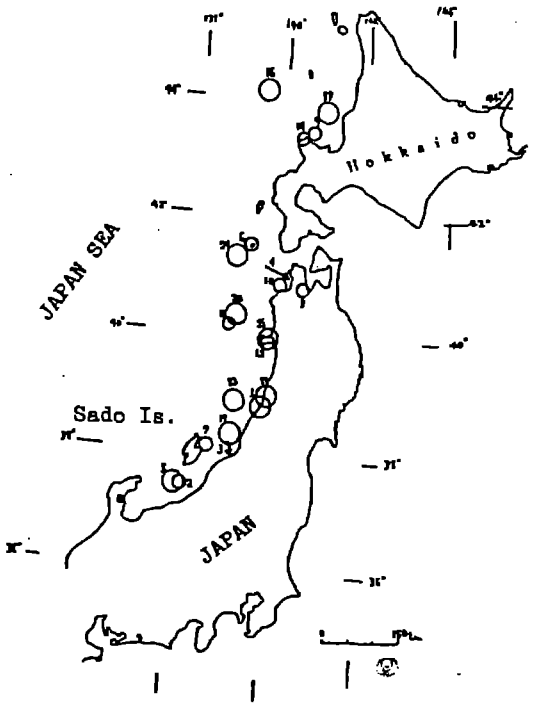

Table 2. Statistics of damages of the Nihonkai-Chubu Earthquake Tsunami After National Land Agency, Japan and Central Meteorological Observatory, Republic of Korea.

country	Japan						Korea
prefecture/ province	Hokkaido	Aomori	Akita	Shimane	other prefectures	total	Gangweon-Do Kyeongsangbug Do
persons							
killed	4	17	83	0	0	104	1
lost	0	0	0	0	0	0	2
injured	24	25	265	5	5	324	2
damaged houses							
entirely & swept	5	447	1,132	0	2	1,584	1
partially	16	865	2,622	0	2	3,505	0
slightly	69	3,108	2,867	0	0	5,954	22
submerged							
above floor	27	62	65	141	3	298	
below floor	28	152	277	277	8	742	19
damaged vessels	637	853	681	319	161	2,651	81

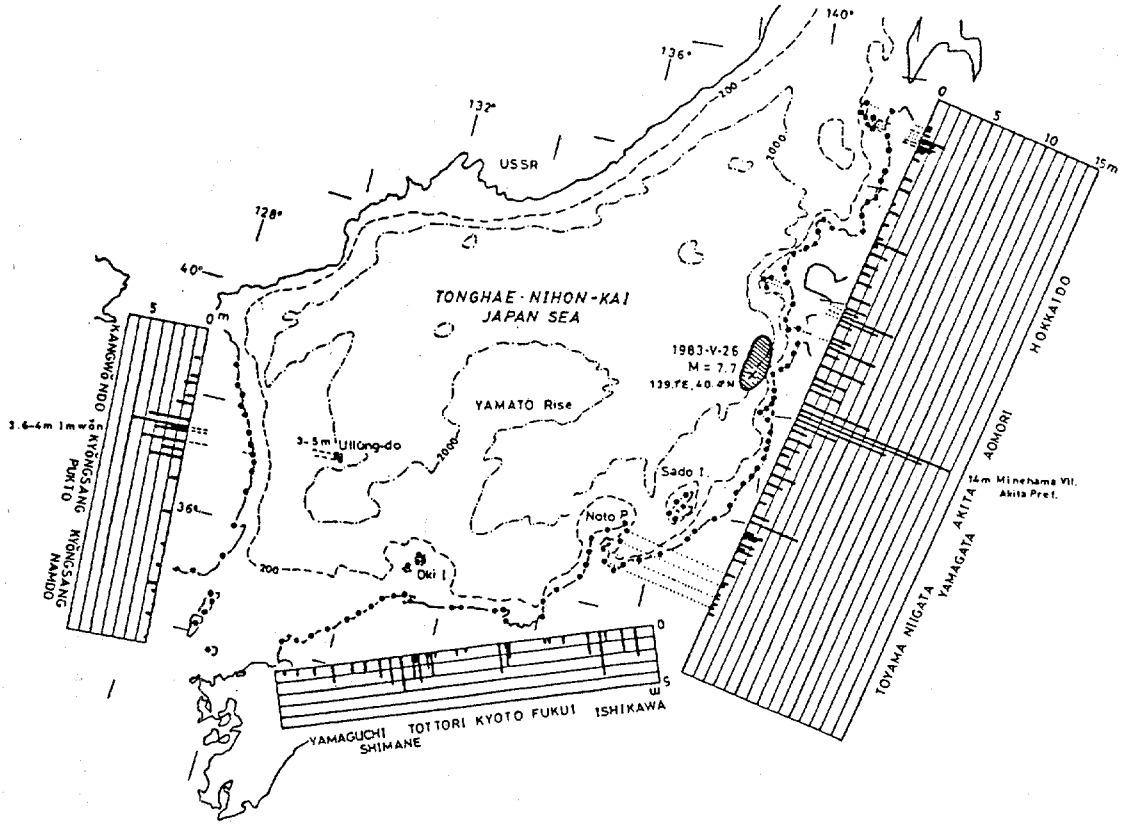

Fig. 2 Schematic distribution of inundation height of the Nihonkai-Chubu Earthquake-Tsunami of May 26th, 1983.

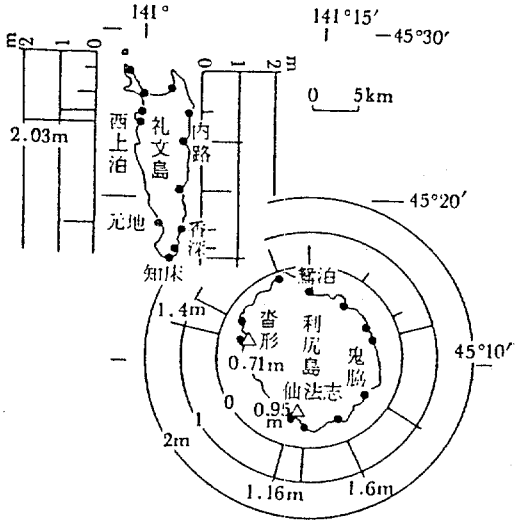

Fig. 3-a Detailed map of Rishiri and Rebun Islands.

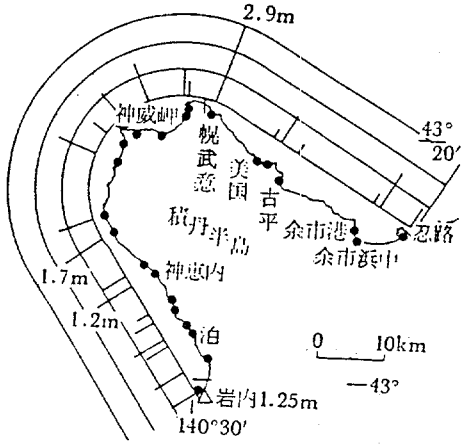

Fig. 3-b Detailed map of Shakotan Peninsula.

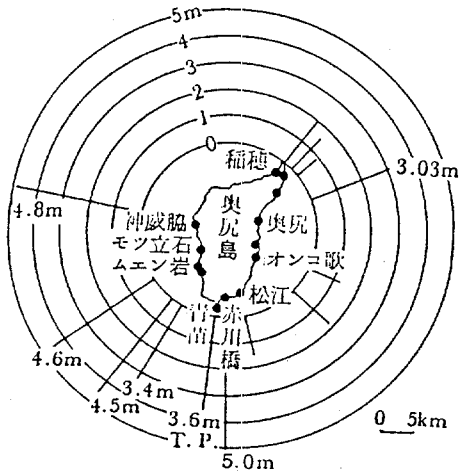

Fig. 3-c Detailed map of Okushiri Island.

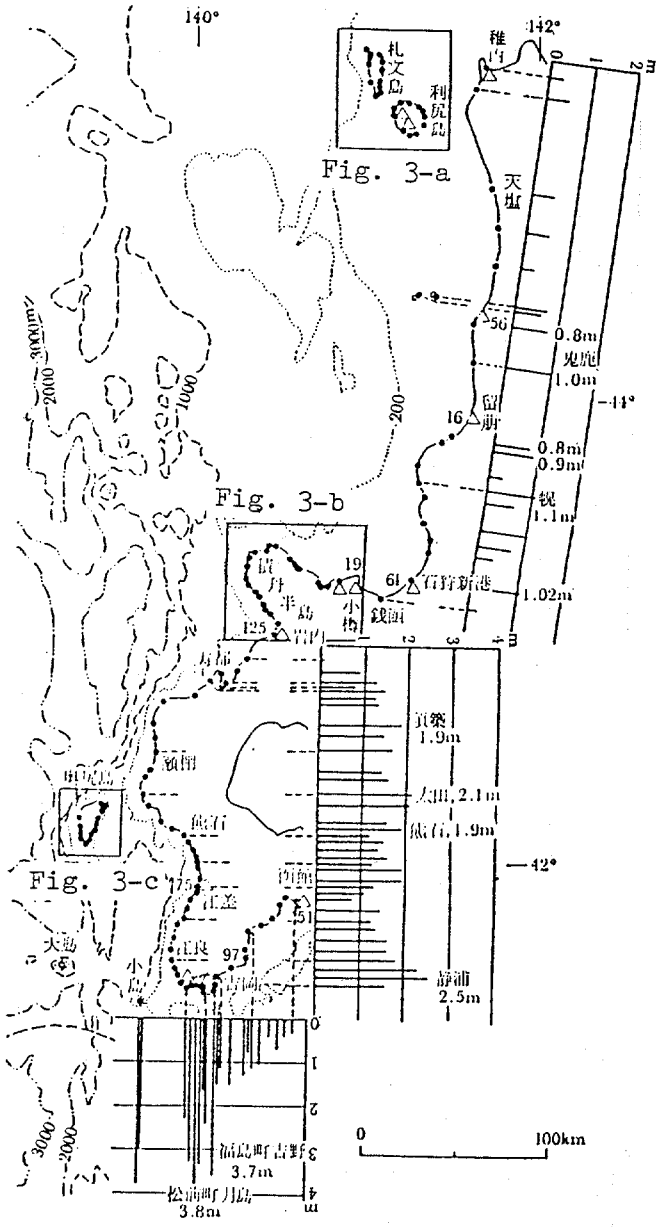

Fig. 3 Distribution of inundation height of the Nihonkai-Chubu Earthquake-Tsunami along the west coasts of Hokkaido Island.

Black circles show the locations of the measured points, and triangles show tide gauge station with tsunami height(cm).

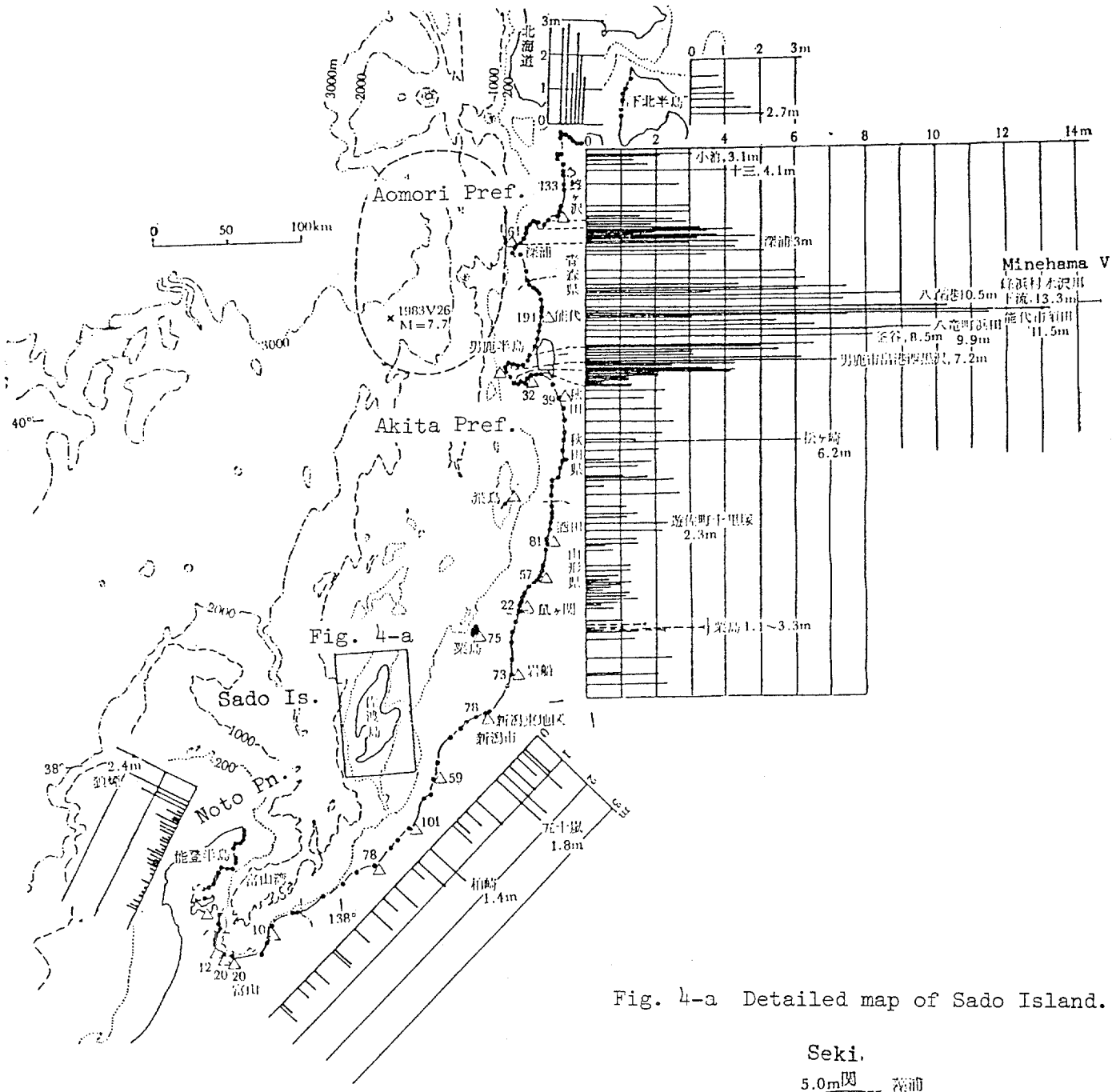

Fig. 4 Distribution of Tsunami height in the northern part of Honshu Island. Broken line shows the tsunami source area given by Hatori(1983).

Fig. 4-a Detailed map of Sado Island.

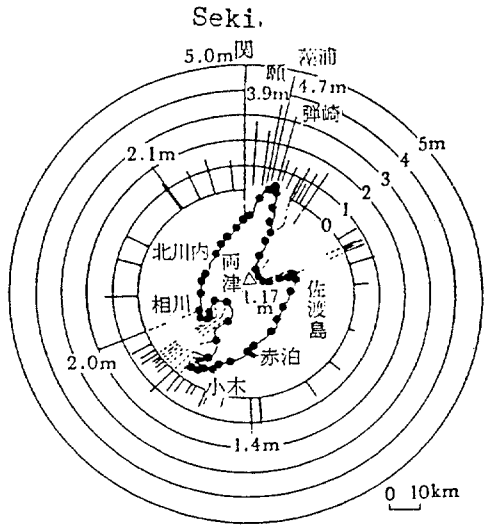

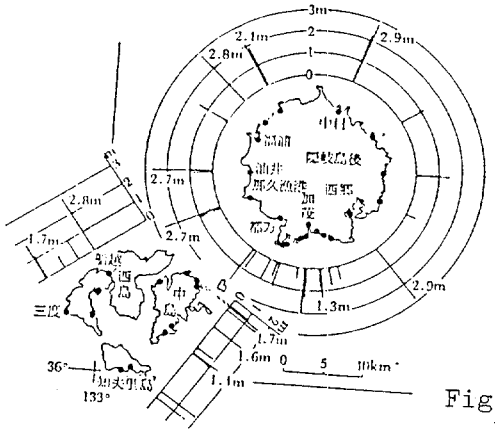

Fig. 5-a Detailed map of Oki Islands.

Fig. 5 Distribution of height of the Nihonkai-Chubu Earthquake-Tsunami in the south part of the Japanese Islands. Notice that higher tsunami was recorded on the coasts of Noto Peninsula and Shimane Prefecture.

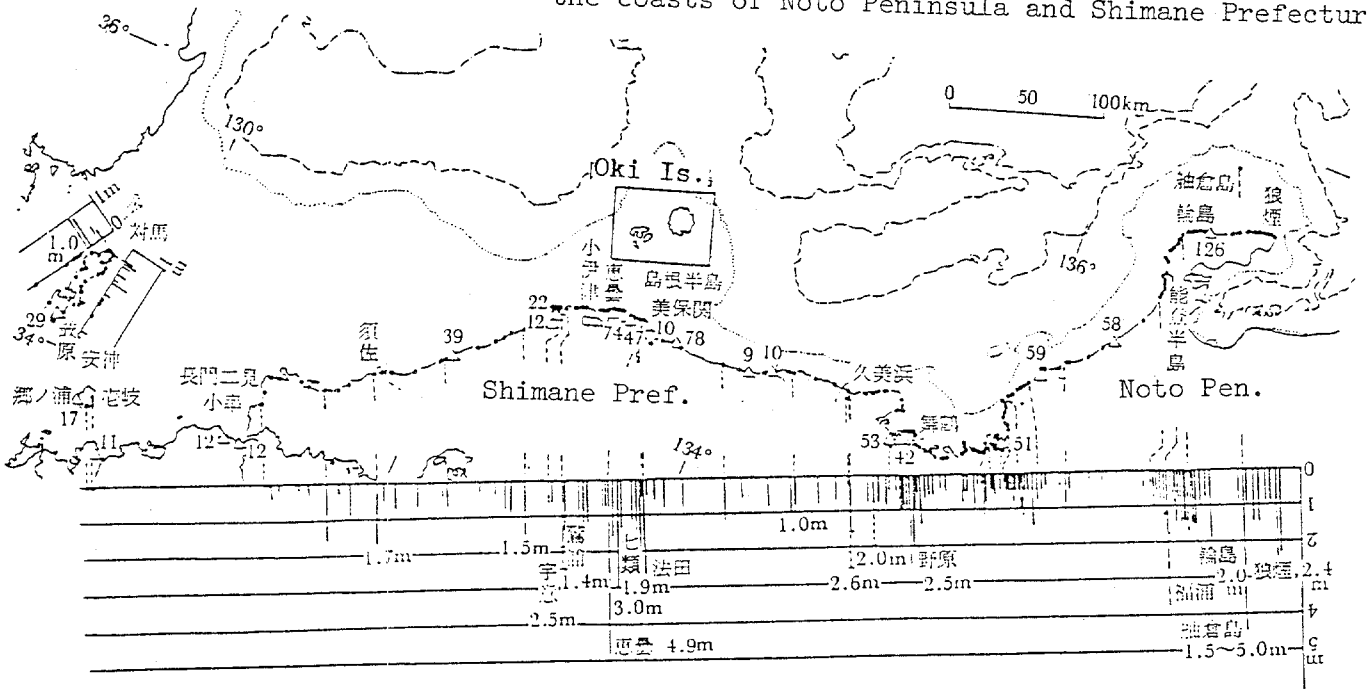

Fig. 6 Distribution of height of the Nihonkai-Chubu Earthquake-Tsunami along the east coast of Korea. No information has come from North Korea till May 1985.

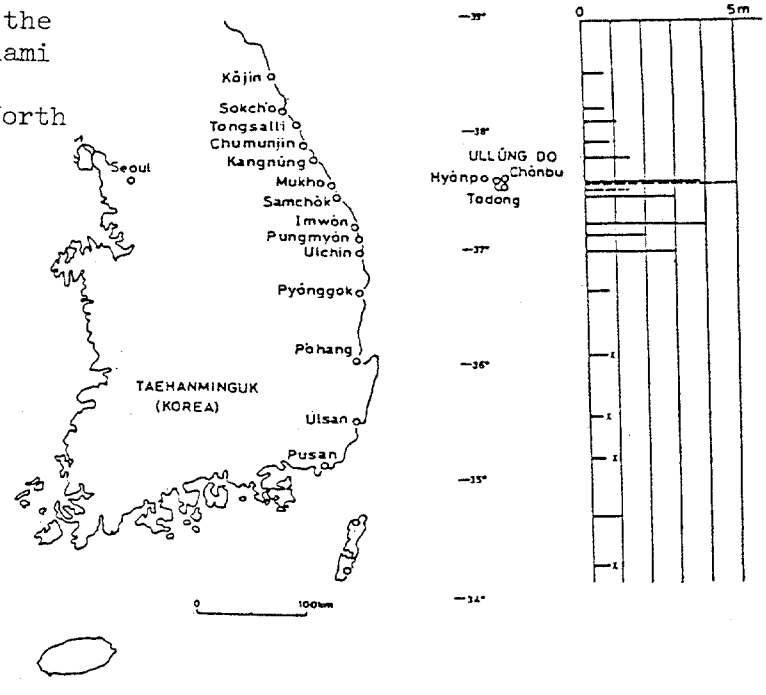

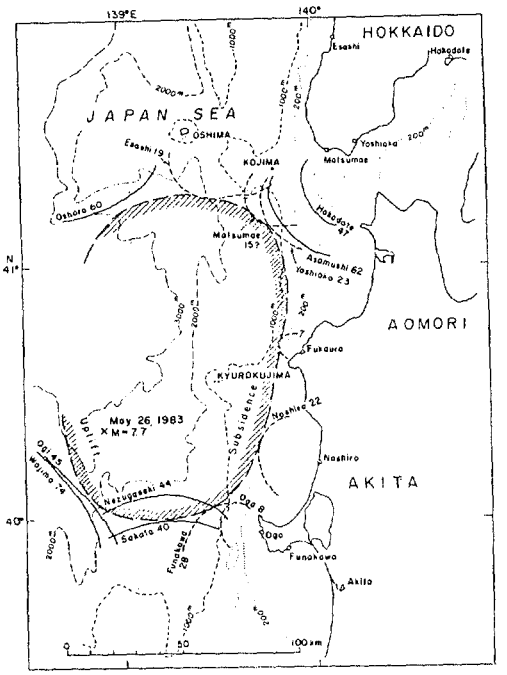

Fig. 7

Estimated source area of the 1983 Japan Sea tsunami. The last wave fronts are shown with the name of tide stations and travel time(min). The senses, up or down, of the initial motion of tsunami are indicated by solid and broken lines, respectively. (After Hatori, 1983)

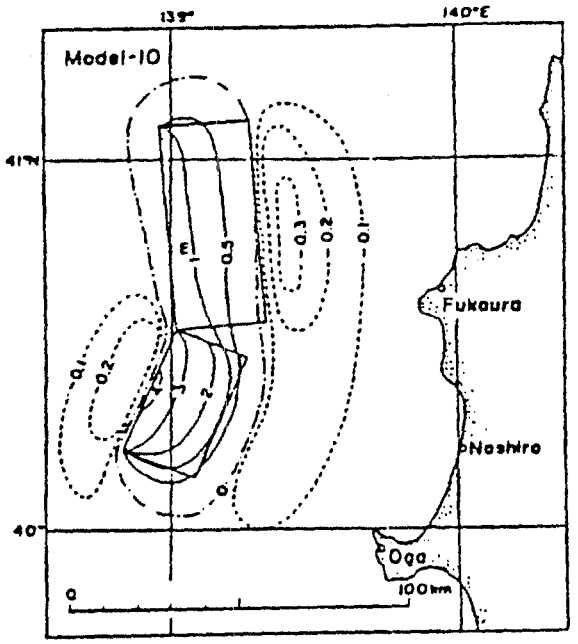

Fig. 8 Initial sea bed displacement caused by the Nihonkai-Chubu Earthquake. After Aida(1984).

Full line shows the area of upheaval and broken line shows that of subsidence.

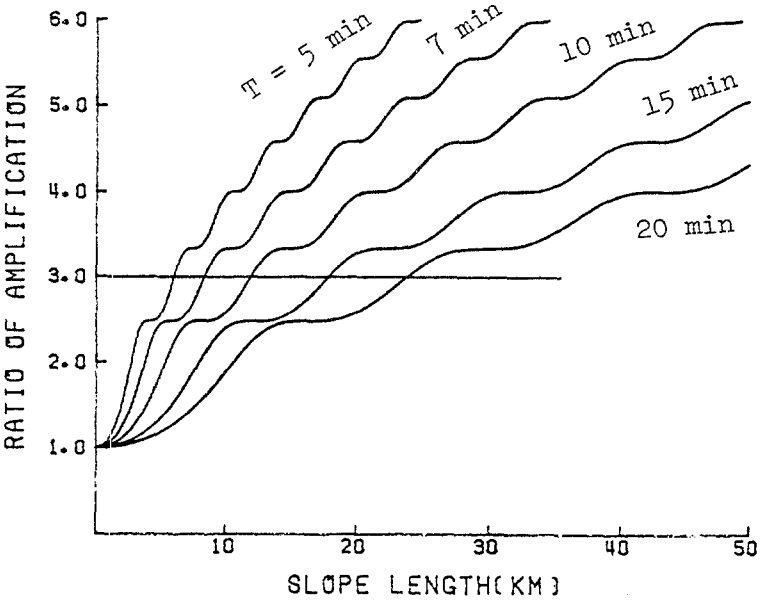

Fig. 11 Tsunami amplification ratio calculated by Shuto's formula (1).

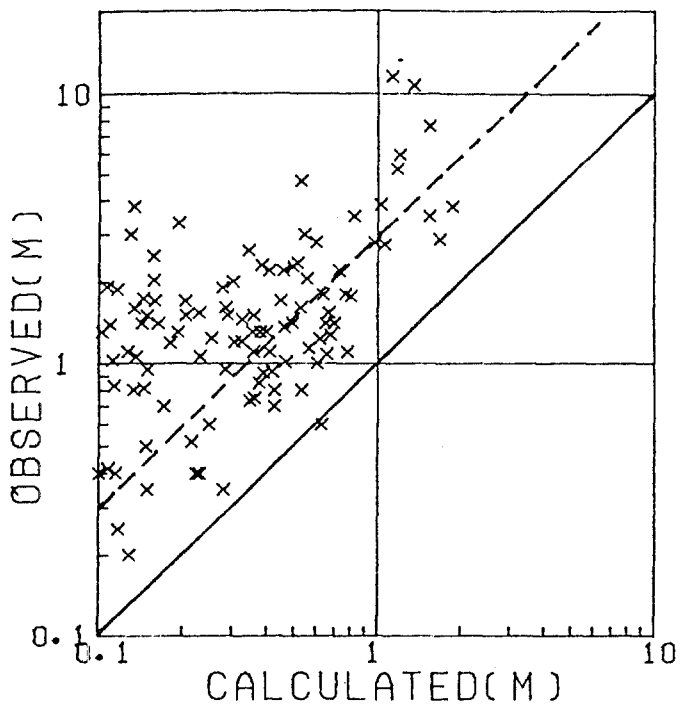

Fig. 12 Comparison of observed tsunami height(h_{obs}) with numerically calculated height(h_{cal}). Full line denotes $h_{obs} = h_{cal}$, and broken line denotes $h_{obs} = 3.0 \times h_{cal}$.

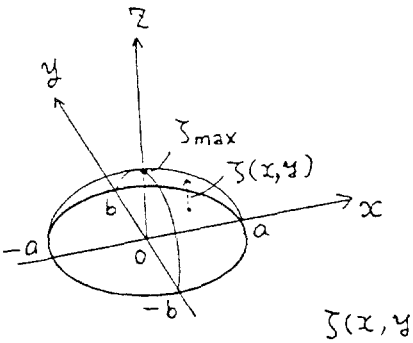

$$\zeta(x,y) = \zeta_{max}\left(1 - \frac{x^2}{a^2} - \frac{y^2}{b^2}\right)$$

Fig. 15 Simplified seabed upheaval model.

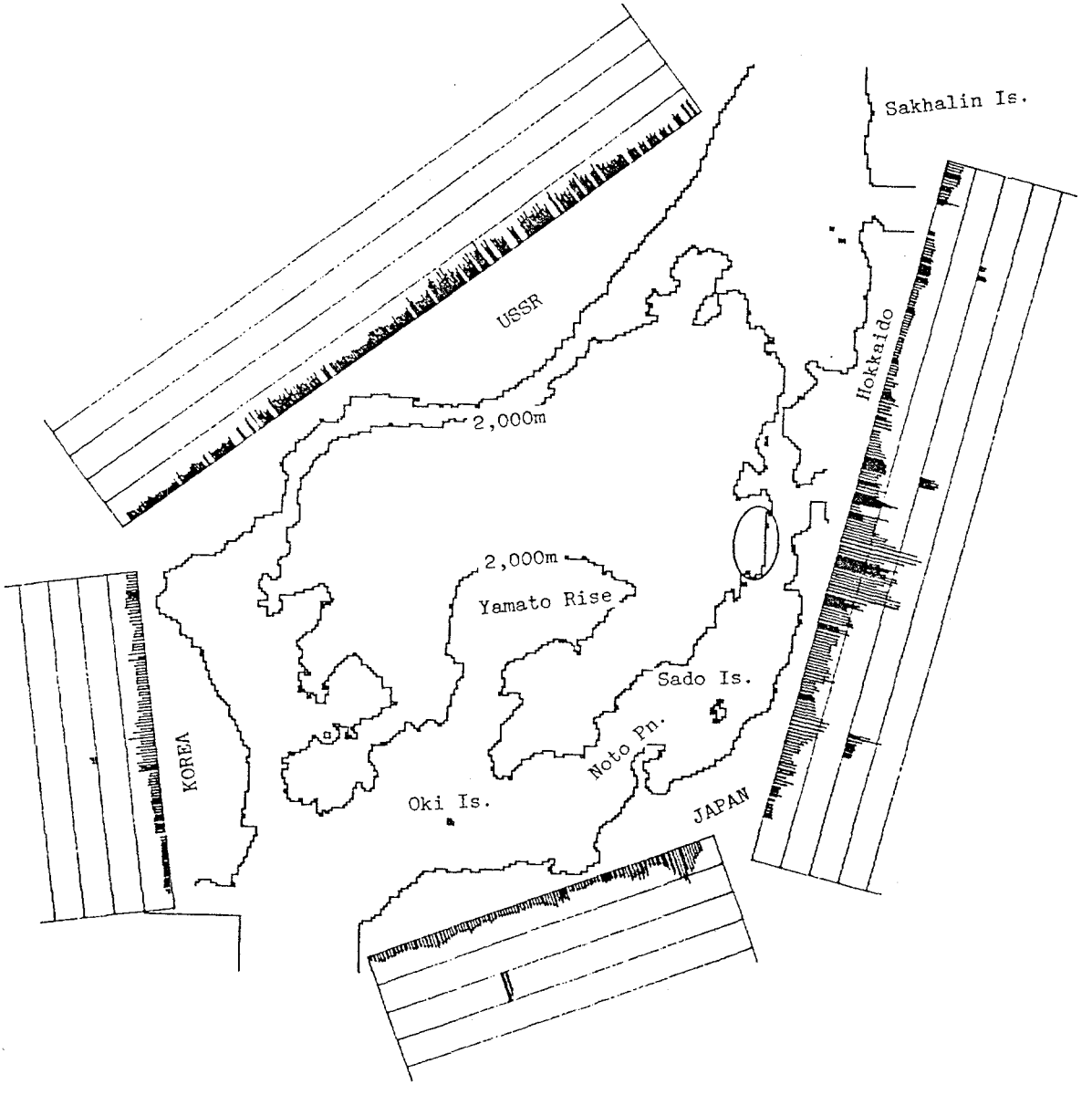

Fig. 16 Tsunami height distribution for the symplified model.

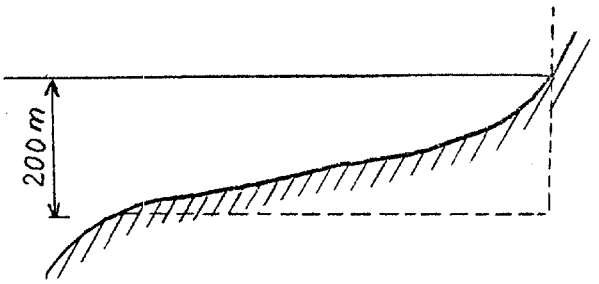

Fig. 9 Actual shape of continental slope region (real line) and assumed shape (broken line) for numerical calculation.

Fig. 10 Result of numerical calculation for the Nihonkai-Chubu Earthquake-Tsunami. One mesh corresponds to 50cm of tsunami height. Notice that the depth in the shelf region is assumed uniform as 200m.

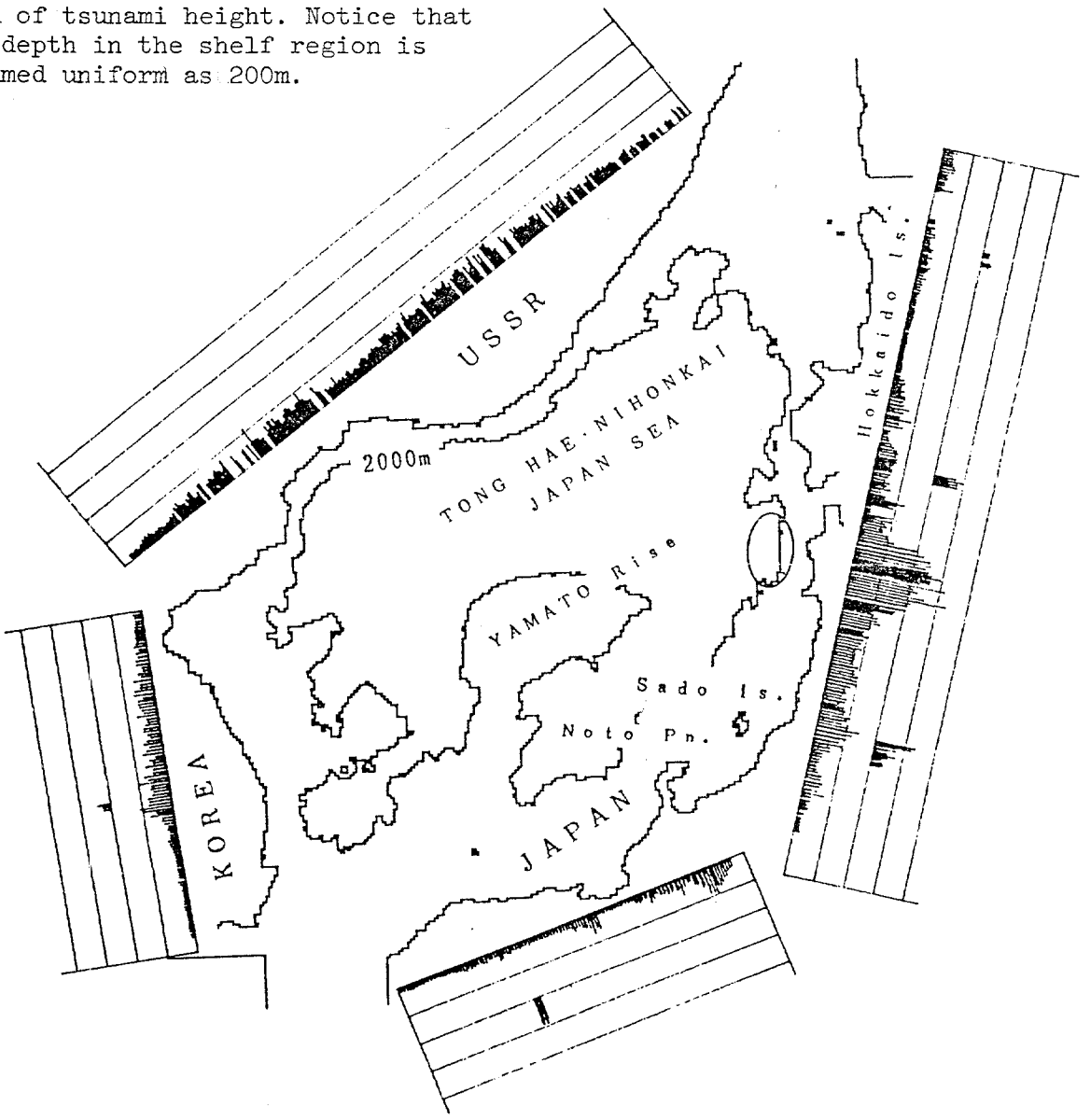

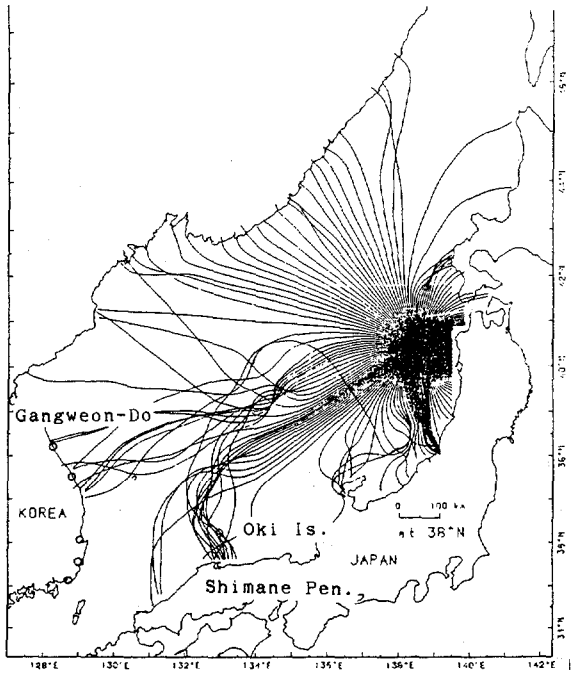

Fig 13 Refraction diagram computed by wave ray method (After Kang, et al., 1985)

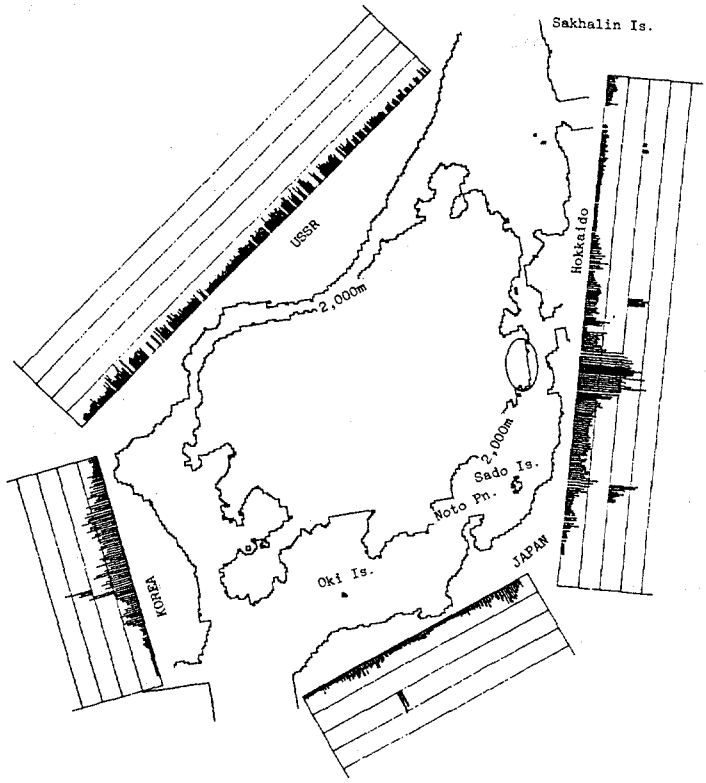

Fig. 14 Result of numerical calculation of the Nihonkai-Chubu Earthquake-Tsunami under the condition that Yamato Rise is removed.

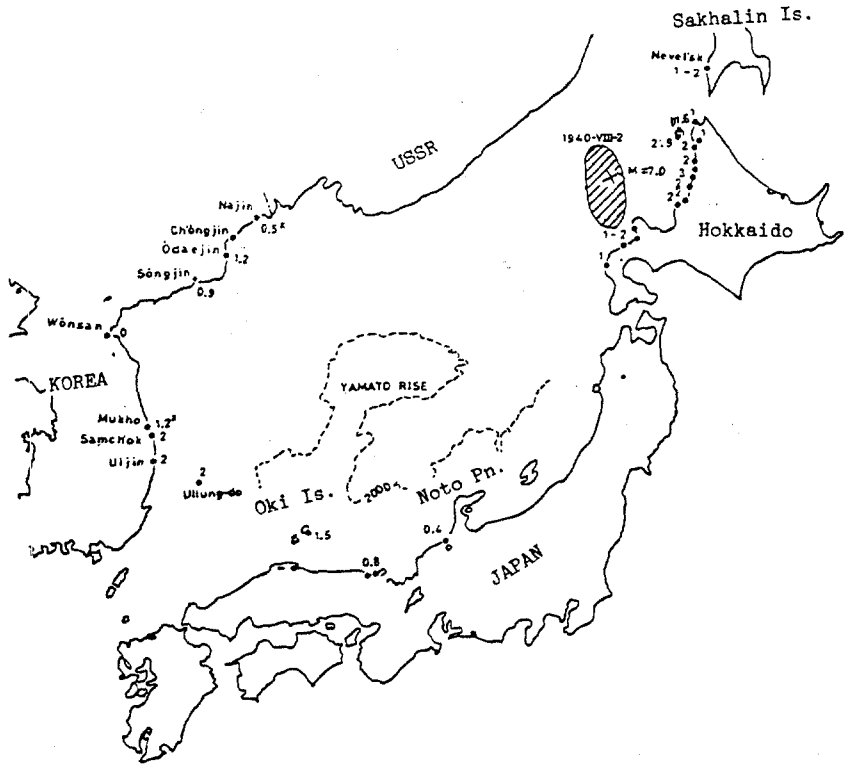

Fig. 17 Distribution of height of the Kamuimisaki-Oki Earthquake-Tsunami of 1940-VIII-2, M = 7.5, m = 2. unit:m.

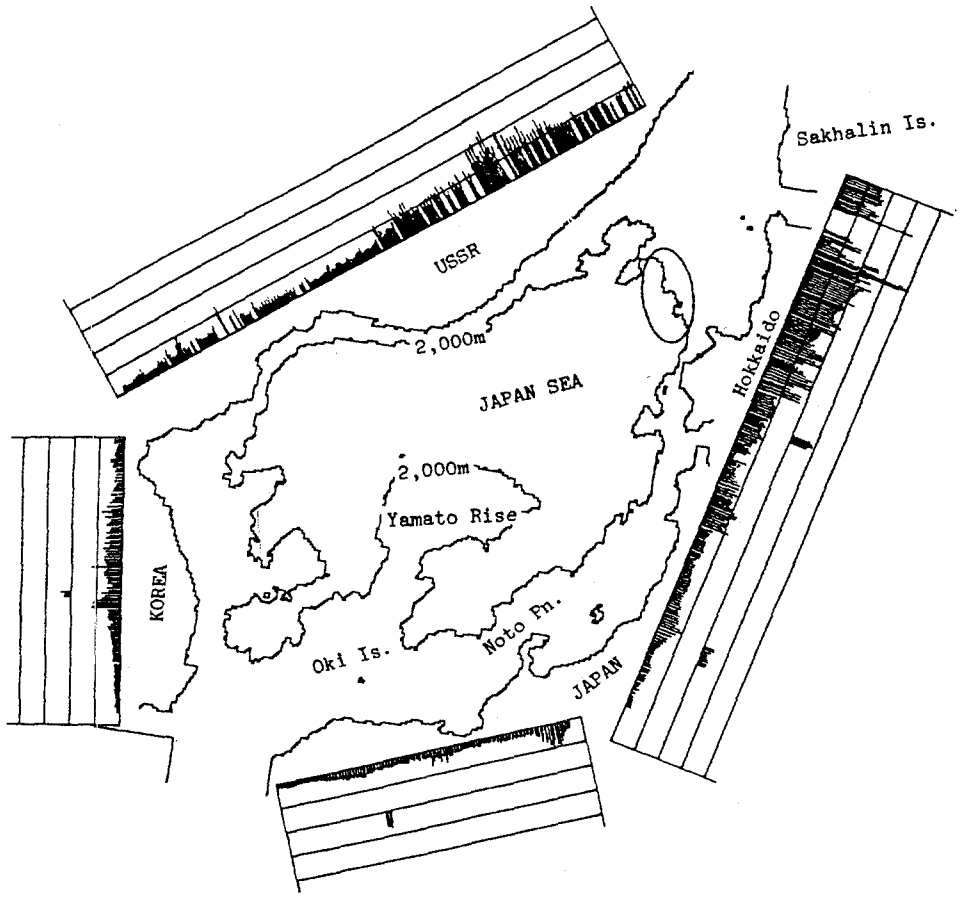

Fig. 18 Result of the numerical calculation of the Kamuimisaki-Oki Tsunami.

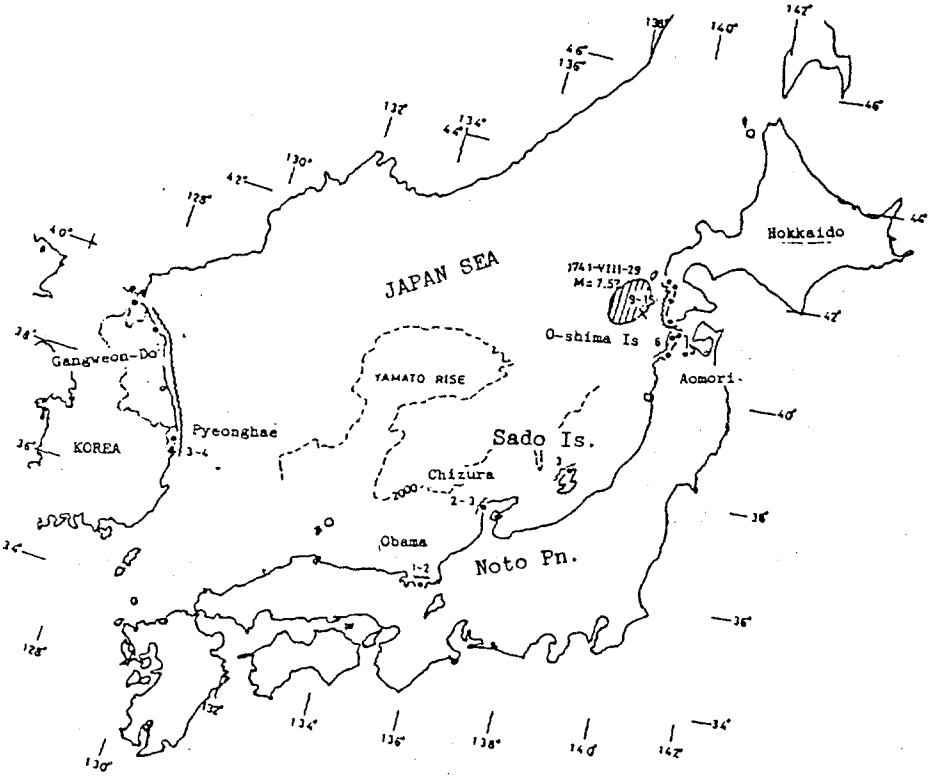

Fig. 19 Distribution of height of the 1741 Kampo Tsunami.

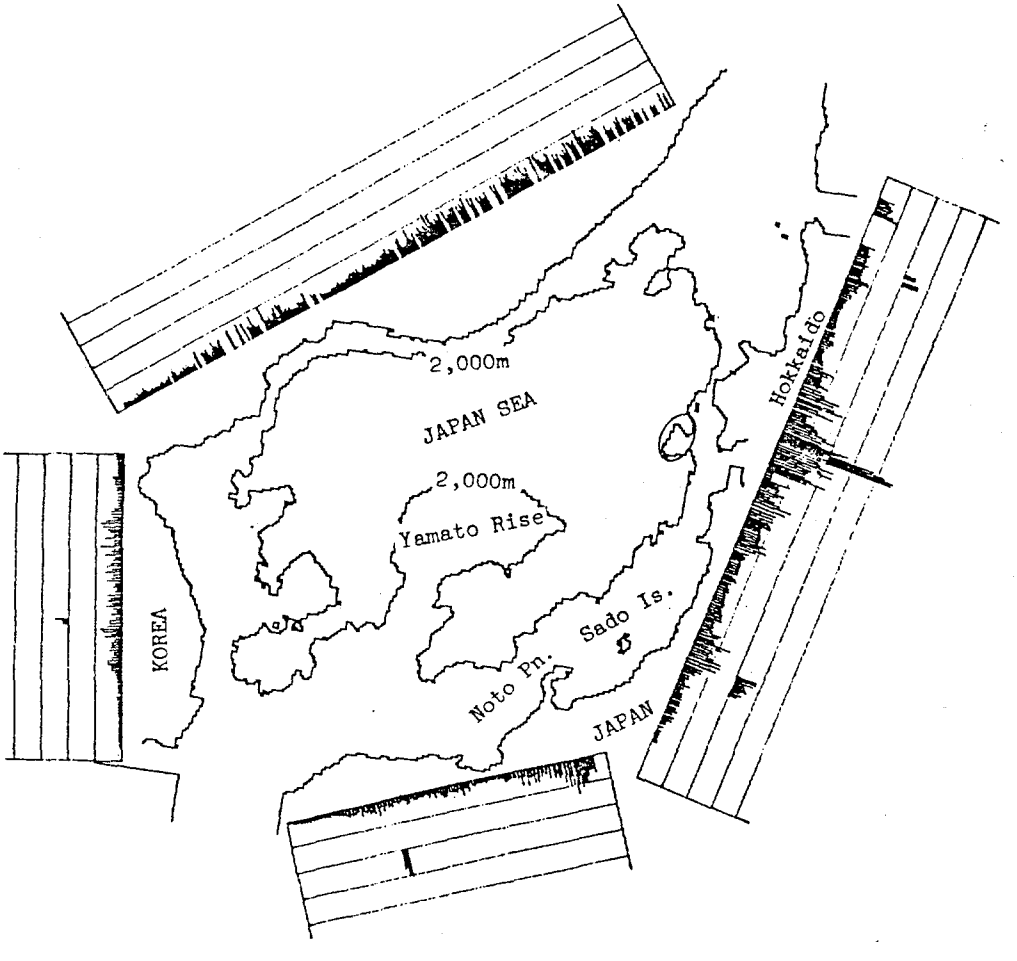

Fig. 20 Result of the numerical calculation of the Kampo Tsunami by using simplified sea bed deformation.

A Study of Numerical Technique on the Tsunami Propagation and Run-up

Nobuo Shuto* , Takao Suzuki**, Ken'ichi Hasegawa *** and Kazuo Inagaki***

* Tohoku University, Sendai, Japan
** The Chubu Electric Power Company Inc., Nagoya, Japan
*** Unic Corporation, Tokyo, Japan

ABSTRACT

Numerical tests are performed to examine the dependence of computed results on the grid size in tsunami simulations, for simplified conditions. In addition to the ordinary CFL condition, the resolution, N, which is defined as the number of grid points per wave length is found essentially important. In order to obtain good results, values of N should be taken to be larger than 20.

With this fact taken into consideration, the 1983 Nihonkai-Chubu earthquake tsunami is computed. The smallest grid size is 30 m. Throughout the simulation, the shallow water theory is used.

Numerical results agree well with tide gauge records, measured run-up heights and inundated areas. The maximum run-up height of 15 m is also reproduced as a result of the lense effect of sea bottom topography in deep sea.

1. INTRODUCTION

Tsunami simulation techniques based upon the finite difference method have been developed and used for tsunami risk evaluation, for example, by Aida(1969), Iwasaki(1979) and Goto and Shuto(1983). Some of the present authors has used the finite element method(1983).

All of these studies use the shallow water theory which is basically the same as the tide and storm surge simulation models, although nonlinear dispersive equations have also been developed by several researchers as recent examples can be found in Goto's paper(1984). Most of the simulation studies were carried out to reproduce historical tsunamis which have inevitable uncertainty about fault models, run-up heights and inundation areas. Therefore, it was not clearly answered whether the shallow water theory gave sufficient results or not.

The 1983 Nihonkai-Chubu earthquake generated a great scale tsunami. Many accurate data of run-up heights, inundated areas and tide gauge records as well as seismic data were obtained and collected. The fault model was resonable determined based on seismic and tsunami data. In addition, evolution of solitons as a result of the dispersion effect was observed and recorded at the front of tsunamis.

Consequently, it is considered that this tsunami can provide a good example to examine the accuracy of numerical simulation and to know the limitation of the shallow water theory.

In application of numerical techniques, the grid size has an influence upon the numerical result. In order to make this influence clear, numerical tests are carried out for a simplified model before simulating the actual tsunami. The resolution which is the number of grid points per wave length is found more important than the rate of allowance for the CFL condition.

With this fact taken into consideration, the 1983 Nihonkai-Chubu earthquake tsunami is computed. The simulation is composed of three steps. The first step is to obtain a rough feature of the tsunami in the whole Japan Sea. The second step is to simulate the tsunami from the source area to the seashore of the Tohoku district where the tsunami gave severe damages. The third step is to reproduce the inundation and run-up in the North Akita Coast where the maximum run-up of 15 m was found. The smallest grid size is 30 m.

The initial profile of the tsunami is calculated with the theory of Manshinha and Smylie (1971) by substituting the Aida fault model-10 (1984). Throughout the simulation, the shallow water theory is used.

Numerical results agree satisfactorily with tide gauge records, measured run-up heights and inundated areas. The maximum run-up height is also reproduced as a result of the lense effect of sea bottom topography in deep sea, which can only be expressed by fine grid size.

2. PRELIMINARY STUDY ON NUMERICAL STABILITY AND CONVERGENCE

A one-dimensional model of linear long waves in shallow water is numerically tested in order to simplify the problem. The following parameters may govern the accuracy of numerical computations.

$$N = L / \Delta x \tag{1}$$

$$M = \Delta t / \Delta t_c \times 100 \tag{2}$$

where L denotes the wave length, Δx the spatial grid size, Δt the time interval for integration and Δt_c the time interval determined from the CFL condition ($= \Delta x / \sqrt{gh}$).

One of the parameters N indicates the resolution, which is the number of grid points included within one wave length. The other parameter M indicates the rate of allowance for the CFL condition, which is usually taken as large as possible within the range where the CFL condition is satisfied.

A progressive sinusoidal wave with unit amplitude is assumed at a boundary of a one-dimensional channel of a constant water depth and its numerical damping is examined. A staggered leap-frog scheme is used in the computation.

The results are shown in Figs.1 and 2. Figure 1 shows that a heavy damping occurs within a travel distance of one wave length even if M is taken as sufficiently large as 90. If N is larger than 20, the damping is not destructive. This situation is more clearly shown as a function of N with M as a parameter in Fig.2. Figure 2 also shows that overshooting can occur depending upon values of N.

If 5 % errors are allowed, numerals in frame in Table 1 give possible combinations of M, N and travel distance. In an actual numerical simulation of tsunamis, the water depth is not constant but variable. In case of a near-source tsunami in Japan, it is very rare that a constant water depth continues over a distance of more than four wave lengths of the tsunami. If no big change in wave profile occurs after a travel over a distance of four wave lengths, the resulted wave profile can be used as the input wave to the next zone of a different water depth. Therefore, an adequate combination of M and N should be selected so as to satisfy this condition.

In order to be free of overshooting, values of N should be larger than 100 as is shown in Table 1. This is impossible in actual simulations. However the effect of overshooting is negligibly small in comparison with damping. From this preliminary study, it is concluded that the resolution N is more important than M. Even for M=10, a satisfactory result is obtained if a large value of N is assumed.

Two-dimensional problems may follow a similar law to one-dimensional problems obtained above, if the same staggered leap-frog scheme is used. As a conclusion, a value of N not smaller than 20 should be selected in order to avoid a numerical damping.

Table 1 Ratio of wave height after a travel to the original height

Resolution N	CFL cond. M	Propagated distance/wave length 1	2	3	4	5	6	7	8	9	10
5	10	0.66	0.52	0.45	0.39	0.35	0.32	0.30	0.28	0.26	0.25
	50	0.71	0.58	0.50	0.45	0.41	0.37	0.35	0.32	0.31	0.29
	90	0.85	0.79	0.78	0.66	0.68	0.63	0.60	0.60	0.53	0.55
10	10	0.97	0.87	0.79	0.73	0.67	0.63	0.60	0.57	0.54	0.52
	50	0.99	0.92	0.84	0.78	0.74	0.70	0.66	0.63	0.60	0.58
	90	0.99	1.02	1.02	0.99	0.94	0.93	0.93	0.92	0.89	0.87
20	10	1.05	1.05	1.03	1.00	0.97	0.95	0.92	0.90	0.87	0.85
	50	1.04	1.05	1.04	1.03	1.01	0.99	0.97	0.94	0.92	0.91
	90	0.98	1.00	1.01	1.03	1.04	1.04	1.05	1.05	1.04	1.05
30	10	0.99	1.04	1.06	1.06	1.05	1.04	1.03	1.02	1.01	1.00
	50	0.98	1.02	1.05	1.06	1.06	1.05	1.05	1.04	1.03	1.03
	90	1.00	1.01	0.99	0.98	0.99	1.00	1.01	1.02	1.03	1.03
60	10	1.00	1.01	0.99	0.98	1.00	1.01	1.02	1.04	1.04	1.05
	50	1.00	1.01	1.01	0.99	0.98	0.99	1.00	1.02	1.02	1.03
	90	1.00	1.00	1.01	1.00	0.99	1.00	1.01	1.01	1.01	1.01
100	10	1.00	1.01	0.99	1.01	1.01	1.01	1.01	1.00	0.99	0.98
	50	1.00	1.00	1.00	0.99	1.00	1.01	1.01	1.01	1.01	1.00
	90	1.00	1.00	1.00	1.00	1.00	1.00	1.00	1.00	1.01	1.01

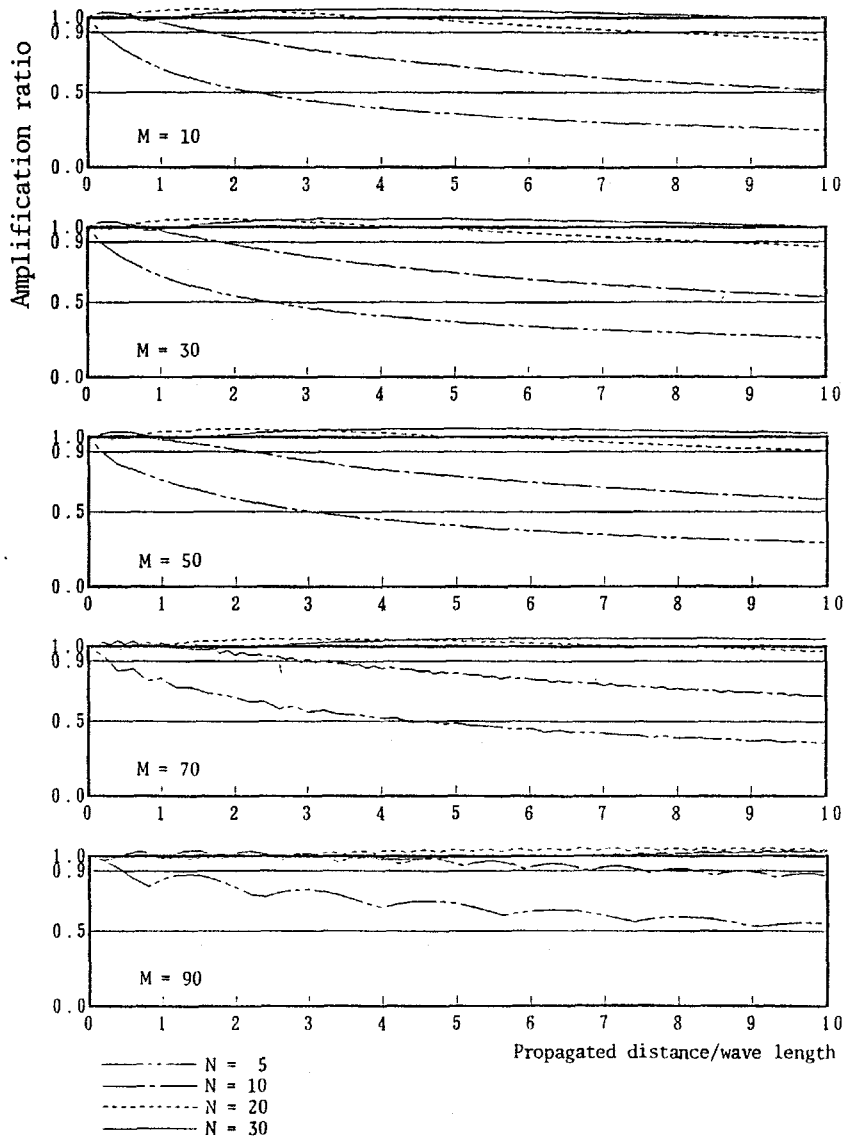

Figure 1 Spatial distribution of amplification ratio

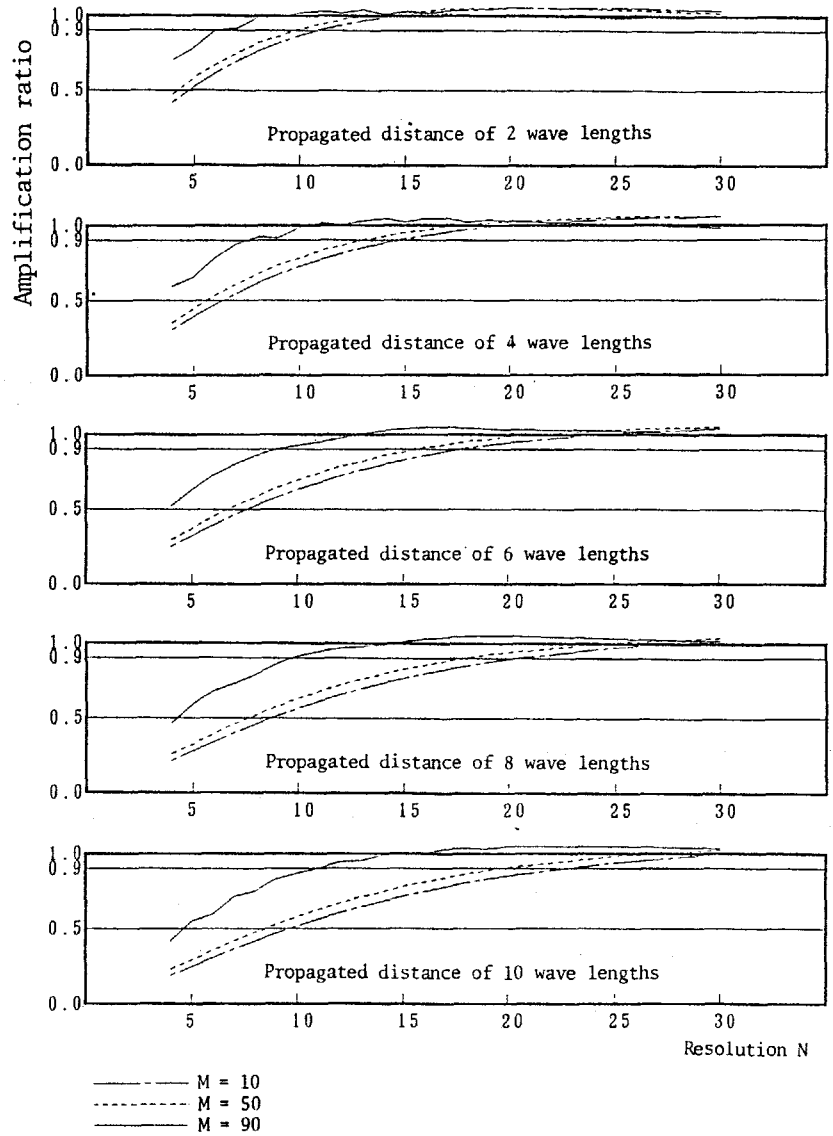

Figure 2 Relationship between resolution N and amplification ratio

3. BASIC EQUATIONS

Two-dimensional equations of shallow water waves are used as the basic equations.

$$\frac{\partial P}{\partial t} + \frac{\partial}{\partial x}\left(\frac{P^2}{D}\right) + \frac{\partial}{\partial y}\left(\frac{PQ}{D}\right) + gD\frac{\partial \eta}{\partial x} + \frac{gn^2}{D^{7/3}}P\sqrt{P^2+Q^2} = 0 \qquad (3)$$

$$\frac{\partial Q}{\partial t} + \frac{\partial}{\partial x}\left(\frac{PQ}{D}\right) + \frac{\partial}{\partial y}\left(\frac{Q^2}{D}\right) + gD\frac{\partial \eta}{\partial y} + \frac{gn^2}{D^{7/3}}Q\sqrt{P^2+Q^2} = 0 \qquad (4)$$

$$\frac{\partial}{\partial t}(\eta-\xi) + \frac{\partial P}{\partial x} + \frac{\partial Q}{\partial y} = 0 \qquad (5)$$

Where P and Q are discharges in the x- and y-directiones, η and ξ vertical displacements of the water surface and sea bottom, g the gravitational acceleration, n the Manning's roughness, and D the total water depth given by $D=h+\eta-\xi$ with the initial water depth h. A staggered leap frog scheme is used. On the offshore open boundary, the characteristics line method is used. In the first and second computation steps in the following section, the boundary condition at land is that the discharge normal to boundary is zero. In the third step where a detailed analysis including run-ups on land is carried out, the moving boundary condition is used.

4. THE 1983 NIHONKAI-CHUBU EARTHQUAKE TSUNAMI

There have been many numerical studies of tsunamis. Most of them aimed to reproduce historical tsunamis, for which data such as run-up heights, inundated areas and fault models are of little reliance.

For the 1983 Nihonkai-Chubu earthquake tsunami, accurate tide gauge records, run-up heights and inundated areas are measured and collected. In addition, the fault parameters are reasonably estimated from seismic data.

To simulate this tsunami, three steps are taken in the computation. The Japan Sea is divided as shown in Fig.3, corresponding to these three steps.

The first step computation area is used to examine the fault model. Propagation of the tsunami is computed for the whole Japan Sea. Travel time, initial movement of sea surface (ebb or flood) and time history of surface elevation are compared between numerical results and tide gauge records.

The second step computation area has nearly the same size as the area usually assumed in any tsunami simulations at present.

In order to reproduce run-up heights and inundation, the third step computation area is introduced.

As the fault model, the Aida model-10 (1984) shown in Fig.4 is used. Supported also by the seismological data of Shimazaki and Mori(1983), this model is believed as the best at present. The vertical displacement of sea bottom at the source area is calculated with the theory of Manshinha and Smylie (1971). The maximum displacement 4.4m is found in southern part of the faults.

4.1 The First Step Result

The first step computation area is so wide that it is not possible to fully satisfy the requirement obtained in Section 2, limited by the capacity of computer memory. The requirement is partially loosened, since this computation is for a rough examination of the fault model through the overall feature of the tsunami.

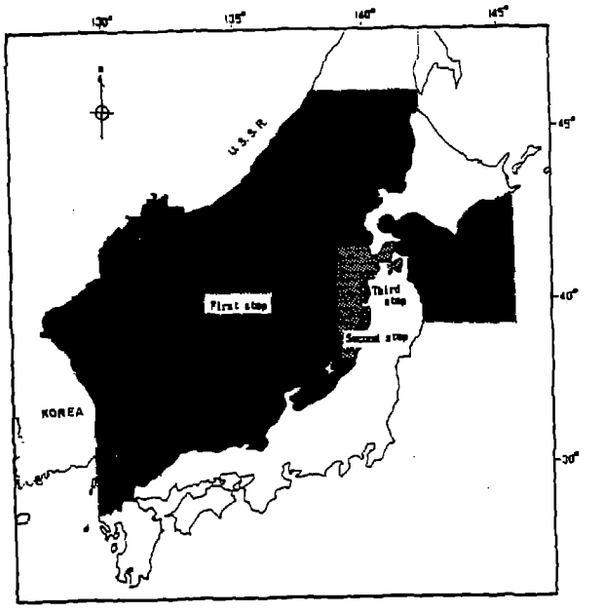

Figure 3 Analyzed area

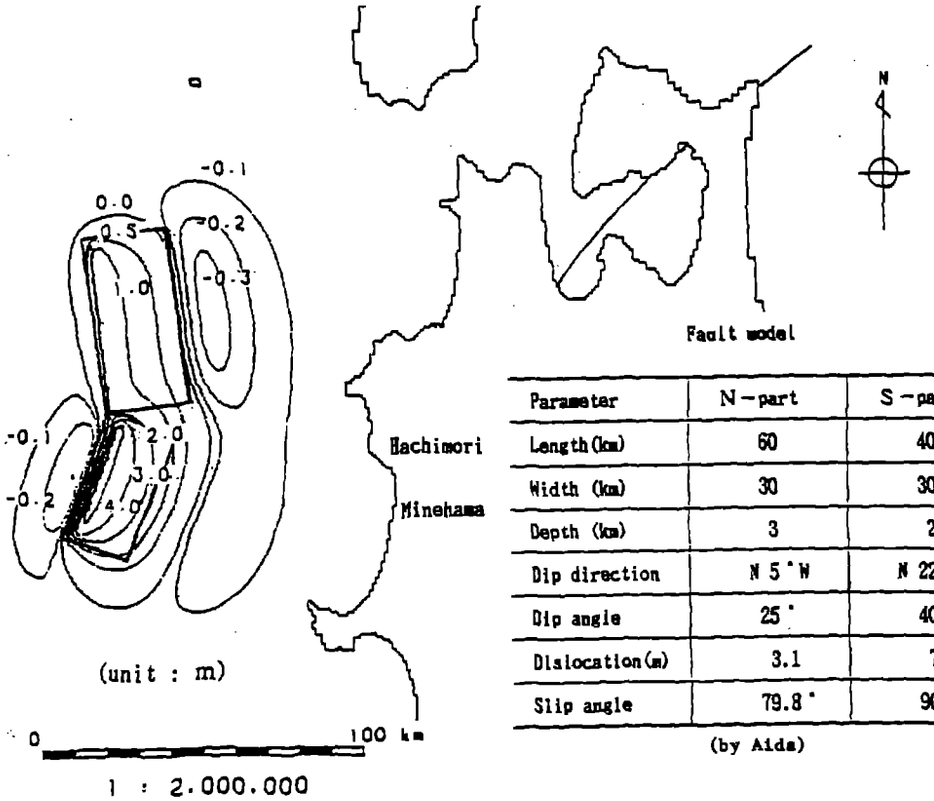

Parameter	N-part	S-part
Length(km)	60	40
Width (km)	30	30
Depth (km)	3	2
Dip direction	N 5°W	N 22°E
Dip angle	25°	40°
Dislocation(m)	3.1	7.6
Slip angle	79.8°	90.0°

(by Aida)

Figure 4 Distribution of vertical displacement

Figure 5(a) shows the distribution of grid size required for the resolution N=20, based upon linear long waves of a period of 7 minutes. Figure 5(b) shows the grid system actually used in the first step computation. The total number of grid points is 136,183.

The travel time and the initial wave motion caused by the tsunami are shown in Fig.6. Numerals indicate the travel time from the source area in minute. Upper ones are from tide gauge records and lower ones are the computed. Upper and lower half circles indicate the observed and computed initial motion of sea water surface. Black means ebb and white means flood. Computed results agree well with the tide gauge records everywhere.

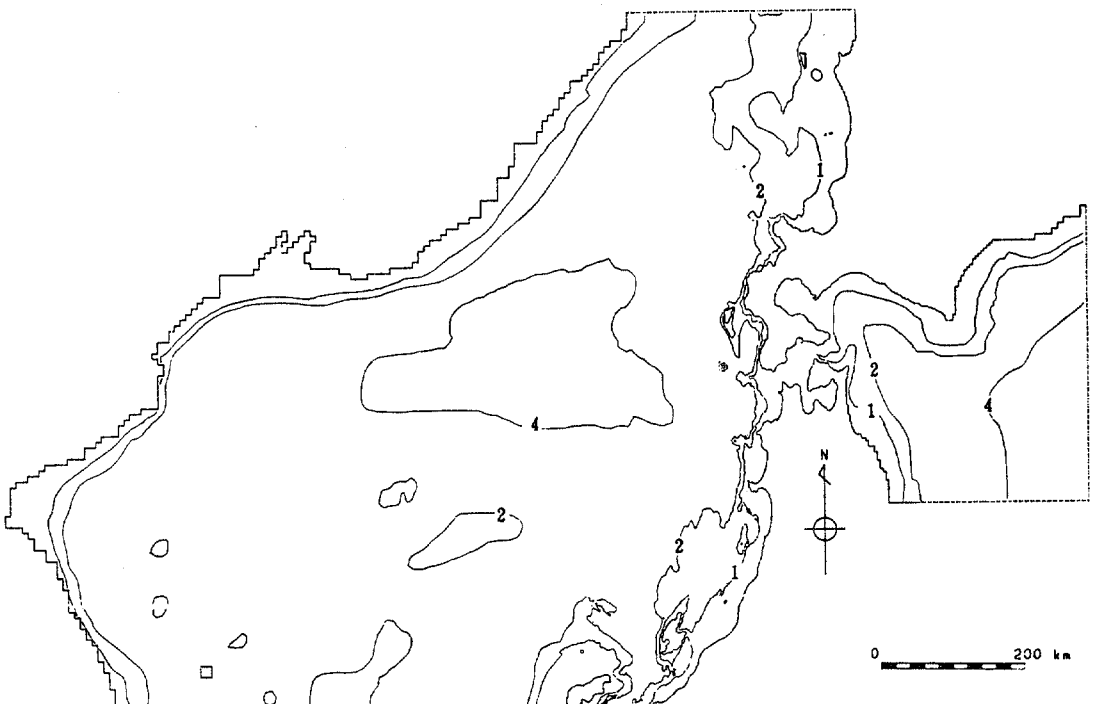

Figure 5(a) Required grid size for the first step computation area(N=20)

Area	Grid size (km)
A	8
B	4
C	2
D	1

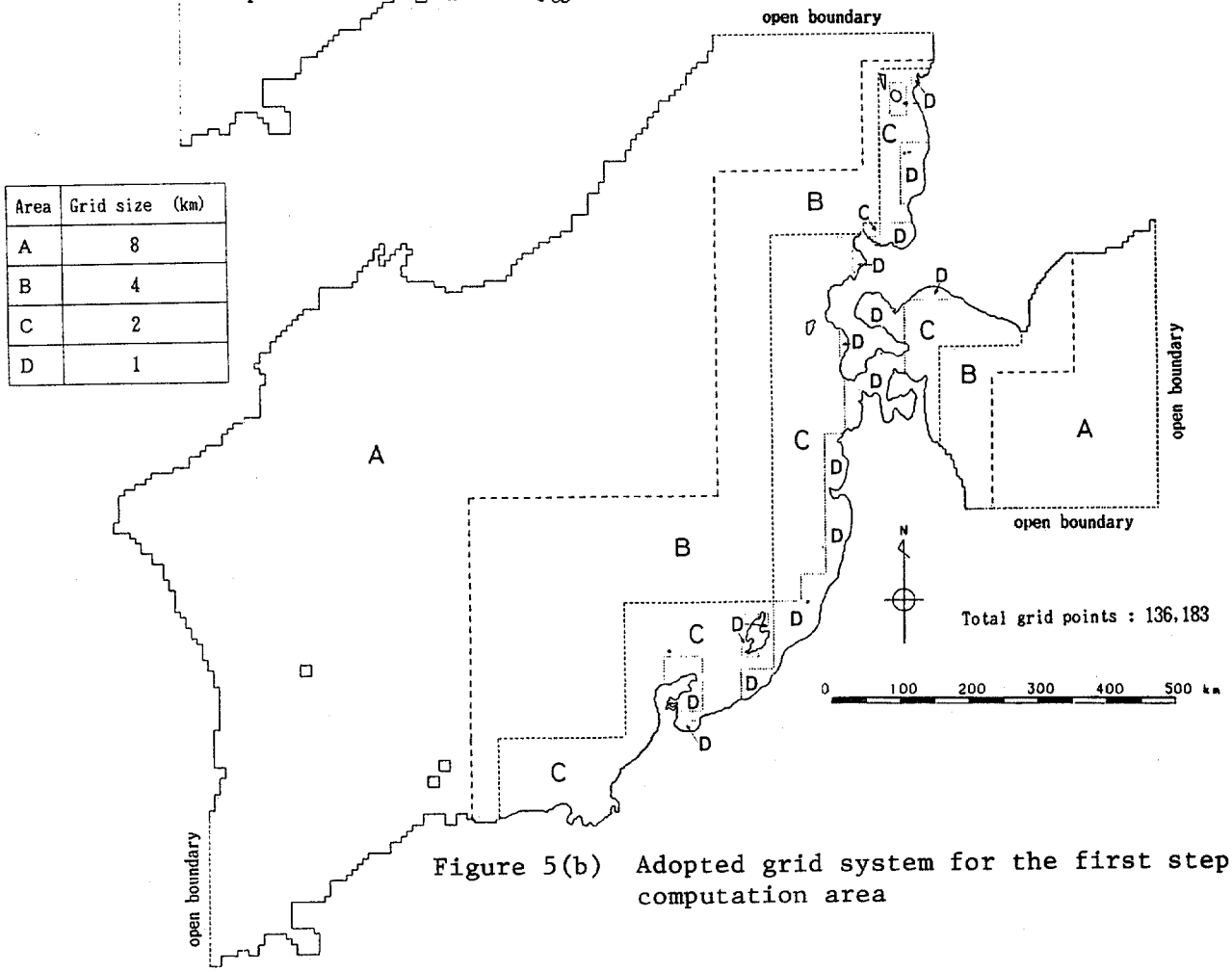

Figure 5(b) Adopted grid system for the first step computation area

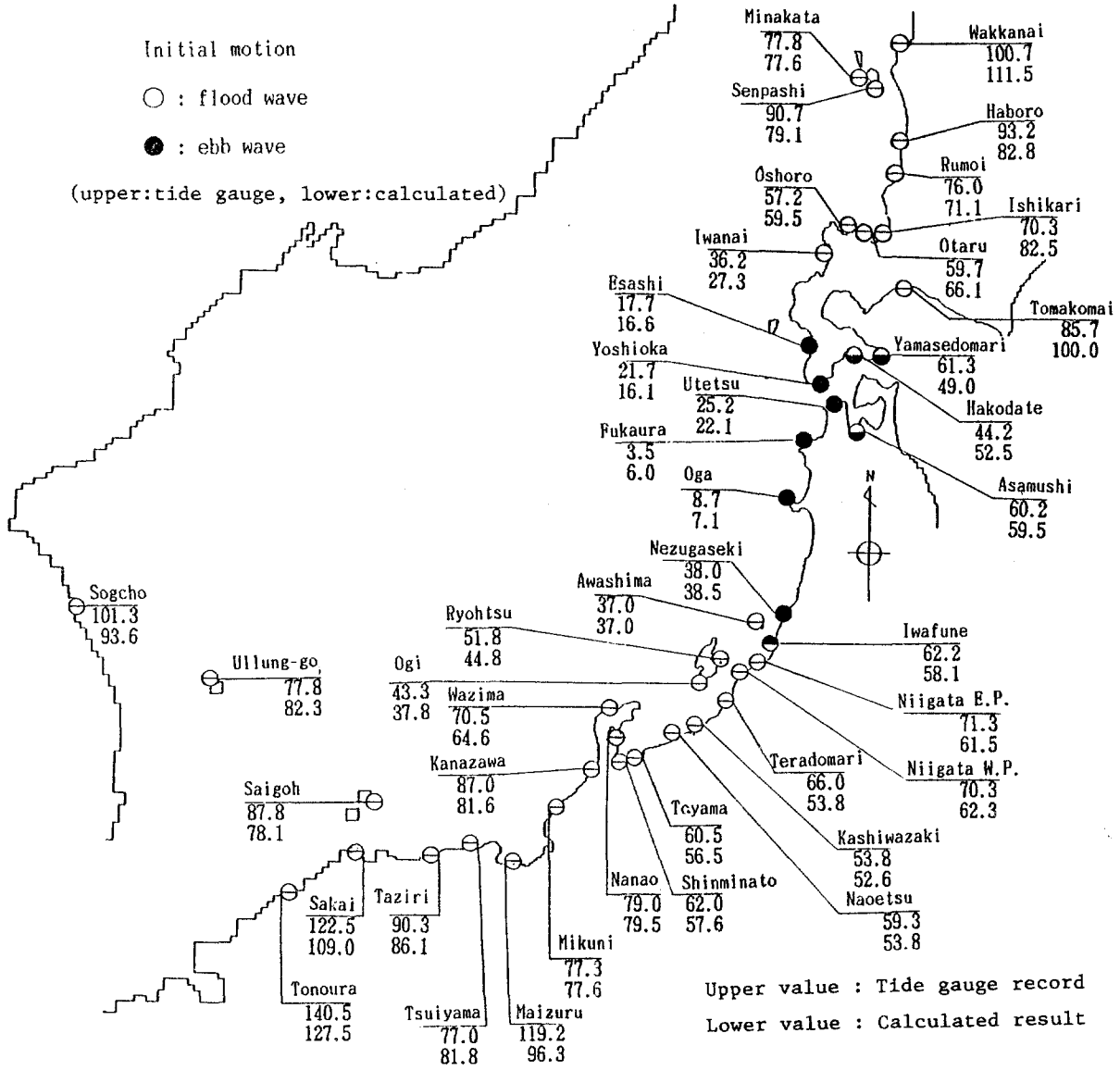

Figure 6 Comparison between tide gauge records and calculated results

Figure 7 provides comparisons between the computed time histories of water surface elevation and the tide gauge records. Although wave profiles are basically similar, agreements between the two are not so well. However, the authors consider that this comparison provides no definite conclution, due to the following reasons. The grid size at seashore in this computation is 1.0 km, therefore neither the local topography around nor the tsunamis at tide gauge stations can be exactly expressed or reproduced. In addition, the effect of low-pass filtering which is inevitably associated with tide gauge wells acts to reduce the amplitude of recorded tsunamis.

From this computation, it is concluded that the Aida model-10 is able to explain the behavior of the tsunami in the whole Japan Sea.

4.2 The Second Step Result

The maximum run-up height of about 15 m was found in Minehama Village on

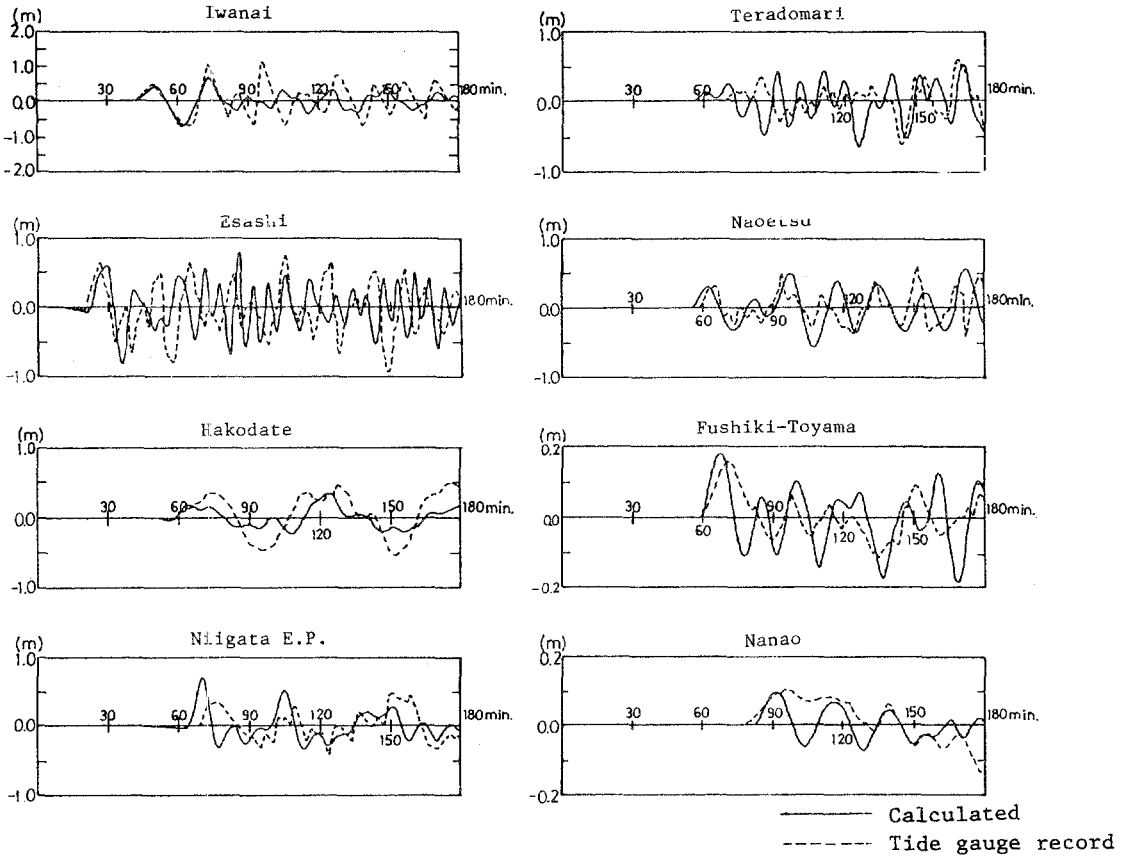

Figure 7 Comparison of the time histories of water surface elevation

the sandy North Akita Coast which has a smooth shoreline 55 km long. The bottom slope is very gentle as 1/200 or 1/300. Around the point of the maximum run-up, extremely high run-up heights were found to distribute along the beach of smooth shoreline. The coast is quite different from a ria, at the head of which tsunamis often give the maximum run-up due to convergence and or resonance. The sea bottom topography is one of the possible causes of high run-up heights for the present tsunami, otherwise it is impossible to explain this concentration of the tsunami.

The grid size of the second step computation is determined so as to strictly satisfy the requirement in Section 2 in the sea deeper than 15 m. Figure 8(a) and (b) show the required (N=20) and adopted grid systems. Values of N in the latter range from 20 to 30. The total number of grid points is 111,226. Although this grid system is sufficient to compute the tsunami propagation from source area to nearshore zone, it is still not sufficient to examine run-up heights.

Figure 9 shows the computed wave rays and travel time. Wave rays start with 2 km intervals from the fringe of the source area. It is clearly recognized that the sea bottom works as a lense and concentrates the tsunami to Minehama Village. Other researchers have already tried but failed to explain the high concentration of the tsunami, because the grid size they used was not fine enough to reproduce this lense effect. This focusing process can only be explained by the fine grid system used in the present study.

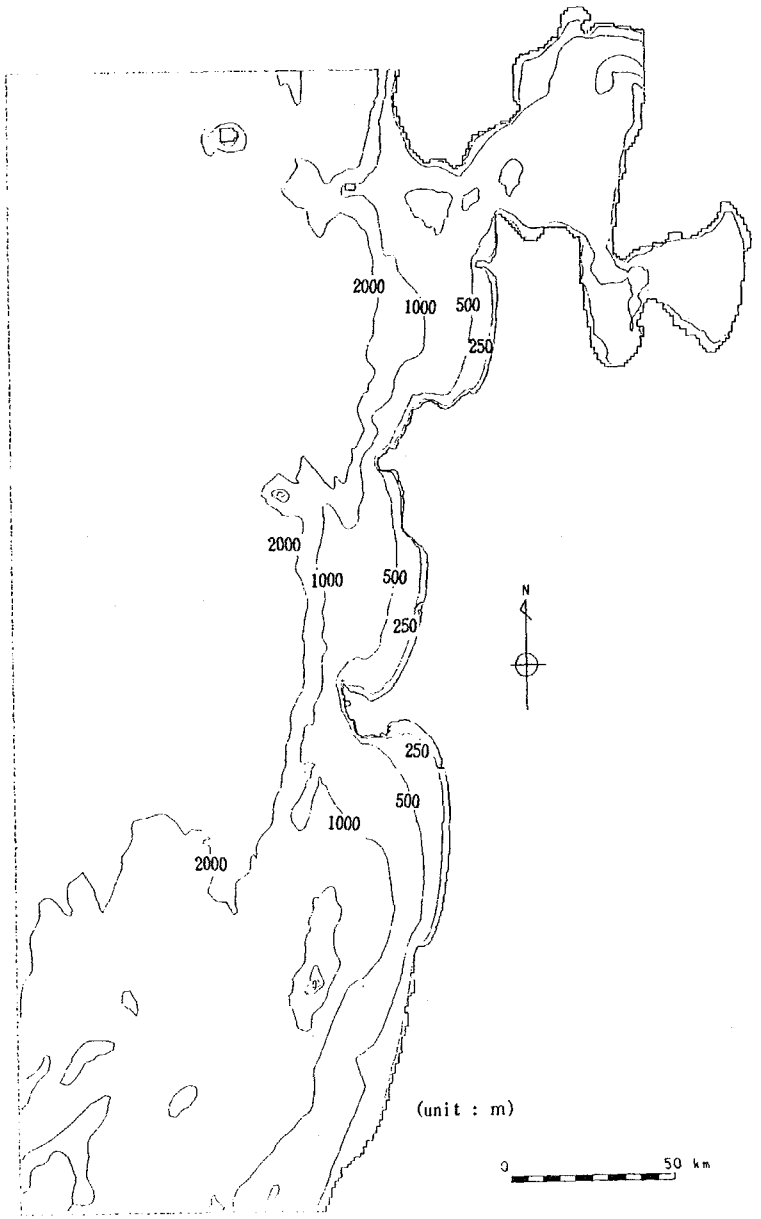

Figure 8(a) Required grid size for the second step computation area(N=20)

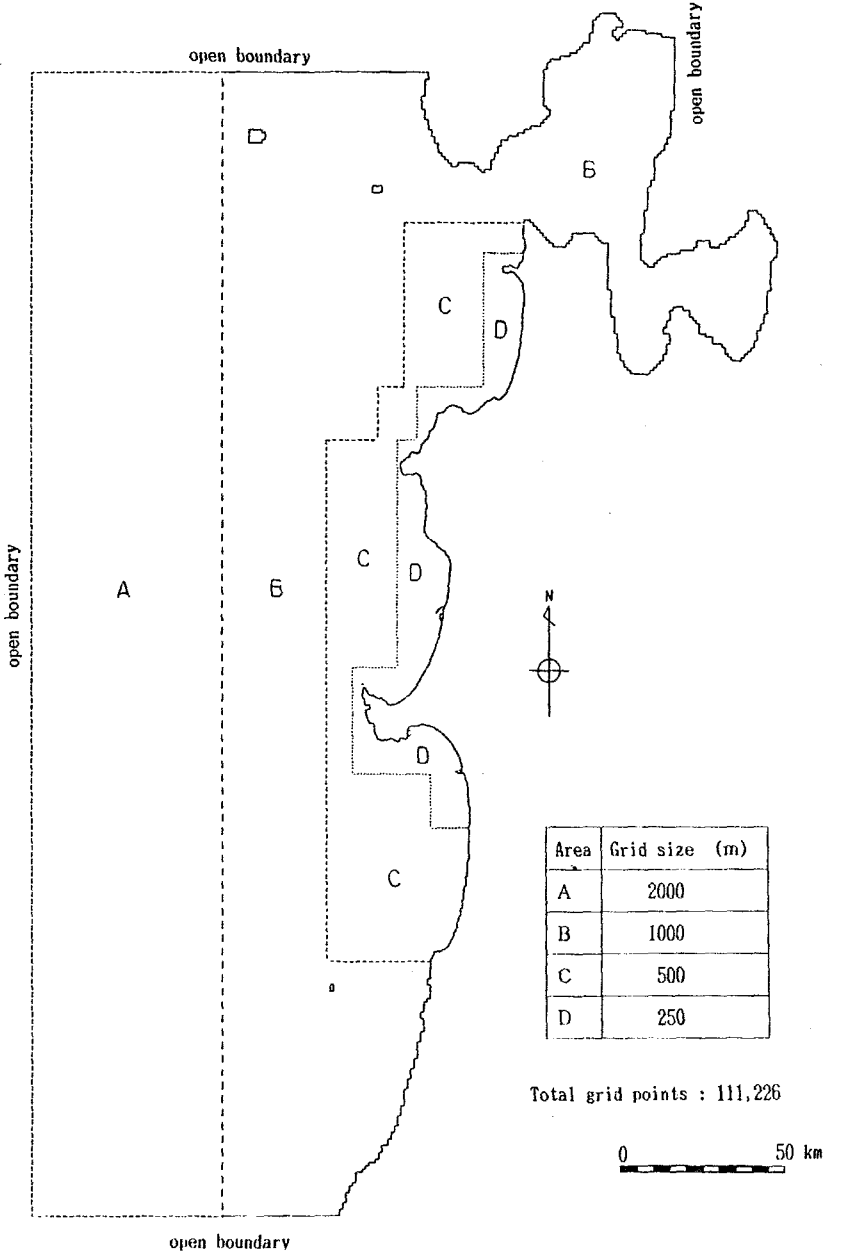

Figure 8(b) Adopted grid system for the second step computation area

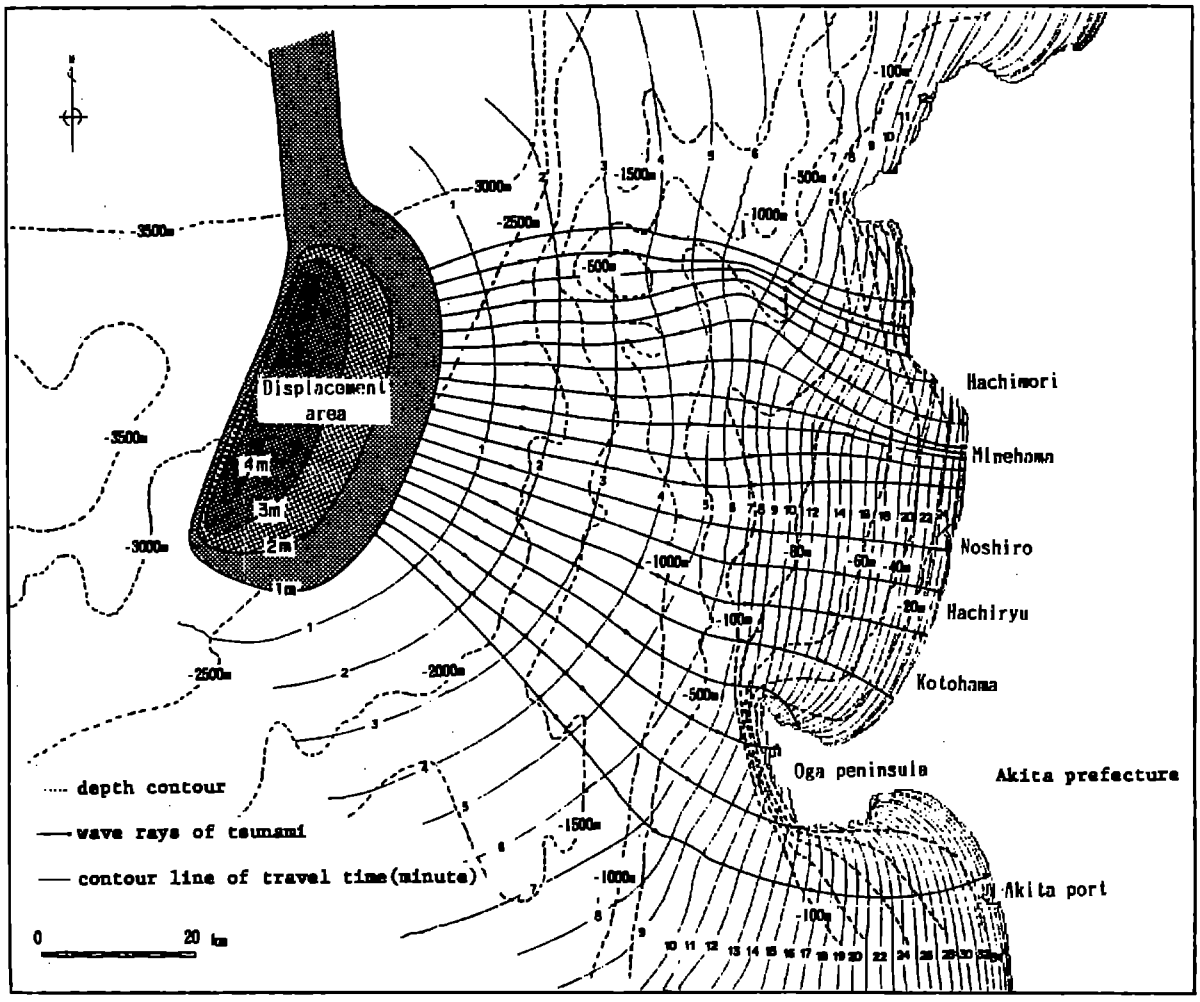

Figure 9 Computed wave rays and travel time

4.3 The Third Step Result

The detailed analysis of run-up and inundation is carried out in the third step computation. The grid size is determined to satisfy N=30, on assuming again the wave period is 7 minutes (Fig.10(a)). Figure 10(b) shows the grid system used in the computation. The minimum size is 30 m. The total number of grid points is 128,646. Time histories of water surface elevation obtained in the second step computation are used as the input at the open boundary. The moving boundary condition is used at the front of the tsunami in area E of Fig.10(b).

The computed run-up heights and inundated areas are compared with the observed data in Fig.11. Bars and lines in the figure give the observed and computed run-up heights. The hached areas in the central and right figures are the observed and computed inundated areas. The computed maximum run-up height coincides with the measured one except for a fact that the former is located at a point 1 km south of the latter.

Every run-up heights are compared in Fig.12. White and black circles in the figure indicate the measured and computed run-up heights. Crosses are the ratio of the computed to the measured ones. This ratio ranges from 0.8 to 1.2 with mean value of 1.04 averaged over 237 points along the coast 40 km long. Agreement is, therefore, fairly well.

Figure 13 is examples of flow patterns in nearshore zone and on land in Minehama Village. Ref lecting the topography of land rich in small ups and

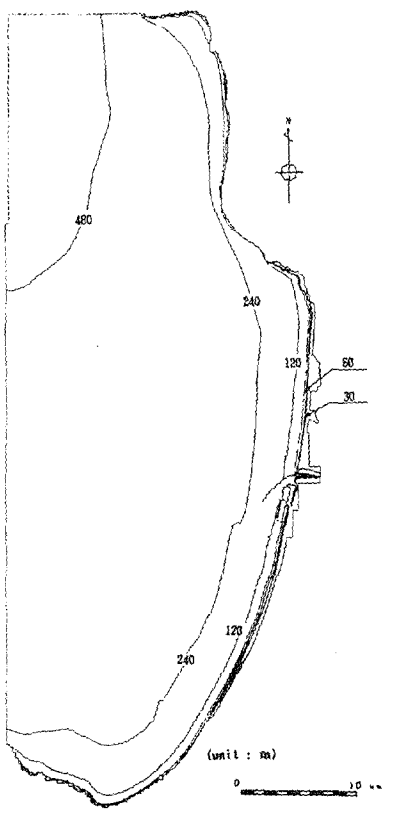

Figure 10(a) Required grid size for the third step computation area(N=30)

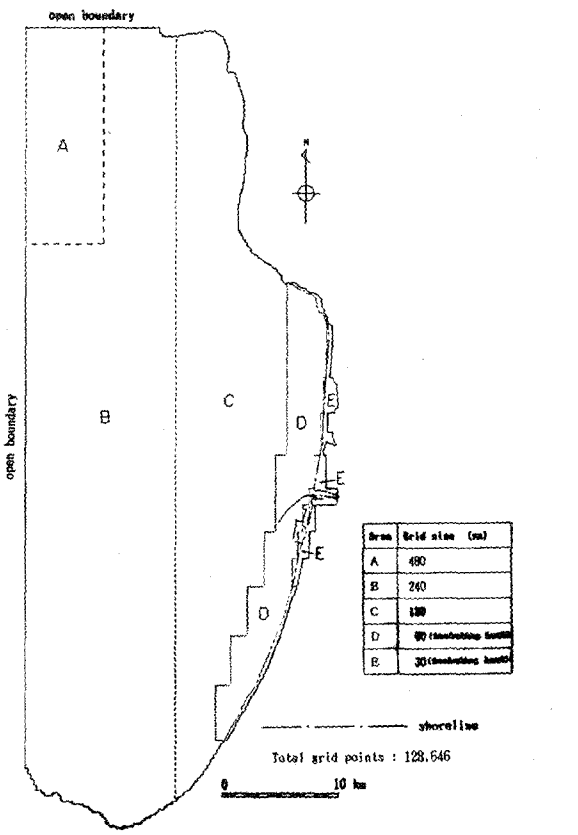

Figure 10(b) Adopted grid system for the third step computation area

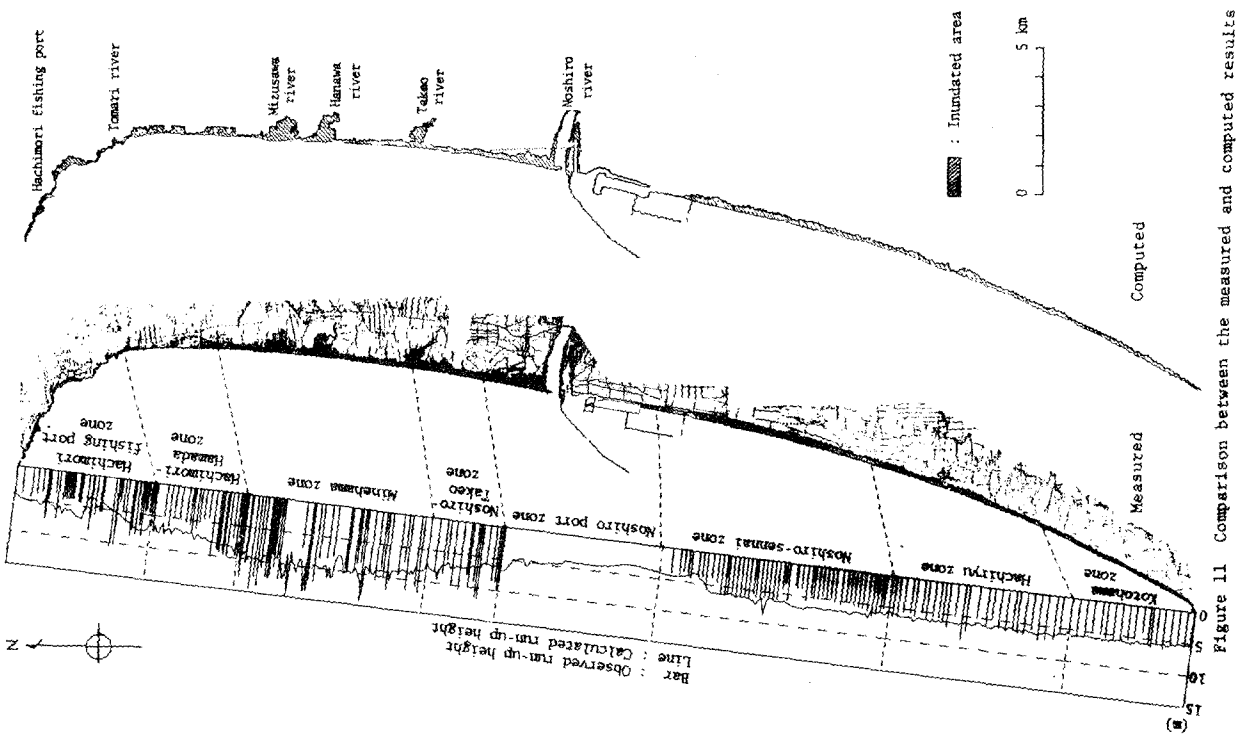

Figure 11 Comparison between the measured and computed results

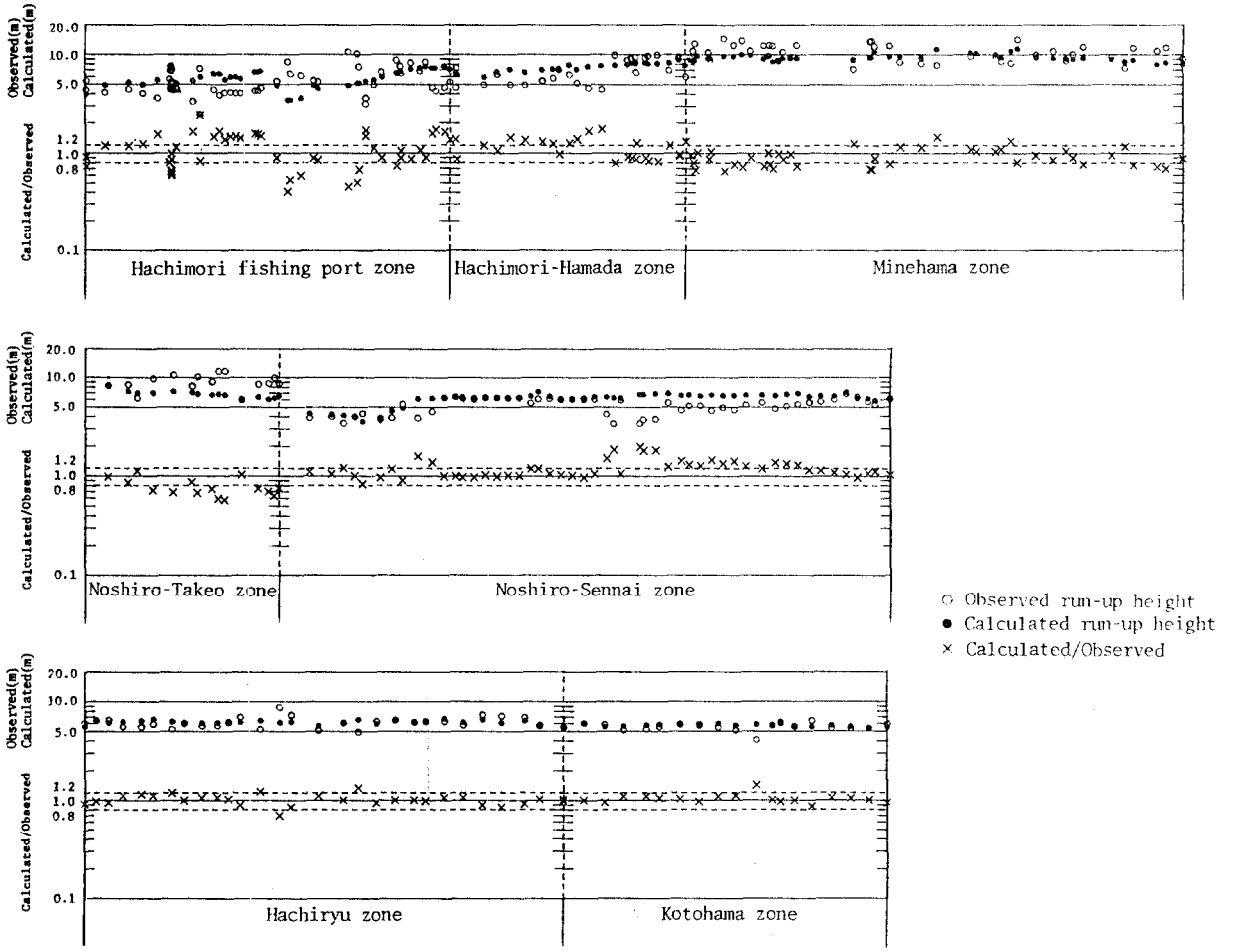

Figure 12 Comparison between the measured and calculated run-up heights

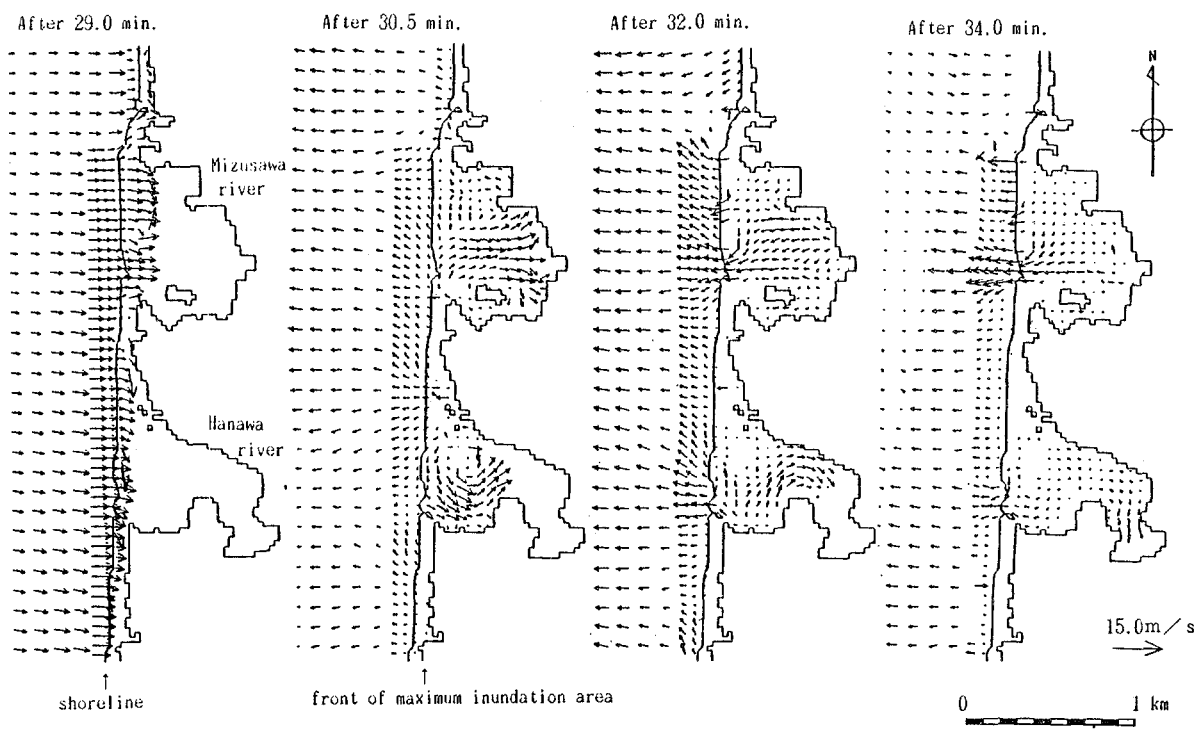

Figure 13 Flow patterns on Minehama inland

downs, water currents on land show complicated movements.

From the third step computation, it is concluded that the shallow water theory can be successfully applied to explain run-ups and inundated areas if used with a careful consideration of the size of grid.

5. CONCLUSIONS

In a usual tsunami simulation, the grid size in deep ocean has been determined with no rule except for the CFL condition. The present study reveals that the resolution N, i.e., the number of grid points per wave length is an important parameter to avoid a possible numerical damping which may destroy the whole picture of the tsunami.

As a result of the one-dimensional analysis, it is recommended to select N larger than 20. With this selected value of N and the wave length of linear long waves which varies from place to place depending on the water depth, the size of the spatial grid can be determined.

With this consideration included, the 1983 Nihonkai-Chubu earthquake tsunami is computed with the shallow water theory. The results agree fairly well with the measured data. The most essential point to reproduce the high run-ups of this tsunami is a sufficiently fine grid system to express the topography in detail, even in deep sea. In the present analysis, this is unintentionally done with no regard to the topography but with a consideration of numerical damping of the waves.

REFERENCES

Aida I., 1969,"A numerical experiment for the tsunami accompanying the Kanto Earthquake of 1932", Bull. Earthq. Res. Inst., Univ. Tokyo, Vol.48, pp 73～86(in Japanese)

Aida I., 1984,"A source model of the tsunami accompanying the 1983 Nihonkai-Chubu Earthquake", Bull. Earthq. Res. Inst., Univ. Tokyo, Vol.59, pp 93～104(in Japanese)

Goto C. and N. Shuto, 1983, "Numerical simulation of tsunami propagation and run-up", Tsunamis;Their Science and Eng., AEPS, pp439～451

Goto C., 1984, "Equations of nonlinear dispersive long wave for a large Ursell number", Proc. Japan Soc. Civil Engrs., No.351, pp193～201 (in Japanese)

Iida K., T. Suzuki, K. Inagaki and K. Hasegawa, 1983, "Finite element method for tsunami wave propagation in Tokai district, Japan", Tsunamis; Their Science and Eng., AEPS, pp293～301

Iwasaki T. and A. Mano, 1979, "Two-dimensional numerical computation of tsunami run-ups in the Eulerian description", Proc. of 26th Conf. on Coastal Eng., JSCE, pp70～74(in Japanese)

Manshinha L. and D. E. Smylie, 1971, "The displacement fields of inclined faults", Bull. Seismol. Soc. America, Vol.61, pp 1433～1440

Shimazaki K. and J. Mori,1983,"Focal mechanism of the May 26, 1983 Japan Sea Earthquake", Programme and Abstracts, Seismol. Soc. Japan, No.2,p15

ALL-UNION CONFERENCE ON TSUNAMI PROBLEM IN GORKY

S. L. Solovjev
Institute of Oceonology, Moscow, USSR

E. N. Pelinovsky
Institute of Applied Physics, Gorky, USSR

All-Union Conference on tsunami problem was held in Gorky on September 18-21, 1984. It was organized by the Tsunami Commission of the Scientific Council on the problem "The study of oceans and seas and the use of their resources" of the USSR State Committee for Science and Engineering in cooperation with the Institute of Applied Physics of the Academy of Sciences of the USSR, Research Radio-Physical Institute and Gorky Zhdanov Polytechnical Institute. One-hundred-and-four representatives of 47 organizations from 19 cities, including 14 Professors and 44 Doctors took part in the conference. One-hundred-and-seven reports whose abstracts were published in Tsunami Conference, Digest of the conference, Editor-in-Chief E. N. Pelinovsky. Gorky Institute of Applied Physics, Academy of Sciences of the USSR (1984).

The reports given at the Conference embraced practically all the aspects of the tsunami problem: wave excitation, their propagation in the open ocean, run-up on the coast, tsunami action on constructions, tsunami regionalization, improvement of the tsunami warning service and the creation of a united automatized system for tsunami observation and population warning, accompanying hydrophysical fields.

Ten reports were dedicated to the problems of tsunami excitation, reconstruction of the tsunami source and to similar problems. The most interesting was the paper by V. K. Gusyakov and L. B. Chubarov (Novosibirks, Krasnoyarsk) "On the comparison of the tsunami effectiveness of the main types of seismic sources of Kuril-Kamchatka zone." In spite of the wide-spread views, on the basis of numerical simulation, the authors showed that for the assigned tectonic dislocation in the seismic source, a steep overthrust, a gently sloping thrust, and any combination of the tsunami along the coast, i.d. they had approximately the same tsunami effectiveness. A horizontal shift is 4-5 times less effective for tsunami excitation and gives another sign distribution of the wave on the coast.

Some problems of the tsunami reflection at a slope were considered by R. Kh. Mazova (Gorky). Although the tsunami energy reflects almost completely at a slope, the variation in the wave form can be radical enough. New results of the hydraulic modeling of the long waves passing underwater barriers were given by G. E. Kononkova, L. M. Voronin, and K. V. Pokazeev (Moscow). In particular, if the barrier was wide, the long wave split into solitons. N. P. Mirchina and E. N. Pelinovsky (Gorky) showed the possibility of the tsunami amplification in separate regions of the coastal zone due to the dispersion effects. V. A. Takhteev (Vladivostok) noted that the presence of the ice sheet did not change significantly the velocity of tsunami propagation. The calculations by E. N. Potetyunko, B. S. Belozyorov, L. D. Filimonova, and I. P. Voloshin (Rostov) showed that the presence of surface-active substance films did not affect tsunami radically, either.

New results of Irkutsk school concerning the solution of the tsunami inverse problem including its solution by the control methods were presented in the reports by O. V. Vasil'ev and V. A. Terletsky. "Methods for determination of the shallow water bottom dislocation exciting the wave of the given mariograms," by G. V. Vasil'eva and V. V. Lobov "On an analytical method of restoration of shallow bottom dislocation, causing the wave of the given characteristics" and by V. G. Trubin "On approximate restoring of bottom dislocation in Cochl-Poisson problem." The formulation of the mathematical problems approaches better the conditions of the tsunami observations in Kuril-Kamchatka zone than previously.

The majority of the reports--more than 20--were traditionally devoted to the various aspects of the tsunami propagation in the ocean and to the related problems. M. A. Belyantsev, V. G. Bukhteev, G. P. Kleshcheva, and N. L. Plink (Leningrad) have continued the numerical simulation of a tsunamis propagation from their sources near the north-western coast of North America to the coastal zone of the USSR. It is shown that, due to the relief peculiarities of the Pacific Ocean, the Soviet coastal zone was screened from these tsunamis.

Two reports by A. G. Marchuk (Novosibirsk) were devoted to the role of waveguides (underwater ridges and shelf) in the transmission of tsunami's energy. In particular, it was shown by ray methods that in the case of the tsunami of May 26, 1983, and possible secondary tsunamis, a certain portion of tsunami's energy propagated round the Sea of Japan, that is along the shelf.

A greater attention, than at the previous tsunami conferences, was paid to the tsunami action on constructions. Seven reports were devoted to this problem. V. V. Yakovlev and T. V. Martynenko (Kiev) considered the diffraction of a solitary wave on a submerged cylinder. Expressions for a vertical and horizontal forces and for a tilting moment (for maximum torque) were obtained. Combining analytical and numerical methods, M. I. Zheleznyak and I. T. Selezov (Kiev) determined the plane dimensions and the extent of the bottom washing out by tsunami waves near vertical solid obstacles. Two reports by V. Kh. Davletshin (Dneprodzerzhinsk) described the results of hydraulic modeling of a solitary wave impact on vertical constructions and cylindrical bearings of off-shore platforms. It was confirmed that the pressure maximum did not coincide in time with the maximum run-ups. The best agreement with the experiments was observed for a nonlinear-dispersion model. A theoretical model proposed by Dorfman and Zheznyak was verified for the maximum run-up on bearings.

Three reports dealt with the problem of searching for new seismic signs of the tsunamigenity of earthquakes. S. A. Kovalev and S. L.Solovjev (Moscow) continued to study P-wave high frequency (1.0-1.6 Hz) records at teleseismic distances. It was confirmed that the time of growth of oscillations up to the maximum value was the sign of the tsunamigenity of an earthquake, but according to this parameter, the transition from non-tsunamigeneous earthquakes to tsunamigeneous ones occurs gradually and occupies a definite band of the parameter.

Six reports were devoted to the investigation of internal waves arising due to underwater earthquakes. V. M. Dryagilev, I. I. Zolotareva, and A. A. Zolotarev (Rostov) studied the interaction of waves excited in a stratified fluid by the bottom uplift with an elastic cover.

The participants of the conference listened with great attention to the communication by V. N. Mitrofanov, E. A. Kulikov, V. A. Dzhumagaliev, N. L. Makovsky (Malokurilsk, Yuzhno-Sakhalinsk) on the registration of the tsunami produced by the Irutup earthquake on March 24, 1984, M = 7.5, with the aid of the bottom cable tide-gauge placed at a distance of 5 km from the Shikotan Island at a depth of 100 m. The tsunami record was marked by a large wave period--80-90 min. The wave height was equal to 9 cm.

V. I. Belokon', A. F. Rodkina, N. A. Smal' (Vladivostok) developed their previous works and showed that tsunamis passing the continent slope could induce the disturbances of the terrestrial magnetic field, several times exceeding the background field oscillations. B. F. Titaev and V. I. Korochentsev (Vladivostok) proposed to use uninhabited underwater apparatus in order to investigate tsunami aftereffects.

Two reports by I. P. Kuz'minykh, Yu. F. Lanin, G. A. Venetsky, V. I. Chekmagov (Obninsk) presented a three-level structure of a "United automatized tsunami system" (UATS) being created in the Far East. The principles of the system operation, the structure of technique complexes, and their specifications were discussed. This project, unlike the previous ones, takes a better account of real conditions of the Kuril-Kamchatka zone.

Some problems of algorithmic and apparatus provision of UATS were considered in reports by I. V. Nikiforov and I. N. Tikhonov (Moscow, Yuzhno-Sakhalinsk) "The experience of a combined processing of seismograms by a computer when the regime of real time is limited," V. V. Sviridov, L. G. Kaurov, T. V. Gavrish (Khar'kov). "On data compression on the basis of an adaptive time discretization in hydrophysical subsystems of UATS," A. I. Zelyony, G. N. Mar, I. V. Nikiforov (Moscow) "Real time adaptive forecasting of sea level fluctuations during the passage of tsunami," A. I. Zelyony, G. N. Mar, I. M. Shenderovich "On tsunami wave space-time detection in a total spectrum of the sea level fluctuations," G. N. Mar and I. M Shenderovich "The use of floating water level recorders for tsunami waves detection and distinction in the real time scale" and "On linearization of statistical characteristics of vibroton-type pressure sensors," A. V. Kalyaev, R. I. Furunkiev, M. I. Garber, G. I. Zaluzhny, S. Yu. Fomin, Yu. D. Kovbas (Taganrog, Minsk, Vladivostok) "A knot multiprocessor computing medium with a hardware algorithm processing for the operative solution of the boundary problems on the basis of nonlinear nonstationary Navie-Stokes and Saint Venant equations," V. K. Krylovich, V. V. Mikhal'kov, A. D. Solodukhin (minsk) "A local acoustic current gauge."

In the reports by V. I. Korochentsov (Vladivostok) and I. N. Didenkulov, A. M. Sutin (Gorky), the problems on the application of hydroacoustic methods for the tsunami sources location and the observation of the passage of waves were touched upon; these ideas had something in common with those proposed at the tsunami conference in Yuzhno-Sakhalinsk in 1981.

It was noted at the conference that investigations of computational methods and tsunami wave run-up should be better coordinated in order to improve short- and long-range tsunami forecasting. For this purpose two working groups "The tsunami effect on the coast and constructions" (chairman E. N. Pelinovsky) and "Computational methods in the tsunami problem" (chairman Yu. I. Shokin) were organized in the frames of the tsunami commission. Some recommendations were taken into consideration, which concerned the practical realization of theoretical investigation and the improvement of the tsunami forecasting system.

The atmosphere at the conference was businesslike and warm and favored the closer relations between specialists of different profiles. The conference showed that the problem of tsunami is intensively studied in the USSR.

APPLICATION FOR MEMBERSHIP

THE TSUNAMI SOCIETY
P.O. Box 8523
Honolulu, Hawaii 96815, USA

I desire admission into the Tsunami Society as: (Check appropriate box.)

☐ Student ☐ Member ☐ Institutional Member

Name _____ Signature _____

Address _____ Phone No. _____

_____

Zip Code _____ Country _____

Employed by _____

Address _____

Title of your position _____

FEE: Student $5.00 Member $25.00 Institution $100.00

Fee includes a subscription to the society journal: SCIENCE OF TSUNAMI HAZARDS.

Send dues for one year with application. Membership shall date from 1 January of the year in which the applicant joins. Membership of an applicant applying on or after October 1 will begin with 1 January of the succeeding calendar year and his first dues payment will be applied to that year.